Construction and noise studies of a continuous wave Raman laser
by Jason K Brasseur

A thesis submitted in partial fulfillment of the requirements for the degree of Doctor of Philosophy in Physics
Montana State University

Abstract:
The first non-resonant cw Raman laser in H2 is presented in this thesis. A time-dependant theory is presented that describes the cw Raman laser in the high pressure limit, so population dynamics can be ignored. The theory is tested in the steady-state regime and it matches well against the experimental data obtained. The theory also predicts the relaxation oscillations of the cw Raman laser and provides insight to minimize these oscillations. The theory predicts the relative intensity noise of the cw Raman laser, which is in good agreement with experimental results. Finally the cw Raman laser linewidth is measured to be 4kHz over a 10ms scan, and the Allan variance of the laser linewidth is experimentally measured.

CONSTRUCTION AND NOISE STUDIES OF A CONTINUOUS WAVE RAMAN LASER

by

Jason K. Brasseur

A thesis submitted in partial fulfillment
of the requirements for the degree

of

Doctor of Philosophy

in

Physics

MONTANA STATE UNIVERSITY – BOZEMAN
Bozeman, Montana

November 1998

APPROVAL

of a thesis submitted by

Jason K. Brasseur

This thesis has been read by each member of the thesis committee and has been found to be satisfactory regarding content, English usage, format, citations, bibliographic style, and consistency, and is ready for submission to the College of Graduate Studies.

Dr. John Carlsten ______________________ 12-1-98
Date

Approved for the Department of Physics

Dr. John Hermanson ______________________ ____________
Date

Approved for the College of Graduate Studies

Dr. Joseph Fedock Joseph J. Fedock 12/3/98
Date

STATEMENT OF PERMISSION TO USE

In presenting this thesis in partial fulfillment of the requirements for a doctoral degree at Montana State University – Bozeman, I agree that the Library shall make it available to borrowers under rules of the Library. I further agree that copying of this thesis is allowable only for scholarly purposes, consistent with "fair use" as prescribed in the U.S. Copyright Law. Requests for extensive copying or reproduction of this thesis should be referred to University Microfilms International, 300 North Zeeb Road, Ann Arbor Michigan 48106, to whom I have granted "the exclusive right to reproduce and distribute my dissertation in and from microform along with the non-exclusive right to reproduce and distribute my abstract in any format in whole or in part."

Signature____________________

Date 12/1/98

ACKNOWLEDGEMENTS

I would like to thank John Carlsten, my advisor, for giving me the opportunity to work on something special, and giving me his passion for physics, for these things I will always be grateful.

I would like to thank R.T. Robiscoe for his endless homework which taught me to think like a physicist. I would like to thank Kevin Repasky and Gregg Switzer for their thoughts and help. I thank Pete Roos for his help on the last experiment and his enthusiasm. Many other past and present members such as Pete Sellin, Lei Meng, Jim Wessel, Rand Swanson and Phillip Battle, thank you. I would like to thank Michael Jefferson and Jan Hall for their help with electronics and frequency locking.

I would like to thank Norm Williams and Eric Anderson for their help with machining and electronics. I thank my friends for their support Monty, Darrell, Margaret, and George.

Finally, I would like to thank my graduate committee for their help and support.

TABLE OF CONTENTS

1. INTRODUCTION 1

References 6

2. THRESHOLD PREDICTIONS AND PROOF OF CONCEPT EXPERIMENT. 7

Theoretical Prediction of Threshold 7
Design Considerations 10
Experimental Apparatus 12
Experimental Results 13
Discussion 16
References 18

3. THEORETICAL DESCRIPTION OF THE CW RAMAN LASER 19

Physical System 19
Polarization of the Medium and the Density Matrix 22
Far-off Electronic Resonance 27
High Pressure and Established Coherence Limits 29
References 32

4. STEADY-STATE CW RAMAN SCATTERING 33

Determination of Constants 33
How the Cw Raman Laser Starts Up 35
Steady-State Limit 38
Experimental Verification of Theory 41
Remarks 45
References 46

5. RELAXATION OSCILLATIONS AND NOISE 47

Motivation for a Linearized Theory 47
Linearization of the Cw Raman Laser Equations 47
Relaxation Oscillations 50
Experimental Elimination of Relaxation Oscillations 52
Predictions of RIN on the Raman Laser 55
Conclusions 59

References 61

6. CW RAMAN LASER LINEWIDTH 62

Motivation for a Linewidth Measurement 62
Measurement of Laser Linewidth 62
Experimental Apparatus and Linewidth Measurements 64
Conclusions 69
References 70

7. CONCLUDING REMARKS 71

APPENDICES 72

Appendix A – Locking 73
Appendix B – Servo Design 78
Appendix C – Piezo Driver 83
Appendix D – AOM Driver 87
Appendix E – AOM Temperature Controlling 90
Appendix F – Pumping System 92
Appendix G – Raman Cavity 94
Appendix H – Math-Cad Programs 97

LIST OF FIGURES

Figure

1.1 Energy Level Diagram 2

1.2 Potential Raman Lasers 4

2.1 Cavity Build Up 9

2.2 Cavity Mode Overlap 11

2.3 Cavity Mode Overlap 11

2.4 Experimental Apparatus 12

2.5 Stokes Output and Photon Conversion Efficiency vs. Pump Power 14

2.6 Pump and Stokes Profiles 15

2.7 Beam Diameters through a Focus 16

3.1 Resonant Cavity 20

3.2 Energy Level Diagram 22

3.3 Energy Level Diagram 24

4.1 Cw Raman Start Up 36

4.2 Conversion Efficiency vs. Time 37

4.3 Pump Coupling Efficiency vs. Time 38

4.4 Conversion Efficiency vs. Times Threshold 40

4.5 Experimental Diagram 41

4.6 Stokes Output and Conversion Efficiency vs. Pump Power (fitted) 42

4.7 Experimental Diagram 43

4.8 Stokes Output and Conversion Efficiency vs. Pump Power (threshold)...... 44

5.1. Raman Start Up 49

5.2 Comparison of Theories 49

5.3 Relaxation Oscillations Frequency and Damping 51

5.4 Damping in 1 oscillation 51

5.5 Experimental Set-Up.. 52

5.6 Stokes RIN 54

5.7 Stokes and Pump RIN as Function of Pump Power.. 55

5.8 Cavity Lineshape 56

5.9 Pump RIN for Theory 57

5.10 Stokes and Pump RIN as Function of Pump Power (Theory) 57

5.11 Stokes and Pump RIN as Function of Pump Power (with input RIN).......... 58

5.12 Low and High AOM Gain.. 59

6.1 Experimental Apparatus 65

6.2 Linewidth Measurement.. 66

6.3 Allan Variance vs. Integration Time 68

A.1 Production of Error Signal 75

A.2 Error Signal 77

B.1 Servo and Overall Response 80

B.2 Servo Circuit Diagram 81

C.1 Piezo Driver Circuit Diagram 85

D.1 AOM Driver Circuit Diagram 89

E.1 AOM Temperature Stability 91

F.1	Pumping System	93
G.1	cw Raman Laser	95
G.2	Cavity Housing	95
G.3	cw Raman Laser	96
G.4	Isolation Shell	96

ABSTRACT

The first non-resonant cw Raman laser in H_2 is presented in this thesis. A time-dependant theory is presented that describes the cw Raman laser in the high pressure limit, so population dynamics can be ignored. The theory is tested in the steady-state regime and it matches well against the experimental data obtained. The theory also predicts the relaxation oscillations of the cw Raman laser and provides insight to minimize these oscillations. The theory predicts the relative intensity noise of the cw Raman laser, which is in good agreement with experimental results. Finally the cw Raman laser linewidth is measured to be 4kHz over a 10ms scan, and the Allan variance of the laser linewidth is experimentally measured.

CHAPTER 1

INTRODUCTION

If you were to take a poll and ask a group of laser physicists: "What do you think the laser field as a whole needs in the future?", the answers would vary, but there would be an underlining theme. They would want to have a narrow linewidth laser at every wavelength in the spectrum, ultra-violet, visible and infrared parts of the spectrum, with a gaussian spatial mode for the output. So why would we want to have all of these lasers? What good would they be?

The needs vary from making more stable atomic clocks to monitoring of atmospheric gasses. Imagine if we could put a small laser system on a smoke stack that could tell us what pollutants a factory was putting out. We could place these laser systems around airports and monitor the wind conditions and monitor for wind shear, by using a laser that is in the "eye" safe region of the spectrum. Both of these lasers are needed in the 2-5 μm infrared region of the spectrum. Now how can we make these dreams of bigger and better things become a reality? Either we can make new lasers, or take existing lasers and externally shift the wavelength.

Currently available lasers in this region have some disadvantages. For example, a lead salt laser can produce laser light into the infrared but it has small output powers (~tens of μW) and needs to be cooled at liquid nitrogen temperatures. An alternative is to take existing lasers and double, or triple the frequency of the laser by using second harmonic generation and other nonlinear effects. We also can make optical parametric oscillators which can form laser frequencies lower than the original laser. However, all of these devices have drawbacks that range from output linewidths to the multi-mode spatial outputs of the optical parametric oscillator to the high thresholds often needed to construct the lasers, typically in the 50 to 100 mW range [1,2]. In addition, the cost of some of these devices is ~$100k and up.

Another method to shift the frequency of a laser is to use Raman scattering. Laser induced Raman scattering, first studied in 1962 [3], occurs when an incident photon interacts with a molecule (or an atom) and generates a red shifted photon resulting from the conservation of energy when the excitation in the molecule occurs. The molecular excitation can be rotational, vibrational, or electronic, which accounts for the possibility of many different wavelengths. For example, figure-1.1 shows the levels involved for vibrational Raman scattering of a 532 nm laser in H_2 to 683 nm. At high intensities the Raman process can have gain and produce stimulated Raman scattering, and, because of the high intensities needed, Raman scattering is most often studied in the high power pulsed regime. Stimulated Raman scattering has also been utilized in the continuous wave (cw) regime to make cw Raman lasers. However, because of the lower intensity of the cw pump

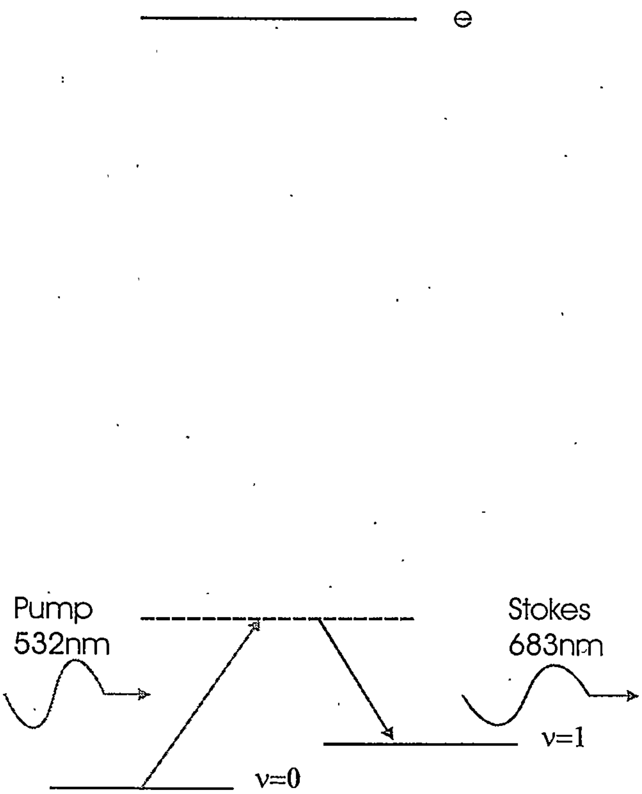

Figure 1.1 Energy level diagram for H_2, to scale.

lasers, these cw Raman lasers generally operate near a molecular (or atomic) resonance to increase the Raman gain and are therefore tunable only over a narrow regions near the resonance.

A few examples of near resonant Raman lasers include a 67μm cw Raman laser in NH_3 [4], a cw sodium Raman laser near the Na D lines [5], a two photon pumped cw Rb Raman laser near 776nm [6], and various cw Raman lasers near the Ne resonances in the He-Ne laser discharge tube [7-9]. In addition, cw Raman lasing is also possible in optical fibers where the long interaction length of the fiber and the small spot in the fiber increase the gain so cw Raman lasing can occur. However, typically input pump powers on the order of a watt are need to pump these Raman fiber lasers [10]. In addition, the Raman shift in the optical fiber is only ~440 cm^{-1} and is inconvenient if one is looking for substantial shifts of wavelength.

Recent developments in mirror coating technology have lead to the availability of new mirrors with reflectivies of 99.995% and higher. To put this number in perspective a bath-room mirror only reflects ~96% of the light that is incident on it while the 4% is typically absorbed, these new mirrors absorb only 10 parts per million an improvement of over three orders of magnitude. These low loss mirrors have been used to build nonconfocal cavities or optical resonators with finesses of 50,000 and higher [11,12] (a Q-factor of ~10^9 and greater). By the use of the nonconfocal cavity we have a focusing geometry which makes the spot size of the beam on the mirrors on the order of 100μm, so the degradation of the finesse (Q-factor) that is due to wavefront distortion is minimized and the high finesse cavity is achieved.

With the advent of this new technology of high finesse cavities it now becomes possible to consider using these cavities to do studies in nonlinear optics with cw lasers in the milliwatt range of power. Specifically, it is now possible to use the high finesse cavities to build a widely tunable cw Raman laser that can be pumped by a laser in the milliwatt range, namely low cost diode lasers. If we consider all of the room temperature diode lasers, and a few gasses to perform Raman scattering in, namely H_2, and CH_4, we can cover the 1-4μm range of the spectrum. Figure-1.2 illustrates this point. This provides a lot more possibilities for new lasers. This thesis will describe a non-resonant cw Raman laser in H_2, the first of its kind [13].

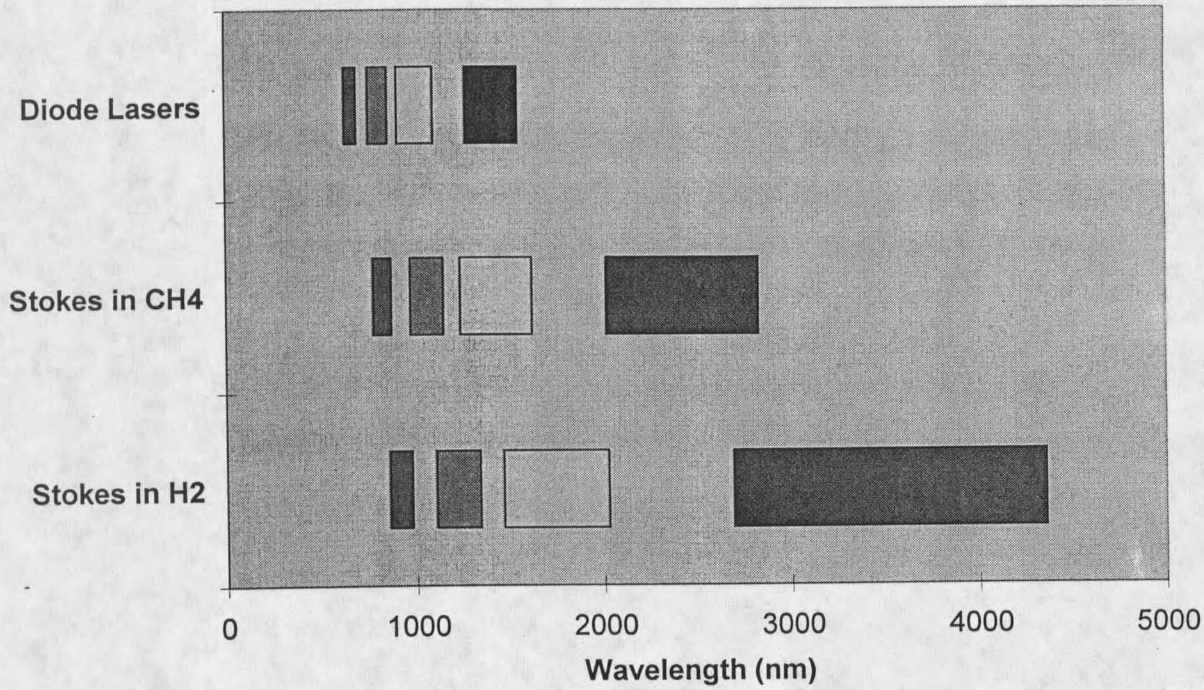

Figure-1.2 Shows the possible cw Raman lasers for various gasses.

This thesis is arranged in the following manner. Chapter 2 describes the proof of concept experiment and familiarizes the reader with the idea of the threshold of the cw Raman laser with a back of the envelope calculation. The output mode of the cw Raman laser is characterized as well. Chapter 3 develops the cw Raman laser equations that will be used throughout this thesis. Chapter 4 studies the steady-state nature of the cw Raman laser. In chapter 5 a linearized theory is developed to explain the relaxation oscillations that the laser is seen to exhibit. Chapter

5 also predicts and explains the amplitude noise on the cw Raman laser. Chapter 6 measures the Raman laser linewidth and the stability of the Raman laser frequency. Chapter 7 gives brief concluding remarks, and a few appendices are included to describe some of the devices and methods used in this thesis. So off to the second chapter.

REFERENCES CHAPTER 1

[1] M. Scheidt, B. Beier, K. -J. Boller, and R. Wallenstein, Opt. Lett. **22**, 1287 (1997).

[2] W. R. Boseburg, A. Drobshoff, J. I. Alexander, L. E. Myers, and R. L. Byer, Opt. Lett. **21**, 1336 (1996).

[3] N. Bloemberg, Amer. J. of Phys. **35**, 989 (1967).

[4] R. Max, U. Huber, I. Abdul-Halim, J. Heppner, Y. Ni, G. Willenberg, and C. O. Weiss, IEEE J. Quantum Electron. **QE-17**, 1123 (1981).

[5] M. Poelker and P. Kumar, Opt. Lett. **17**, 399 (1992).

[6] G. Grynberg, E. Giacobino, and F. Biraben, Opt. Commun. **36**, 403 (1981).

[7] S. N. Jabr, Opt. Lett. **12**, 690 (1987).

[8] P. Franke, A. Feirisch, F. Riehle, K. Zhao, and J. Helmcke, Appl. Opt. **28**, 3702 (1989).

[9] X. W. Xia, W. J. Sandle, R. J. Ballagh, and D. M. Warrington, Opt. Commun. **96**, 99 (1993).

[10] P. Persephonis, S. V. Cherikov, and J. R. Taylor, Electron. Lett. **32**, 1486 (1996).

[11] K. S. Repasky, L. E. Watson, and J.L. Carlsten, Appl. Opt. **34**, 2615 (1995)

[12] R. S. Repasky, J. G. Wessel, and J. L. Carlsten, Appl. Opt. **35**, 609 (1996).

[13] J. K. Brasseur, K. S. Repasky, and J. L. Carlsten, Opt. Lett. **23**, (1998).

CHAPTER 2

THRESHOLD PREDICTIONS, AND PROOF OF CONCEPT EXPERIMENT

Theoretical Prediction of Threshold

As stated in the previous chapter, this thesis presents the first non-resonant cw Raman laser in H_2. In this chapter we will go though the initial thought process that led to the realization of a cw Raman laser.

An important concept when describing lasers is the threshold condition, since this is when the light exiting the cavity exhibits laser-like qualities, i.e. coherence. Threshold happens when the gain equals the loss in a system. To predict the threshold of the cw Raman laser we start with the single-pass gain G in a focused geometry[1]:

$$G = \frac{1}{2}\frac{4\alpha}{\lambda_p + \lambda_s}\tan^{-1}\left(\frac{\ell}{b}\right)P_p. \qquad 2.1$$

Where G is the Raman gain per pass, α is the Raman gain coefficient, λ_p (λ_s) is the wavelength of the pump (Stokes) field, ℓ (b) is the interaction length (confocal parameter[2]) of the beam, and P_p is the incident pump power. The factor of one half accounts for the standing wave that is formed inside of the resonant cavity instead of a traveling wave. The Raman gain coefficient, α, has the following functional form[3]:

$$\alpha = \frac{D(\nu_p - \nu_v)}{(\nu_i^2 - \nu_p^2)^2} = \frac{D\nu_s}{(\nu_i^2 - \nu_p^2)^2} \qquad 2.2$$

Where D is a constant that incorporates the pressure of the gas at the linewidth of the transition, ν_p (ν_s) is the pump (Stokes) frequency, and ν_i (ν_v) is the resonant electronic (vibrational) frequency of the transition. Equation 2.2 assumes that the pump frequency ν_p is far from the resonance ν_I. For diatomic hydrogen, ν_I=8.48x10^{4}cm^{-1}, and ν_v=4155cm^{-1}. Note that ν_i corresponds to a resonance at 118nm in the UV, so ν_I^2-ν_p^2 will be a slowly varying function for ν_p in the visible and the IR parts of the spectrum. Thus the cw Raman laser in H_2 is expected to be broadly tunable. For a pump wavelength of 532nm (18,800 cm^{-1}), α is 2.5x10^{-9} cm/W in the high-pressure limit[3]. To generate a spontaneous Stokes photon in a single pass we need on the order of 300kW of pump power. Since typical cw lasers are in the milli-watt to watt range, we need a way of increasing our cw power to have cw Raman lasing.

One way to increase the circulating power of the pump laser is to pump an optical cavity, or a high finesse cavity (HFC). To see this effect, we start with an interferometer and focus on the intensity build up inside of the HFC. Because we are looking at an interference effect, we sum the electric field to build up the intensity inside of the HFC. Figure 2.1 demonstrates how the fields build up inside of the HFC.

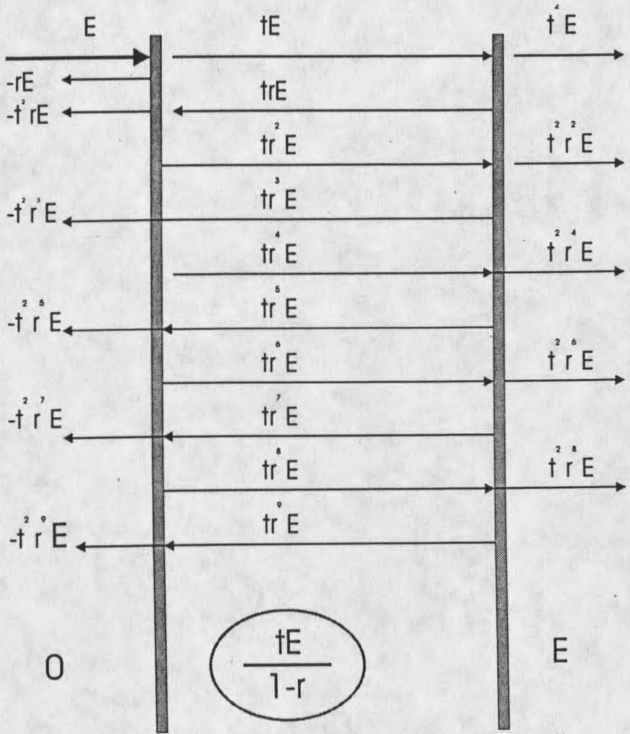

Figure 2.1 Electric field buildup inside high finesse cavity

Where r (t) is the electric field reflectivity (transmission) which is just the square root of the intensity reflectivity, R, (transmission, T). We see that, in the absence of mirror absorption, all of the optical power is coupled into the HFC and the field builds by a factor of t/(1-r) or the power contained inside the cavity increases as the square of t/(1-r) [4]. Thus our gain becomes the following:

$$G = \left(\frac{1}{2}\right)\frac{4\alpha}{\lambda_p + \lambda_s}\tan^{-1}\left(\frac{\ell}{b}\right)\left(\frac{\sqrt{T_p}}{1-\sqrt{R_p}}\right)^2 P_{incident} \qquad 2.3$$

where T_p (R_p) is the transmission (reflectivity) of the mirrors at the pump wavelength, and $P_{incident}$ is the optical power incident on the HFC.

The mirrors of the HFC can be coated for both the pump and the Stokes wavelengths. Now we need to think about how the Stokes reflectivity figures into the cw Raman laser threshold. We have the gain per pass as given by equation 2.3, now we need to find the loss per pass. This is:

$$Loss = 1 - R_s \tag{2.4}$$

where R_s is the mirror reflectivity at the Stokes wavelength. By equating the gain and loss equations (2.3 and 2.4) and solving for $P_{incident}$, we arrive at the following condition for the threshold of the cw Raman laser:

$$P_{threshold} = \frac{2(1-R_s)}{\tan^{-1}\left(\frac{\ell}{b}\right)}\left(\frac{\lambda_s + \lambda_p}{4\alpha}\right)\left(\frac{1-\sqrt{R_p}}{\sqrt{T_p}}\right)^2 \tag{2.5}$$

To get an approximate value for the threshold let us choose some typical numbers. The manufacture of the mirrors can produce mirrors with coatings for multiple wavelengths with reflectivies of 0.9998 and absorption of 15 ppm or less [5]. The laser used to pump the Raman cell has a wavelength of 532nm, which would correspond to a Stokes output of 683nm. The cavity length is approximately 7cm with 25cm radius of curvature mirrors, corresponding to a confocal parameter, b, of 17.3cm. If these parameters are plugged into 2.5, we predict a threshold of 0.7mW, which is dramatically less then the 300kW for a single pass. The only assumption is that the optical cavity is resonant at both the pump and Stokes wavelengths.

Design Considerations

Thus the threshold of the cw Raman laser is predicted to be on the order of a milliwatt. Now we need to think about how one of these lasers can be made. In order to make the cw Raman laser work we need to make a cavity that is doubly resonant. At first this seems like an insurmountable task, because we have finesses on the order of 15,000 or the ratio of the free spectral range (FSR) of the cavity to the linewidth of the HFC is 15,000. Figure 2.2 illustrates this seemable impossible task.

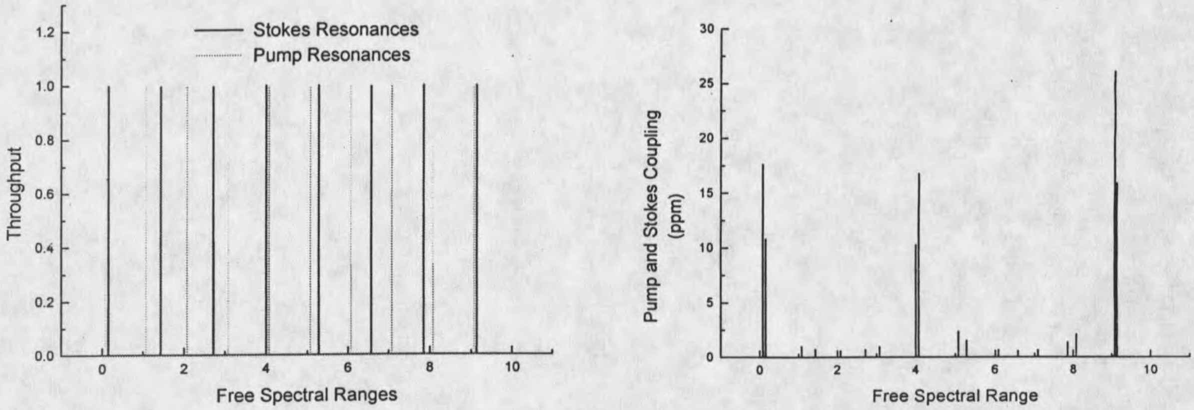

Figure 2.2 Overlap of pump and Stokes cavity modes

We see that over a scan of seven FSRs the overlap of the Stokes modes to the pump modes is on the order of 10^{-6}, this would increase the threshold from a milliwatt to a watt! However, we have overlooked the Raman linewidth. For 10atm. of H_2, the Raman linewidth (FWHM) is 510MHz [3]. For a FSR of 2GHz, we only need to scan seven FSRs before we have a significant overlap. Figure 2.3 illustrates how the Raman linewidth relaxes the mode overlap constraint. We see the

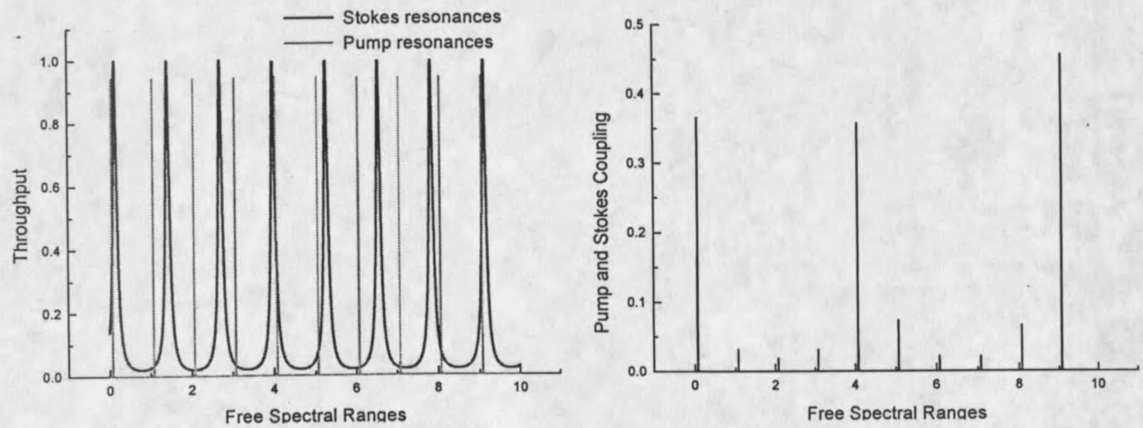

Figure 2.3 Overlap of pump and Stokes cavity modes with the Raman linewidth included.

overlap approaches 50% in a few places, this would double the threshold from a milliwatt to 2 milliwatts. To ensure that the Stokes and pump cavity resonances fall within a Raman linewidth, either the pump laser or the Raman cavity must be scanned until an overlap occurs, ~7 FSR or ~20GHz (for a 2-3GHz FSR) of tuning is required for either the cavity or the pump laser.

In addition to the requirement that the pump and Stokes resonances overlap, the pump laser needs to be stable enough to maintain the intensity build-up in side of the HFC. For the cavities described in this thesis, the pump laser must be stable to about 10kHz (cavity linewidth/10). As a result, the pump laser must undergo some frequency and phase stabilization. Appendix A describes the Pound-Drever-Hall [6] method for locking, which is used to stabilize the pump laser.

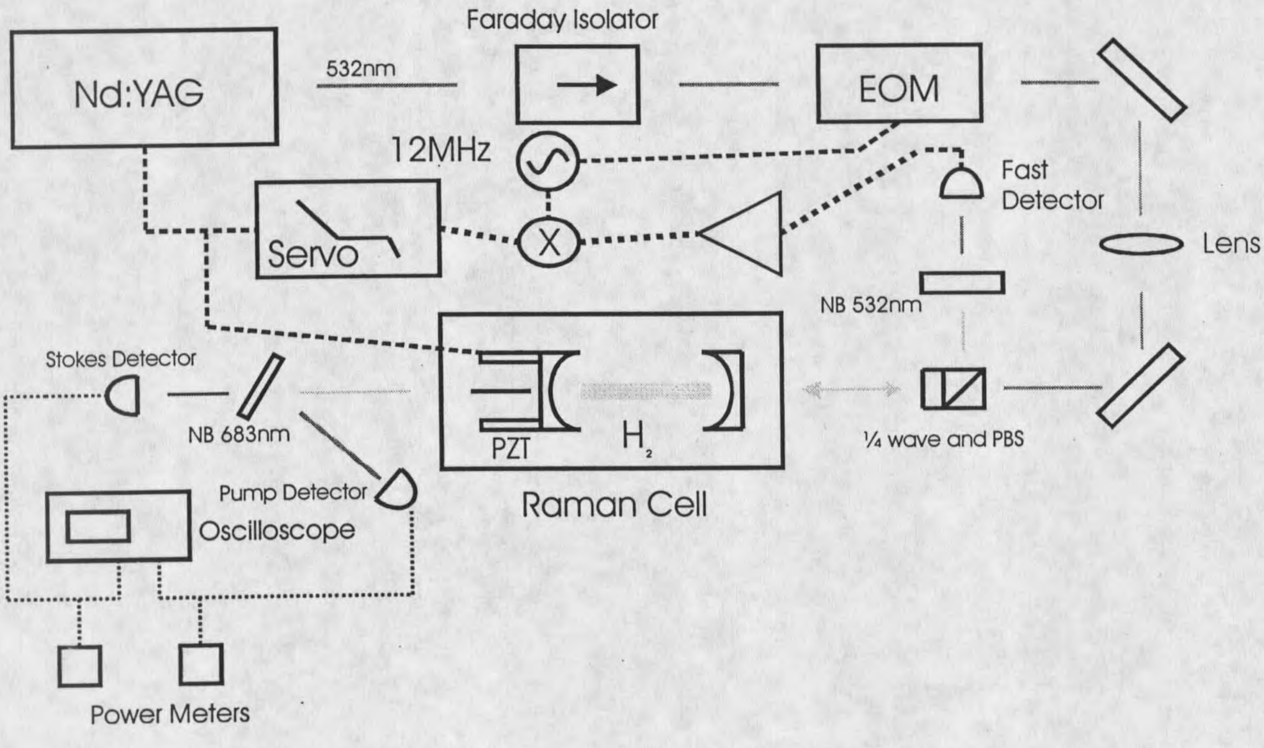

Figure 2.4 Experimental diagram of the cw Raman laser

Experimental Apparatus

The apparatus used to make the first cw Raman laser in H_2 is shown above in figure 2.4. For this experiment we chose to use a frequency-doubled Nd:YAG [7] laser with an output up to 200mW. The output of this Nd:YAG laser at 532nm was sent through a Faraday isolator to minimize the optical feedback to the Nd:YAG laser. An electro-optic modulator (EOM) was used to place sidebands on the carrier frequency required for locking the pump laser to the optical cavity. The pump laser beam traveled through a two-element lens pair used to mode match the pump beam to the cavity. A polarizing beam splitter (PBS) cube in conjunction with a quarter-wave plate allowed for monitoring of the beam reflected from the cavity. A fast detector (>12MHz) was then used to measure the error signal. A low noise amplifier gave the signal 30dB of amplification in power before the signal was mixed to dc. The error signal entered the servo, and the slow corrections were sent to temperature tune the pump laser, while the fast corrections were sent to the pump laser piezoelectric transducer (PZT). The entire apparatus was placed on a floating platform to minimize the effects due to vibrations.

Experimental Results

The Raman cavity used in this experiment has a design similar to the high finesse cavity described in References 8 and 9, and diagrams of the latest Raman cavity used in this thesis can be seen in appendix G. The cavity mirrors had a radius of curvature of 50cm and were spaced by 7.28cm by ULE 7971, an ultra-low expansion material made by Corning. The cavity was filled with 10atm. of H_2, resulting in a Raman linewidth (FWHM) of 510MHz. The output of the cw Raman laser was measured at the exit of the cavity, with a narrow-band (NB) filter at 683nm placed in the beam at a slight angle to separate the pump and Stokes beams. The output power of the laser was varied, and the pump laser was locked to the cavity. The average pump and Stokes powers were measured, and a photodiode was used to monitor the amplitude noise of the Stokes beam.

Figure 2.5a shows the power of the total Stokes power radiated from the cavity as a function of the pump power incident on the cavity and Figure 2.5b shows the Stokes photon

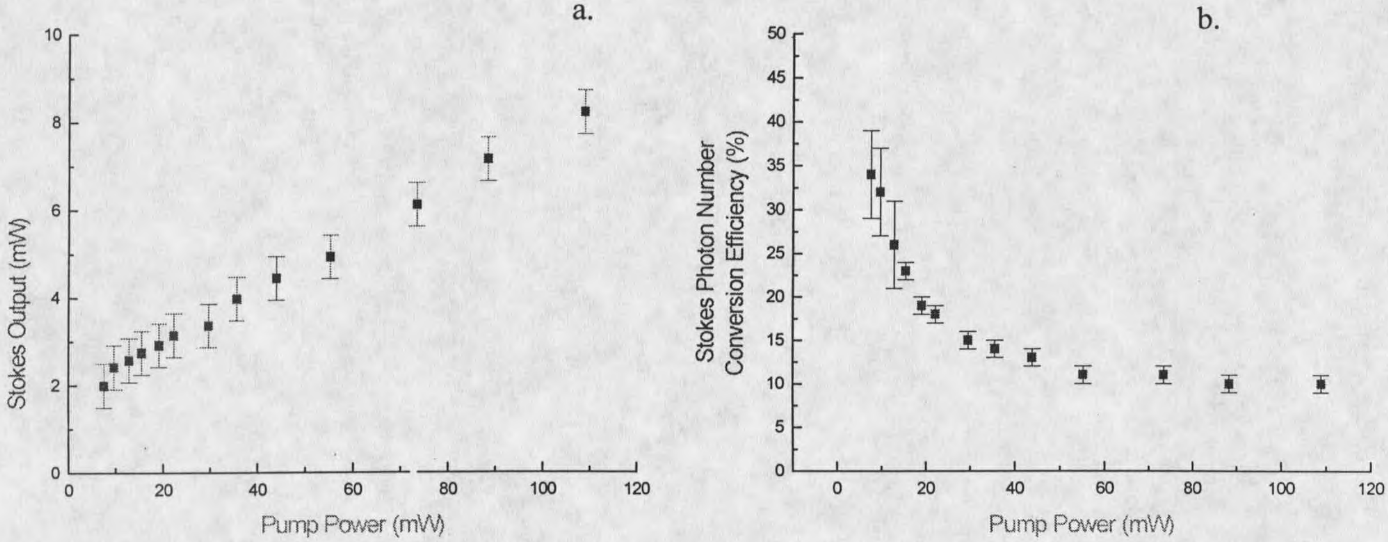

Figure 2.5 Shows the output of the Raman laser: (a) shows the output power of the cw Raman laser while (b) shows the photon number conversion efficiency

number conversion efficiency as a function of pump power. The cw Raman laser has a threshold of ~2mW. The maximum photon conversion efficiency is 35% at a pump power of 7.6mW. The cw Raman laser had a maximum output of 8.2mW at 109mW of pump power.

The theory predicts a threshold of 1.2mW for mirror reflectivities (transmissions) of 0.99983 (92 ppm). However, in this experimental setup we see an experimental threshold of ~2mW. This difference can be attributed to the accuracy of the overlap of the double resonance of the pump and Stokes beams.

The intensity fluctuations on the pump and the Stokes beams at the exit of the cavity are less than 1% for high pump powers and increase to 5% for low pump powers. The intensity fluctuations, which are in a frequency band of 30-300kHz, are believed to be relaxation oscillations caused by the interaction between the locking servo loop with the intensity buildup in the cavity, which occur on a time scale of 1-10μs. The cw Raman laser is more efficient at lower pump powers, causing a larger initial oscillation in the locking signal, which is feedback in to the servo which maintains the oscillations.

The spatial profile and the longitudinal mode characteristics of the output of the cw Raman laser are useful pieces of information. Because we are using a nonconfocal cavity with spherical mirrors, one would expect a gaussian beam at the exit of the cavity. To confirm this result the output of the cw Raman laser is sent through a pelin-broca prism to spatially separate the pump and the Stokes beams. The transverse structure of the beam is measured by imaging the pump and the Stokes beam on a charge coupled device (CCD) camera. These results can be seen in figures 2.6a and 2.6b.

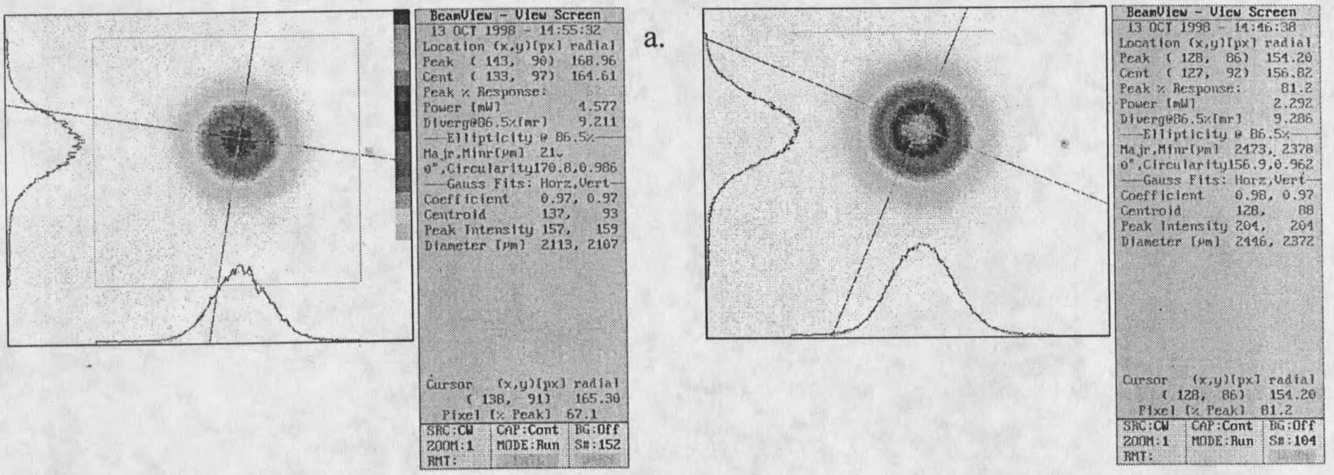

Figure 2.6 Shows the output beam spatial profiles: (a) shows the pump beam while (b) shows the Stokes beam

Figure 2.6a is the spatial profile of the pump beam, and Figure 2.6b is the spatial profile of the Stokes beam. We see that both the pump and the Stokes beams have are circular (>96%) and the gaussian fits are excellent (>0.97). To see the longitudinal dependence of the Stokes beam the Stokes beam was measured through a focus and waist measurements were made at various places throughout the focus. Figures 2.7a and Figure 2.7b show the vertical and horizontal waist as at various places while the beam is focused.

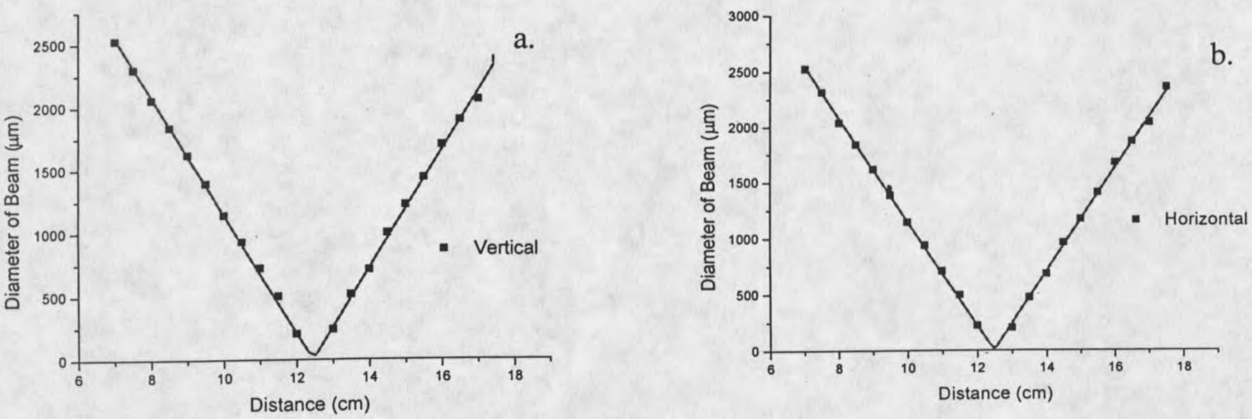

Figure 2.7 Shows the output Stokes beam of the cw Raman through a focus: (a) shows the vertical while (b) shows the horizontal dependencies.

The beam diameter data is fit to the following equation [10]:

$$D(z) = 2 \cdot \sqrt{\frac{\lambda z_o}{\pi}\left(1 + \left(\frac{z - x_o}{z_o}\right)^2\right)^{1/2}} \qquad 2.6$$

where λ (z_0) is the wavelength (Rayleigh range) of the beam and x_0 accounts for any displacement in the origin. We see that the beam obeys gaussian beam propagation, however, there is a slight astigmatism that is attributed to the pelin-broca prism, which was used to spatially separate the pump and Stokes beams.

Discussion

The proof of concept experiment was just presented. The experimental threshold matches our back of the envelope calculation for the threshold of the cw Raman laser within experimental error, and the Stokes output propagates according to gaussian optics as expected. However, there are many exciting unexpected subtleties. When one takes a closer look at the photon conversion efficiency, we see that as we increase the pump power the efficiency increase initially from zero (below threshold) to ~34% and then falls to ~10% at higher pump powers.

This is peculiar, for a diode laser the conversion efficiency increases as more current is supplied to the diode and eventually levels off but is does not drop by a third. Another gem is when the cw Raman laser lases it is prone to oscillate at a frequency that is highly dependent on the pump power which makes one think of relaxation oscillations. In order to explain and predict these phenomena, we need to develop a time dependent theory for the cw Raman laser. This is discussed in chapter 3.

REFERENCES CHAPTER 2

[1] P. Rabinowitz, A. Stein, R. Brickman, and A. Kaldor, Opt. Lett. **3**, 147 (1978).

[2] The confocal parameter of a beam that is mode matched to the cavity is given by $b = \sqrt{\ell(2R - \ell)}$ where ℓ is the length of the cavity and R is the radius of curvature of the mirrors, see A. Yariv, *Quantum Electronics* (John Wiley & Sons, Inc., New York, NY., 1975) page 134.

[3] W.K. Bischel and M. J. Dyer, J. Opt. Soc. Am. B **3**, 677 (1986).

[4] The intensity buildup inside a high-finesse cavity can be found from the standard electric field summation used in optics texts. See, for example, E. Hecht and A Zajac, *Optics* (Addison-Wesley, Reading, Mass., 1979), page 305.

[5] The high reflectivity mirrors were purchased from Research Electro-Optics, Boulder Colorado.

[6] R. W. P. Drever, J. L. Hall, F. W. Kowalski, J. Hough, G. M. Ford, A. G. Manley, and H. Wood, Appl. Phys. B **31** 97 (1981).

[7] The Lightwave Electronics laser used in this thesis has 200mW of single frequency, single mode optical power and a linewidth of <10kHz.

[8] K. S. Repasky, L. E. Watson, and J.L. Carlsten, Appl. Opt. **34**, 2615 (1995)

[9] R. S. Repasky, J. G. Wessel, and J. L. Carlsten, Appl. Opt. **35**, 609 (1996).

[10] A. Yariv, *Quantum Electronics* (John Wiley & Sons, Inc., New York, NY., 1975) page 111.

CHAPTER 3

THEORETICAL DESCRIPTION OF THE CW RAMAN LASER

Physical System

Typically the theory describing Raman scattering in H_2 can be mathematically described as amplifier theory. The main reason for this is the most important independent variable is the propagation distance of the optical beam through a Raman cell. Even when the optical beam undergoes many focuses in a multi-pass cell, the important variable is still the interaction length. However, in a resonant cavity, where the beam is folded back on top of itself, we lose the ability to trace out the beam on a pass per pass basis. In fact, we have two traveling waves each traveling in opposite directions interfering to form a standing wave inside of the cavity which has no apparent preference to direction. If we look at this standing wave at time scales larger than ℓ/c, or 0.2ns for a 7cm cavity, the standing wave appears to be uniform throughout the cavity and the amplitude of the standing-wave increases uniformly with time as more light is pumped into the cavity. This is true of any laser that is formed by a resonant cavity. In Sargent, Scully and Lamb's **Laser Physics** [1], we a have a traditional treatment of a two level laser system. We will extend this treatment to the Raman system.

The goal of the theory, that we are getting ready to derive, is to find time dependent expressions for the pump and Stokes fields. Because we are dealing with fields, it is natural to start with Maxwell's equations.

$$\nabla \cdot D = 0 \qquad \nabla \times E = -\frac{\partial B}{\partial t}$$

$$\nabla \cdot B = 0 \qquad \nabla \times H = J + \frac{\partial D}{\partial t} \qquad 3.1A.d$$

where $D = \varepsilon_o E + P$, $B = \mu_o H$, and $J = \sigma E$. To simply the boundary conditions we assume the presence of a lossy medium described by σ which incorporates the losses due to the H_2 by scattering and losses due to transmissions and absorptions in the mirrors. Now if we take the curl of the first equation we arrive at Maxwell's wave equation:

$$-\nabla^2 E + \mu_o \sigma \frac{\partial E}{\partial t} + \mu_o \varepsilon_o \frac{\partial^2 E}{\partial t^2} = -\mu_o \frac{\partial^2 P}{\partial t^2} \qquad 3.2$$

This is a common result that is seen everywhere in physics. This equation is true for both the pump and the Stokes fields. Let us start by examining the spatial dependence of our fields. We can separate the time and spatial dependence of equation 3.2 and arrive the at following second order differential equation.

$$\nabla^2 u(z) = -k^2 u(z) \qquad 3.3$$

Figure 3.1 is an illustration of the resonant cavity, so we can see our boundary conditions for equation 3.3.

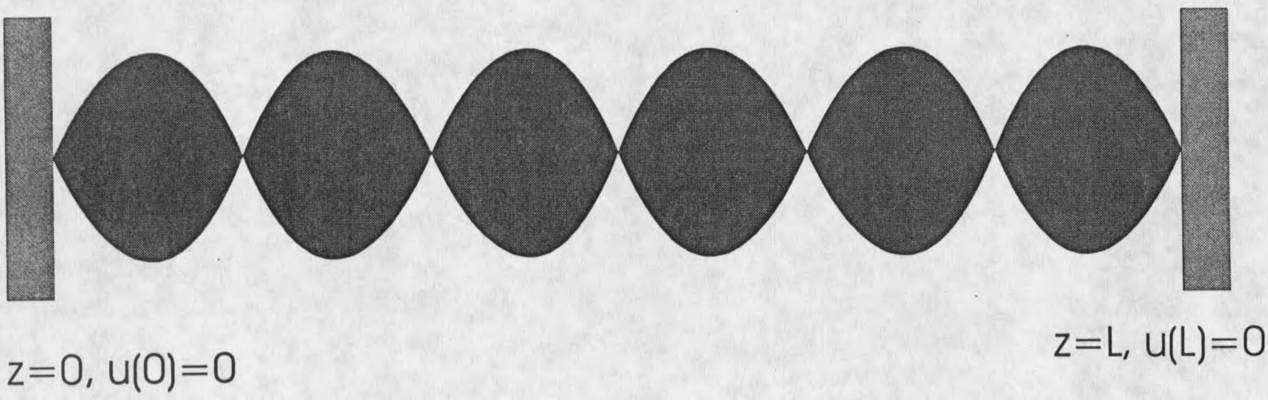

Figure 3.1 Shows the spatial dependency of a resonant cavity

When we apply these boundary conditions to equation 3.3 we arrive at the following solution:

$$u_n(z) = B_n \sin(k_n z) \qquad 3.4$$

where $k_n c = \Omega_n = \frac{n\pi c}{\ell}$. This results from separating our fields and our polarization into the following dependencies:

$$E(z,t) = \frac{1}{2}\sum_n A_n(t) u_n(z) + c.c. \qquad 3.5$$

where $A_n(t)$ is the complex electric field amplitude of mode n. We can further set

$$A_n(t) = E_n(t)\exp\{-i[\nu_n t + \phi_n(t)]\}, \qquad 3.6$$

where the amplitude coefficient $E_n(t)$ and the phase $\phi_n(t)$ vary little in an optical period, and $\nu_n + \dot{\phi}_n$ is the oscillation frequency of the mode. So the expansion of our field becomes

$$E(z,t) = \frac{1}{2}\sum_n E_n(t)\exp\{-i[\nu_n t + \phi_n]\} u_n(z) + .c.c \qquad 3.7$$

similarly we find that we can express our polarization as

$$P(z,t) = \frac{1}{2}\sum_n \mathcal{P}_n(t)\exp\{-i[\nu_n t + \phi_n]\} u_n(z) + c.c. \qquad 3.8$$

Now we take these expressions for the field and the polarization and plug them into equation 3.2, and use the fact that E_n, ϕ_n, and P_n vary little in an optical period to set the terms containing $\ddot{E}_n$, $\ddot{\phi}_n$, $\ddot{\mathcal{P}}_n$, $\sigma\dot{E}_n$, $\sigma\dot{\phi}_n$, $\dot{\phi}_n\mathcal{P}_n$, and $\dot{\mathcal{P}}_n$ equal to zero. This approximation leaves us with the following equation describing the pump and Stokes fields:

$$\Omega_n^2 E_n - i\left(\frac{\sigma}{\varepsilon_o}\right)\nu_n E_n - 2i\nu_n \dot{E}_n - \left(\nu_n + \dot{\phi}_n\right)^2 E_n = \frac{\nu_n^2}{\varepsilon_o}\mathcal{P}_n \qquad 3.9$$

where we have used $\Omega_n = k_n c$ and multiplied the equation by c^2. To make this equation more manageable let us assume that the cavity is resonant at both the pump and Stokes wavelengths, i.e. $\Omega_n = \nu_n + \dot{\phi}_n$, and that we only have one mode of the pump or Stokes to worry about. This leaves us with the following equation:

$$\dot{E}_a = -\frac{1}{2}\left(\frac{\sigma}{\varepsilon_o}\right)E_a - \frac{1}{2i}\left(\frac{\nu}{\varepsilon_o}\right)\mathscr{P}_a \qquad 3.10$$

where the subscript, a, will be used to denote either the pump (p) or the Stokes (s) field, the first term corresponds to a loss term due to the medium and the mirrors, and the last term correspond to a gain term. Now we need to find an expression for the polarization of the medium, P.

Polarization of the Medium and the Density Matrix

To find an expression for the polarization of the medium let us start with an energy level diagram. Figure 3.2 shows the energy levels involved vibrational Raman scattering in H_2 (to scale) with a 532nm laser used for the cw Raman laser. Note that the virtual level (dashed line) is associated with the first electronic level (labeled $|2\rangle$) so the cw Raman laser is far off the electronic resonance. The pump laser establishes a polarization of the medium between the ground state, $|1\rangle$, and the electronic state, $|2\rangle$, which in turn produces a Stokes field that establishes a polarization of the medium between the electronic state and the vibrational

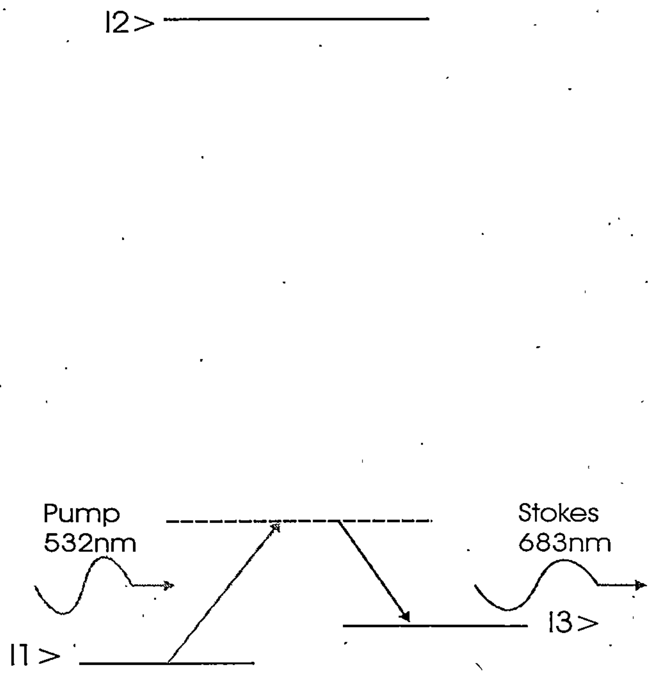

Figure 3.2 Energy level diagram of H_2, to scale

state, $|3\rangle$. The strength of the polarization depends on the level of interaction between the levels or the coherence between the states. We now need to arrive at an expression for the coherence between various states. This is easily done by introducing the density matrix.

We start with the Schrödinger picture of quantum mechanics, and define the wavefunction, $\Psi(x,t)$, which is a solution to Schrödinger's wave equation, $H\Psi = E\Psi$. Because of our geometry, i.e. the resonant cavity, we assume the spatial dependence goes like $u_n(z)$ of equation 3.4. So all that we are left to find is the time dependence of the wavefunction. We can expand the wavefunction in the following manner:

$$|\Psi(t)\rangle = \sum_n c_n(t)|n\rangle \qquad 3.11$$

where $c_n(t)$ are called Schrödinger probability amplitudes, and $|n\rangle$ are the eigenstates of the system. In the Schrödinger picture of quantum mechanics to evolve the wavefunction in time, we evolve these probability amplitudes, not the eigenstate as in the Heisenberg picture. The change in the wavefunction as a function of time arises when a time dependent perturbation, V(t), is applied to the system. This causes the probability amplitudes to change in the following manner:

$$\dot{c}_n(t) = -i\omega_n c_n(t) - \frac{i}{\hbar}\sum_k \langle n|V|k\rangle c_k - \frac{1}{2}\gamma_n c_n \qquad 3.12$$

where ω_n is the frequency of oscillation of the unperturbed wavefunction. The second term and takes into account the perturbation on the system, and the last term results from phenomenologically adding in decay of an excited state. Now we want to change these probability amplitudes into something more physical, i.e. a population in a given state or a coherence between states. So we define the density matrix:

$$\rho_{ab} = c_a c_b^* \qquad 3.13$$

When a=b, we have the population in the in the state a, and when $a \neq b$ we find out how the states a and b are correlated or the coherence between the states. So the density matrix evolves according to the following equation:

$$\dot{\rho}_{ab} = \dot{c}_a c_b^* + c_a \dot{c}_b^* \qquad 3.14$$

Now let us examine our system more closely. First of all let us define our potential

$$V(t) = -\frac{1}{2} \wp E(t) e^{-i\omega t} \qquad 3.15$$

where $\wp$ is the electronic dipole term, E(t) is due to either the pump or the Stokes field depending on the transition, and ω is the frequency associated with the field.. The parity of our potential is odd due to the electronic dipole term. Let us revisit our energy level diagram, figure 3.3.

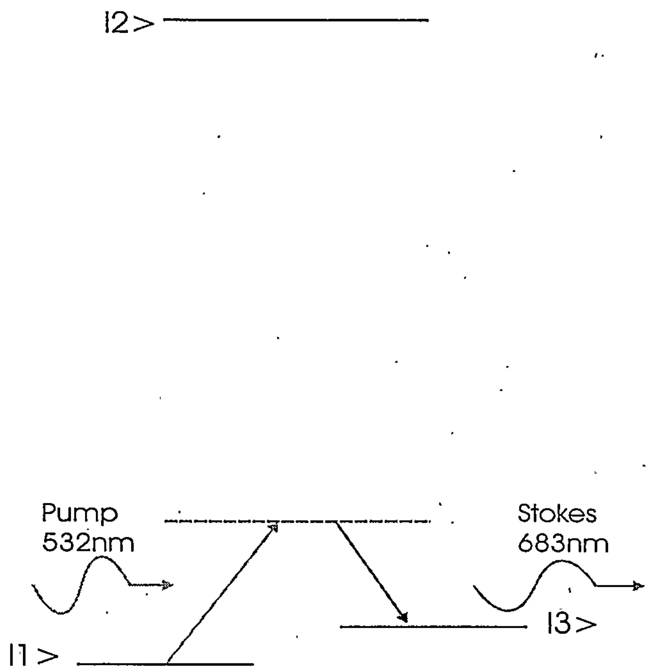

Figure 3.3 Shows the energy level diagrams of H_2 scale

Figure 3.3 illustrates the parity of the different states of the H_2 atom. We see that the states $|1\rangle$ and $|3\rangle$ are even while the state $|2\rangle$ is odd. The parity reduces the amount of work that we have to do when we evaluate the density matrix. This is because $\langle odd|odd|odd\rangle = 0$ and $\langle even|odd|even\rangle = 0$ while $\langle odd|odd|even\rangle = ?$ and $\langle even|odd|odd\rangle = ?$.

Now let us look at the sum contained in equation 3.12, $\sum_n \langle k|V|n\rangle = \sum_n V_{kn} = \sum_n V_{nk}^*$, and use the parity argument. We find that we are left with only two non-zero terms, V_{21} and V_{23}. When we evaluate these integrals, we find

$$V_{21} = -\frac{1}{2}\wp E_p(t)\exp[-i(\omega_p t+\phi)]u_p(z) + CRT \text{, and} \qquad 3.16$$

$$V_{23} = -\frac{1}{2}\wp E_s(t)\exp[-i(\omega_s t+\phi)]u_s(z) + CRT \qquad 3.17$$

where $\wp \approx \wp_{21} \approx \wp_{23}$, and CRT denotes the counter rotating term. The CRT can be neglected because it leads to a rapidly oscillating term. We now know our potentials, so we can begin to write the elements of our density matrix.

Now to make the density matrix equations more manageable and to emphasize the spatial and time dependencies, let us redefine some variables and constants. Let us start by redefining our density matrix to incorporate the pump and Stokes fields as $\sigma_{21} \equiv \rho_{21}e^{i\omega_p t}$, $\sigma_{31} \equiv \rho_{31}e^{i(\omega_p-\omega_s)t}$, $\sigma_{23} \equiv \rho_{23}e^{i\omega_s t}$, and $\sigma_{aa} \equiv \rho_{aa}$. Our pump and Stokes fields are represented by $\alpha \equiv -\frac{\wp}{2\hbar}E_p(t)e^{-i\phi}u_p(z)$, and $\beta \equiv -\frac{\wp}{2\hbar}E_s(t)e^{-i\phi}u_s(z)$ respectively. The decay of the populations and the coherence will be defined as $\gamma_{ab} \equiv \frac{1}{2}\left(\gamma_a + \gamma_b\right)$ [2], and the frequency difference will be defined as $\omega_{21} \equiv \omega_2 - \omega_1$, and the detuning from the excited state will be represented as $\Delta_p \equiv \omega_p - \omega_{21}$, and $\Delta_s \equiv \omega_s - \omega_{23}$ which are identical when the pump and Stokes energy difference is identical to the vibrational energy. Because we only have a three level system we have an additional constraint on or density matrix equations which is $\sigma_{11} + \sigma_{22} + \sigma_{33} = 1$, we define the population difference $D_{ab} = \sigma_{aa} - \sigma_{bb}$. With these definitions and constraints, we can write our density matrix equations [3]

$$\dot{D}_{21} = -b(1+D_{21}) - 4\,\mathrm{Im}(\alpha^*\sigma_{21}) - 2\,\mathrm{Im}(\beta^*\sigma_{23}) \qquad 3.18a$$

$$\dot{D}_{23} = -bD_{23} - 4\,\mathrm{Im}(\beta^*\sigma_{23}) - 2\,\mathrm{Im}(\alpha^*\sigma_{21}) \qquad 3.18b$$

$$\dot{\sigma}_{21} = -(1-i\delta_p)\sigma_{21} + i\alpha D_{21} - i\beta\sigma_{31} \qquad 3.18c$$

$$\dot{\sigma}_{23} = -(1-i\delta_s)\sigma_{23} + i\beta D_{23} - i\alpha\sigma_{31}^* \qquad 3.18d$$

$$\dot{\sigma}_{31} = -(1-i(\delta_p - \delta_s))\sigma_{31} - i\beta^*\sigma_{21} + i\alpha\sigma_{23}^* \qquad 3.18e$$

where the population decays are set equal, $\Gamma = \gamma_{22} = \gamma_{33}$, as well as the coherence decays, $\gamma = \gamma_{21} = \gamma_{23} = \gamma_{31}$. The equations are divided by the coherence decay leading to the following definitions: $b = \Gamma / \gamma$, and $\delta = \Delta / \gamma$. We have a set of expressions for our density matrix, so we can return to our field equation and write an expression for the polarization term.

We can write the slowly varying piece of the polarization as

$$\mathcal{P}_a(t) = 2\exp[i(\omega t + \phi)]\frac{1}{\mathcal{N}_a}\int_0^\ell dz u_a^*(z)(Tr(\wp\rho)) \qquad 3.19$$

where N is a normalization factor which is just

$$\mathcal{N}_a = \int_0^\ell dz u_a(z) u_a^*(z). \qquad 3.20$$

To help us evaluate the polarization let us think back to the infinitely deep square potential well of undergraduate Quantum Mechanics. The solution to Schrödinger's equation had the form

$$\psi_{well}(x) = \sum_n A_n \sin\left(\frac{n\pi}{\ell}x\right) = \sum_n \psi_n(x) \qquad 3.21$$

where ℓ is the length of the cavity. The importance of the solution is the orthogonality of the eigenstates of the wavefunction, or mathematically $\langle n | m \rangle = \delta_{nm}$. So if we examine our coherence terms of ρ, we see that ρ_{21} (ρ_{23}) has the same spatial dependence as the pump (Stokes) fields. As a result, only one term survives the spatial integration for either the pump or the Stokes polarization term, $\mathcal{P}$. This leaves

$$\mathcal{P}_p(t) = 2x_{12}e\rho_{21}\exp(i(\omega_p t + \phi)) = 2x_{12}e\sigma_{21}\exp(i\phi), \text{ and} \qquad 3.22a$$

$$\mathcal{P}_s(t) = 2x_{32}e\rho_{23}\exp(i(\omega_s t + \phi)) = 2x_{32}e\sigma_{23}\exp(i\phi) \qquad 3.22a$$

for the complex polarization induced by the pump and Stokes fields. When we take these results and plug them into equation 3.10 with the appropriate change of variables, i.e. α, and β, we arrive at the following 7 equations which describe the Raman process [3]:

$$\dot{\alpha} = -\frac{1}{2}\left(\frac{\sigma_p}{\varepsilon_o}\right)\alpha + \frac{i\omega_p}{\varepsilon_o} ex_{12}\sigma_{21} + K(t) \qquad 3.23a$$

$$\dot{\beta} = -\frac{1}{2}\left(\frac{\sigma_s}{\varepsilon_o}\right)\beta + \frac{i\omega_s}{\varepsilon_o} ex_{32}\sigma_{23} \qquad 3.23b$$

$$\dot{D}_{21} = -b(1+D_{21}) - 4\,\mathrm{Im}(\alpha^*\sigma_{21}) - 2\,\mathrm{Im}(\beta^*\sigma_{23}) \qquad 3.23c$$

$$\dot{D}_{23} = -bD_{23} - 4\,\mathrm{Im}(\beta^*\sigma_{23}) - 2\,\mathrm{Im}(\alpha^*\sigma_{21}) \qquad 3.23d$$

$$\dot{\sigma}_{21} = -(1-i\delta_p)\sigma_{21} + i\alpha D_{21} - i\beta\sigma_{31} \qquad 3.23e$$

$$\dot{\sigma}_{23} = -(1-i\delta_s)\sigma_{23} + i\beta D_{23} - i\alpha\sigma_{31}^* \qquad 3.23f$$

$$\dot{\sigma}_{31} = -(1-i(\delta_p-\delta_s))\sigma_{31} - i\beta^*\sigma_{21} + i\alpha\sigma_{23}^* \qquad 3.23g$$

where K(t) of equation 3.23a accounts for the optical pumping of the HFC. These seven non-linear coupled differential equations describe the cw Raman laser. Thankfully we do not have to solve these equations in the present state. We are about to unleash a flurry of approximations for our system. However, we will go one approximation at a time, this will take more time and paper but it will provide the reader with a host of equations that can be used to describe the cw Raman laser if one of the approximations or constraints is relaxed.

<u>Far Off Electronic Resonance</u>

The first approximation that will be made is the pump laser is far off resonance, $\omega_{21} >> \omega_p$. This simple assumption has many repercussions. The energy needed to reach the excited is 84,800cm^{-1} which exceeds the thermal energy by several orders of magnitude, as a result the population in the excited state is assumed to be zero, $\sigma_{22}=0$ and $\dot{\sigma}_{22}=0$. Similarly the coherence associated with this excited state, σ_{23} and σ_{21}, do not vary with time, i.e. $\dot{\sigma}_{23}=\dot{\sigma}_{21}=0$ [4-7]. Equations 3.23e and 3.23f give rise to the following steady state values for the coherences

$$\sigma_{21}=\frac{1}{1-i\delta_p}\left(i\alpha D_{21}-i\beta\sigma_{31}^{*}\right) \tag{3.24a}$$

$$\sigma_{23}=\frac{1}{1-i\delta_s}\left(i\beta D_{23}-i\alpha\sigma_{31}^{*}\right). \tag{3.24b}$$

Now we can use the fact that the population in the excited state is zero, $\sigma_{22}=0$, to express D_{21} and D_{23} in terms of D_{13}. This results in the following expressions:

$$D_{21}=\frac{-\left(D_{13}+1\right)}{2} \tag{3.25a}$$

$$D_{23}=\frac{D_{13}-1}{2}. \tag{3.25b}$$

The fact that the process is assumed to be resonant with the vibrational state, i.e. $\delta_p \approx \delta_s \equiv \delta >> 1$, and using equations 3.24a – 3.25b, our seven coupled differential equations reduce to the following four equations[4]:

$$\dot{\alpha}=-\frac{1}{2}\left(\frac{\sigma_p}{\varepsilon_0}\right)\alpha+\frac{i\omega_p}{2\omega_s}g(D_{13}+1)\alpha+\frac{i\omega_p}{\omega_s}g\beta\sigma_{31}+K(t) \tag{3.26a}$$

$$\dot{\beta}=-\frac{1}{2}\left(\frac{\sigma_s}{\varepsilon_0}\right)\beta+\frac{ig}{2}(1-D_{13})\beta+ig\alpha\sigma_{31}^{*} \tag{3.26b}$$

$$\dot{\sigma}_{31}=-\sigma_{31}+\frac{i}{\delta}\sigma_{31}(|\alpha|^2-|\beta|^2)-\frac{i}{\delta}\alpha\beta^{*}D_{13} \tag{3.26c}$$

$$\dot{D}_{13}=b(1-D_{13})+\frac{2i}{\delta}\left(\alpha^{*}\beta\sigma_{31}-\alpha\beta^{*}\sigma_{31}^{*}\right) \tag{3.26d}$$

where $g = \frac{\omega_s e x_{32}}{\varepsilon_o} = \frac{\omega_p e x_{12}}{\varepsilon_o}$. These equations are valid for any non-resonant cw Raman laser.

High Pressure and an Established Coherence Limits

The next approximation that will be made answers the following questions. What happens when the number of atoms inside the cavity increases? How is the population difference equation, 3.26d, dependent on pressure. When do we have to worry about ground state depletion? To answer these questions let us perform a back of the envelope calculation to calculate the number of atoms available for the Raman process.

In 10 atm. of H_2 we have approximately $2.7\text{x}10^{20}$ molecules/cc. Now we need to calculate an interaction volume. A typical Raman cell has 1m radius of curvature mirrors spaced by 7cm which gives an interaction volume through one focus of approximately $7\text{x}10^{-3}$ cm^3, so the number of atoms available is about $1.9\text{x}10^{18}$ atoms. If all of the atoms were converted into Stokes photons, we would have 13kW of Stokes with the lifetime of the vibrational state being 40μs. This exceeds the 10mW power expected to radiate from the cavity by ~3 orders of magnitude, so it is a safe assumption that the ground-state is not depleted. So $\dot{D}_{13}$ is set to zero and D_{13} is set to 1, i.e. all of the atoms are in the ground-state. As a result we are reduced to the following three equations:

$$\dot{\alpha} = -\frac{1}{2}\left(\frac{\sigma_p}{\varepsilon_o}\right)\alpha + \frac{i\omega_p}{\omega_s} g\alpha + \frac{i\omega_p}{\omega_s} g\beta\sigma_{31} + K(t) \qquad 3.27a$$

$$\dot{\beta} = -\frac{1}{2}\left(\frac{\sigma_s}{\varepsilon_o}\right)\beta + ig\alpha\sigma_{31}^* \qquad 3.27b$$

$$\dot{\sigma}_{31} = -\sigma_{31} + \frac{i}{\delta}\sigma_{31}\left(|\alpha|^2 - |\beta|^2\right) - \frac{i}{\delta}\alpha\beta^* \qquad 3.27c$$

We have two field equations and a coherence equation which describe the cw Raman laser in the high-pressure, non-resonant regime.

Let us take a look at the coherence equation. In pulsed Raman scattering this equation plays an important role because the powers are high (100's of killiwatts) and the pulses are short (10's of nanoseconds), resulting in the conversion process and the establishing of a coherence on similar time scales. However, the HFC has buildup times of about 1-10μs which is about 3 orders of magnitude slower than the pulsed system so the coherence is well established in the cw Raman regime. So equation 3.27c is set to zero, and we are on resonance with the vibrational state we have $|\alpha|^2 - |\beta|^2 << \delta$, this leaves the following two equations:

$$\dot{\alpha} = -\frac{1}{2}\left(\frac{\sigma_p}{\varepsilon_0}\right)\alpha + \frac{i\omega_p}{\omega_s} g\alpha - \frac{\omega_p}{\omega_s \delta} g|\beta|^2 \alpha + K(t) \qquad 3.28a$$

$$\dot{\beta} = -\frac{1}{2}\left(\frac{\sigma_s}{\varepsilon_0}\right)\beta + \frac{1}{\delta} g|\alpha|^2 \beta. \qquad 3.28b$$

These equations describe the cw Raman laser in the high-pressure and an established coherence limit. Recall, to make the density matrix more manageable we transformed our fields to stress certain (time and spatial) dependencies. However, now our equations are simple so we can transform our field equations into something familiar:

$$\dot{E}_p = -L_p E_p - \frac{\omega_p}{\omega_s} G|E_s|^2 E_p + k(t) \qquad 3.29a$$

$$\dot{E}_s = -L_s E_s + G|E_p|^2 E_s \qquad 3.29b$$

where the second term of equation 3.28a is dropped because we are not concerned with phase effects. The constants were transformed according to $L_a = \frac{1}{2}\left(\frac{\sigma_a}{\varepsilon_0}\right)$, $G = \left(\frac{\wp}{2\hbar}\right)^2 \frac{g}{\delta}$, and

$k(t) = \left(\frac{2\hbar}{\wp}\right)K(t)$. These are the equations that will be used throughout the thesis. In chapter 4 we will determine the constants of the equations and examine the steady-state limit of these equations. In chapter 5, we will study noise on the cw Raman laser and we will use a linearized version of these equations that we will perturb to predict relaxation oscillations and amplitude noise.

REFERENCES CHAPTER 3

[1] M. Sargent, M. O. Scully, and W. E. Lamb, *Laser Physics* (Addison-Wesley), Reading Mass. (1974) page 96.

[2] This seems to imply that the coherence and population decays are related, which is not generally the case. In order to account for decay, we placed in a decay term in equation 3.12 which leads to the relation $\gamma_{ab} \equiv \frac{1}{2}(\gamma_a + \gamma_b)$. In practice we use the experimentally determined decay constants.

[3] J. V. Moline, J. S. Upped, and R. G. Harrison, Phys. Rev. Lett. **59**, 2868 (1987).

[4] R. G. Harrison, Weiping Lu, and P. K. Gupta, Phys. Rev. Lett. **63**, 1372 (1989).

[5] M. G. Raymer, J. Mostowski, and J.L. Carlsten, Phys. Rev. A. **19** 2304 (1979).

[6] D. Grischkowsky, M. M. T. Loy, and P. F. Liao, Phys. Rev. A **12** 2514 (1975).

[7] M. Takatsuji, Phys. Rev. A, **11** 619 (1975).

CHAPTER 4

STEADY-STATE CW RAMAN SCATTERING

Determination of Constants

In chapter 3, we derived the cw Raman laser equations for a non-resonant system in the high pressure limit. However, we did not calculate the values for the various constants. Let us start by reviewing the results of the last chapter. The cw Raman laser equations are

$$\dot{E}_p = -L_p E_p - \frac{\omega_p}{\omega_s} G \left| E_s \right|^2 E_p + k(t) \tag{4.1a}$$

$$\dot{E}_s = -L_s E_s + G \left| E_p \right|^2 E_s \tag{4.1b}$$

E_p (E_s) is the pump (Stokes) field, and ω_p (ω_s) is the pump (Stokes) frequency. The losses due to the mirrors at the pump (Stokes) frequency are given by L_p (L_s). The gain of the Raman system is given by G, and the cavity is optically pumped by $k(\omega,t)$. Each of these constants can be found by setting the appropriate constant or constants equal to zero. The gain (G) is found by setting L_s equal to zero in equation 4.1b. This yields the following differential equation:

$$\dot{E}_s = G \left| E_p \right|^2 E_s . \tag{4.2}$$

Assuming that E_p varies little in a single pass transit time of the cavity, we have the following solution:

$$E_s = E_{s0} \exp\left(G \left| E_p \right|^2 t \right). \tag{4.3}$$

Comparing this result to equation 5 of reference 1 while making the appropriate scaling for optical power and setting $t = \ell / c$, we arrive at the following expression for the gain

$$G = \frac{1}{2}\left(\frac{1}{4}\alpha \cdot c\sqrt{\frac{\varepsilon_0}{\mu_0}}\right) \qquad 4.4$$

where α is the plane-wave gain coefficient and c is the speed of light. Because we are using a two mirrored cavity as our resonator, we have a standing wave instead of a traveling wave, which accounts for the extra factor of one half. By setting G and k(t) equal to zero in equations 4.1a and 4.1b, we arrive at the following expression for the fields containing L_p and L_s

$$E_{p(s)} = E_0 \exp(-L_{p(s)}t). \qquad 4.5$$

Using the transit time, $t = \ell / c$, and the field left after one reflection, $\sqrt{R}E$, we arrive at the following expression for the losses:

$$L_{p(s)} = -\frac{c}{2\ell}\ln R_{p(s)} \qquad 4.6$$

where ℓ is the length of the cavity and $R_{p(s)}$ is the reflectivity of the mirrors at the pump (Stokes) wavelength. To determine the optically pumping constant, k(t), we calculate the field that enters the cavity per transit time of the cavity. This yields:

$$k(t) = \frac{c}{\ell}\sqrt{T_p}E_{p_{in}} \qquad 4.7$$

where T_p is the transmission of the mirrors at the pump wavelength and E_{pin} is the pump -field incident on the cavity. To check this result, we set the gain, G, equal to zero in equation 4.1a. This gives the following inhomogeneous differential equation:

$$\dot{E}_p = -L_p E_p + k(t) \qquad 4.8$$

which has the solution

$$E_p(t) = \frac{k}{L_p}\left(1 - exp(-L_p t)\right) \tag{4.9}$$

when we apply the boundary condition $E_p(O) = O$. If we take the limit of equation 4.9 as $t \to \infty$, we find that the field approaches the discrete sum limit of $\frac{\sqrt{T_p}E_{pin}}{1-\sqrt{R_p}}$ with the approximation that $\ln(\sqrt{R}) = \sqrt{R} - 1$ [2].

How the Cw Raman Laser Starts Up

We have expressions for each of the constants in equations 4.1a and 4.1b. Now we need to see how the cw Raman laser starts up. Equations 4.1a and 4.1b are the field equations describing what happens inside the Raman cavity, so we need to calculate the power exiting the cavity.

To calculate the fields produced outside of the cavity let us briefly think about the field inside of the cavity. There is a standing wave that is formed by two traveling waves, mathematically:

$$E_{inside} = E\,exp(i(kx - \omega t) + E\,exp(i(-kx + \omega t) = 2E\cos(kx)\cos(\omega t)$$

So we have only one half of the peak field incident on a mirror at a given time so we multiply the internal field by $\frac{1}{2}\sqrt{T}$ for each mirror where T is the transmission of the mirror. So the four fields produced outside the cavity are

$$E_{p_{ffront}} = -\sqrt{R_p}E_{p_{in}} + \frac{1}{2}\sqrt{T_p}E_p \tag{4.10a}$$

$$E_{p_{back}} = \frac{1}{2}\sqrt{T_p}E_p \tag{4.10b}$$

$$E_{s_{front}} = \frac{1}{2}\sqrt{T_s}E_s \tag{4.10c}$$

$$E_{s_{back}} = \frac{1}{2}\sqrt{T_s}E_s \tag{4.10d}$$

To calculate the optical power we use the complex Poynting vector $S = \frac{1}{2}E \times H^*$, where the optical intensity is the magnitude of S, and the optical intensity is the power per area. So we arrive at the following expression for the optical power [3]:

$$P = \frac{1}{2}\sqrt{\frac{\varepsilon_O}{\mu_O}}|E|^2 A \tag{4.11}$$

where A is a scaled area of the beam to account for the transverse structure of the beam and the overlap of the pump and Stokes modes. For the optical power contained in the cavity we average the area through a focus and include a mode filling parameter. The end result is the following scaled area [1]:

$$A = \frac{\ell\left(\lambda_p + \lambda_s\right)}{4\tan^{-1}\left(\frac{\ell}{b}\right)} \tag{4.12}$$

where $\lambda_{p(s)}$ is the pump (Stokes) wavelength and b is the confocal parameter of the beam. We now know how to convert the results into something we would measure in an experiment so we can begin to solve equations 4.1a and 4.1b.

Using the mirror characteristics given by the quote of the mirror manufacture (R=0.9998, A=20ppm), the threshold predictions from chapter II, the plane-wave gain coefficient α=2.5*10^{-9} cm/W [4], and the length of the cavity $\ell = 7.3cm$, we can model the cw Raman laser by integrating equations 4.1a

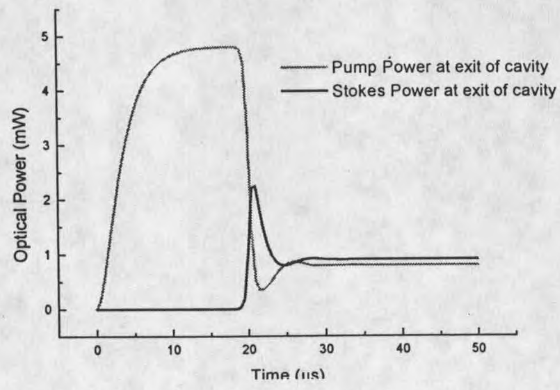

Figure 4.1 Shows how the cw Raman laser starts.

and 4.1b in a Math-Cad program seen in appendix H. Figure 4.1 shows the output pump and Stokes powers at the exit of the cavity for an input power of six times threshold. We see that the power exiting the cavity increases until a Stokes field is produced. Notice that the cw Raman laser actually overshoots the steady-state output, and we have a couple of relaxation oscillations that were mentioned in chapter II. These oscillations will be explained in chapter 5.

One might ask: how well does the process work, or what is the conversion efficiency of the process? To answer this question we need to define what we mean by conversion efficiency. Because the photon produced by the Raman process has less energy than the input photon, a pure power conversion efficiency may be misleading to the performance of the cw Raman laser. A more insightful measurement would be the photon conversion efficiency, this will tell us what percent of the pump photons are converted to Stokes photons. The photon conversion efficiency can be calculated by using the following equation:

$$\% = \frac{\lambda_s}{\lambda_p}\frac{P_s}{P_p} \times 100\% \qquad 4.13$$

where P_s is the total Stokes power radiated from the cavity, P_p is the pump power at the front of the cavity, and λ_s/λ_p is a factor that takes into account the difference in energies of the pump and Stokes photons. Figure 4.2 shows the predicted photon conversion efficiency as a function of time [5]. We can see that when the Stokes field is initially generated the photon conversion efficiency approaches 100%, but it then drops to the steady-state value of ~40%.

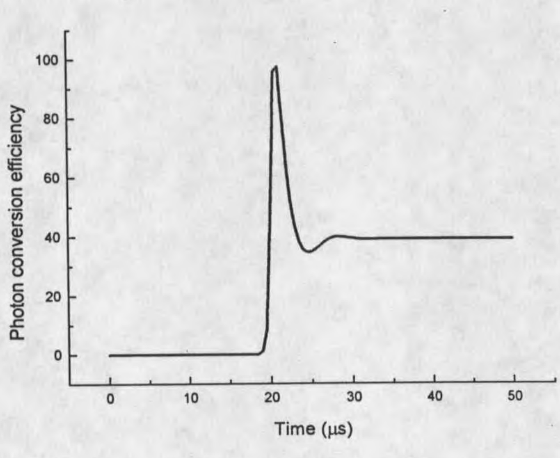

Figure 4.2 Shows the conversion efficiency as a function of time.

So the question becomes: why does the conversion efficiency drop to about 40%, and what is the upper limit to the steady-state photon conversion efficiency? Clearly the conversion efficiency is dependant on the input pump power, however, the amount of the pump power that is coupled into the optical cavity is dependant on the interference of the pump field inside of the cavity, which changes when the pump is converted into Stokes. To see this effect we can look at the pump power at the front of the cavity as a function of time. Figure 4.3 shows the percent of the pump power coupled into the cavity as a function of time. Notice before the pump is converted into Stokes, the coupling efficiency approaches 100%; however, when the pump is converted to Stokes, the coupling efficiency drops to about 40% until is reaches the steady-state value of 60%. Figure 4.3 is very helpful when we think about the maximum conversion efficiency that we would expect in the steady-state limit [5]. When a pump photon is converted into a Stokes photon, one less pump photon is left to interfere with the pump beam incident on the cavity, so the amount of pump that is coupled into the cavity decreases. The maximum photon conversion efficiency one would expect is 50%. Given two photons one is converted and one is used in the interference. We now know how the process starts and we are starting to understand the subtleties of the cw Raman laser.

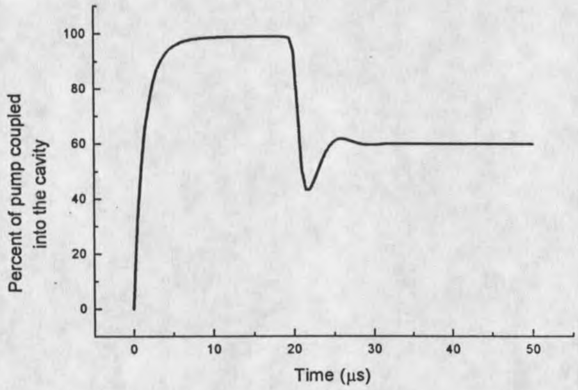

Figure 4.3 Shows the pump coupling efficiency as a function of time

Steady-State Limit

In the steady state, equations 4.1a and 4.1b are set to zero, and we solve for the pump and Stokes fields. This results in the following expressions for the pump and Stokes fields,

$$E_p = \sqrt{\frac{L_s}{G}} \qquad 4.14a$$

$$E_s = \sqrt{\frac{\omega_s\left(k - L_p E_p\right)}{\omega_p G E_p}}. \qquad 4.14b$$

From equation 4.14a, we see that in the steady-state limit, the pump field inside the cavity is constant regardless of the pumping rate after threshold is reached. Thus we expect that the Raman process will reduce the amplitude noise of the pump laser which we will examine in chapter V.. At threshold the Stokes field becomes nonzero; this happens when $k = L_p E_p$ from equation 4.14b. To write the threshold in terms of the pump field incident on the cavity we use equations 4.7 and 4.14a and arrive at the following threshold condition:

$$E_{p_{thres}} = \frac{\ell L_p}{c}\sqrt{\frac{L_s}{T_p G}}. \qquad 4.15$$

where $E_{p_{thres}}$ is the incident pump field required for threshold. Once again equations 4.14a and 4.14b are the pump and Stokes fields inside the cavity. Using the method to arrive at equations 4.10a - 4.10d, we find the following expressions for the steady-state value of the fields exiting the cavity:

$$E_{pss_{front}} = -\sqrt{R_p}E_{p_{in}} + \frac{1}{2}\sqrt{T_p \frac{L_s}{G}} \qquad 4.16a$$

$$E_{pss_{back}} = \frac{1}{2}\sqrt{T_p \frac{L_s}{G}} \qquad 4.16b$$

$$E_{sss_{front}} = \frac{1}{2}\sqrt{T_s}\sqrt{\frac{\omega_s\left(k - L_p E_p\right)}{\omega_p G E_p}} \qquad 4.16c$$

$$E_{sss_{back}} = \frac{1}{2}\sqrt{T_s}\sqrt{\frac{\omega_s\left(k - L_p E_p\right)}{\omega_p G E_p}}. \qquad 4.16d$$

As before we can convert these fields into optical power according to equations 4.11 and 4.12.

One question that we now can answer is: What is the photon conversion efficiency, in the steady-state, as a function of pump power? We use equations 4.7 and 4.13 through 4.16d to arrive at the following expression for the photon conversion efficiency:

$$\% = \frac{1}{2} T_s \left(\frac{\lambda_s}{\lambda_p}\right)\left(\frac{\left|E_s\right|^2}{\left|E_{p_{in}}\right|^2}\right) \qquad 4.17$$

If we take the derivative of equation 4.17 with respect to $E_{p_{in}}$ and use equation 4.14b and set the result equal to zero we arrive at the following expression for pump field for the maximum conversion efficiency:

$$E_{max} = 2\left(\frac{\ell L_p}{c}\sqrt{\frac{L_s}{T_p G}}\right) = 2E_{p_{thres}}. \qquad 4.18$$

So we have a maximum in the photon conversion efficiency at four times the threshold, in power, of the cw Raman laser. Figure 4.4 is a plot of equation 4.17 for the quoted mirror reflectivities [5]. We see that the maximum does indeed occur at four times threshold, but we see that the photon conversion efficiency drops off at higher pump powers. If we recall that the pump field inside of the cavity stays constant regardless of the pump power at the

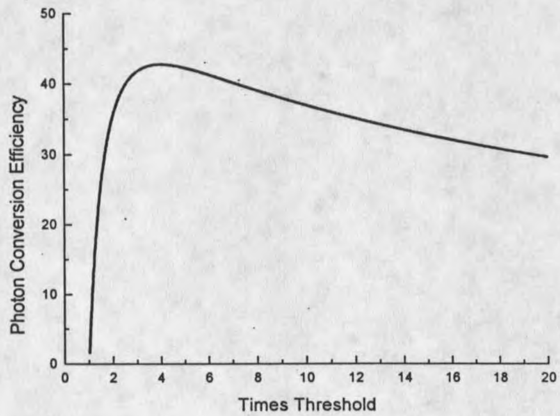

Figure 4.4 Shows conversion efficiency as a function of pump power.

front of the cavity, it makes sense that the efficiency falls off at higher pump powers. The reason for this is: the harder we try to pump the laser the less efficient we are at coupling the light into the cavity, because there is only a fixed amount of light in the cavity to interfere with the reflected pump at the entrance of the cavity which is required for efficient coupling. We now have an idea of how the cw Raman laser should work, now let us compare the theory to some experimental results.

Experimental Verification of Theory

Let us start by examining the experimental data of chapter 2. So we can refresh our memory, let us review the experimental apparatus of the first-version of the cw Raman laser as

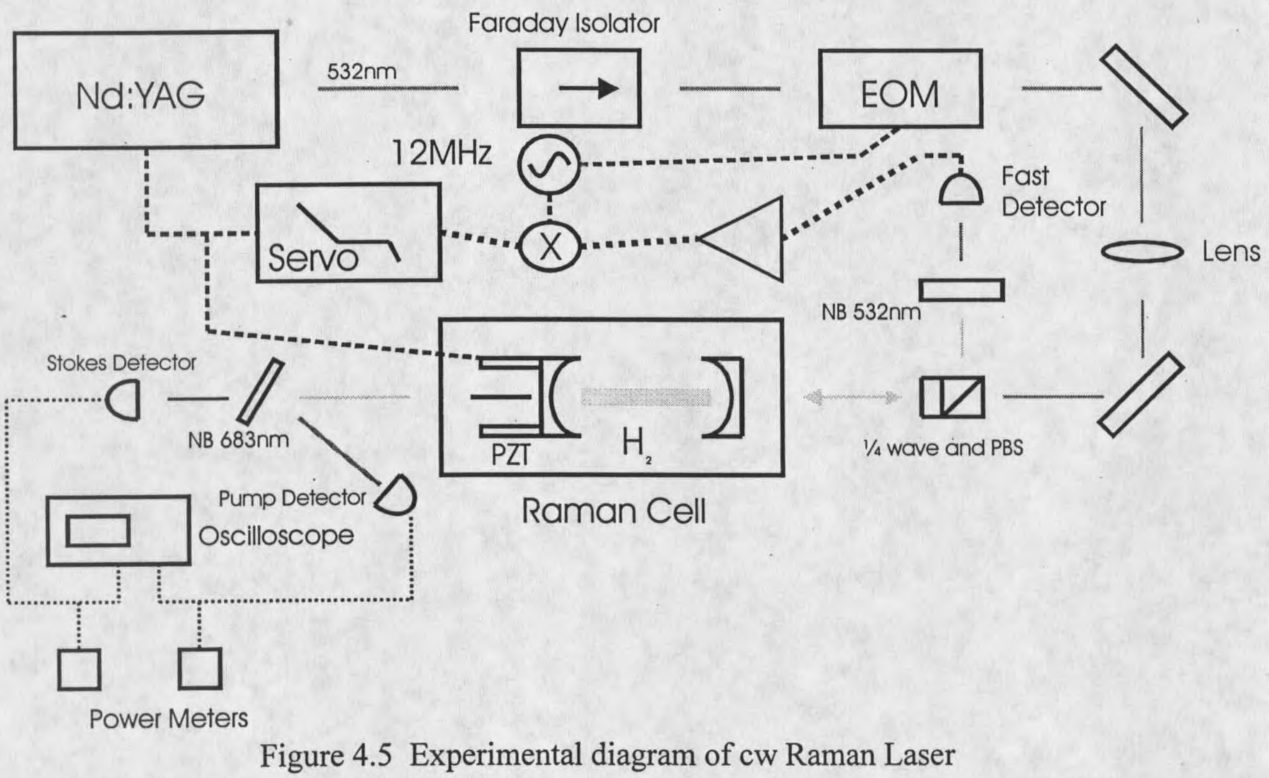

Figure 4.5 Experimental diagram of cw Raman Laser

seen in figure 4.5. The output of this Nd:YAG laser at 532nm was sent through a Faraday isolator to minimize the optical feedback to the Nd:YAG laser. An electro-optic modulator (EOM) was used to place sidebands on the carrier frequency required for locking the pump laser to the optical cavity. The pump laser beam traveled through a two-element lens pair used to mode match the pump beam to the cavity. A polarizing beam splitter (PBS) cube in conjunction with a quarter-wave plate allowed for monitoring of the beam reflected from the cavity. A fast detector (>12MHz) was then used to measure the error signal. A low noise amplifier gave the signal 30dB of amplification in power before the signal was mixed to dc. The error signal entered the servo, and the slow corrections were sent to temperature tune the pump laser, while the fast corrections were sent to the pump laser piezoelectric transducer (PZT). The entire apparatus was placed on a floating platform to minimize the effects of vibrations.

Figure 4.6a shows the theoretical fit of output power of the cw Raman laser versus the pump power, while figure 4.6b shows the theoretical fit of the conversion efficiency of the cw Raman Laser. The theory was fit with the following experimental parameters: mirror reflectivity (transmission) was 0.99984 (112ppm) [6] for both the pump and Stokes wavelengths. Notice the

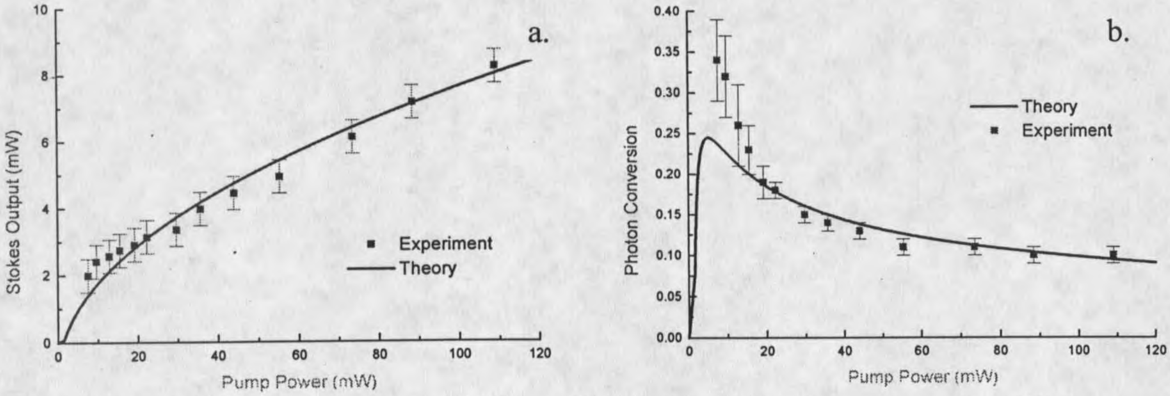

Figure 4.6 Shows the output of the cw Raman laser: (a) shows the output Stokes power as a function of pump power (theory overlaid) (b) show the photon number conversion efficiency as a function of pump power (theory overlaid)

theoretical fits are good at the higher pump powers, but do not match well for the lower pump powers. Recall, from chapter 2, that relaxation oscillations are present and more predominant at lower pump powers.

The apparatus used in the previous experiment did not have the dynamic range in pump power required to accurately study the region near the threshold of the cw Raman laser, so the experimental apparatus was changed to allow for accurate, near threshold measurements. Figure 4.7 shows the experimental setup used to measure the threshold of the cw Raman laser.

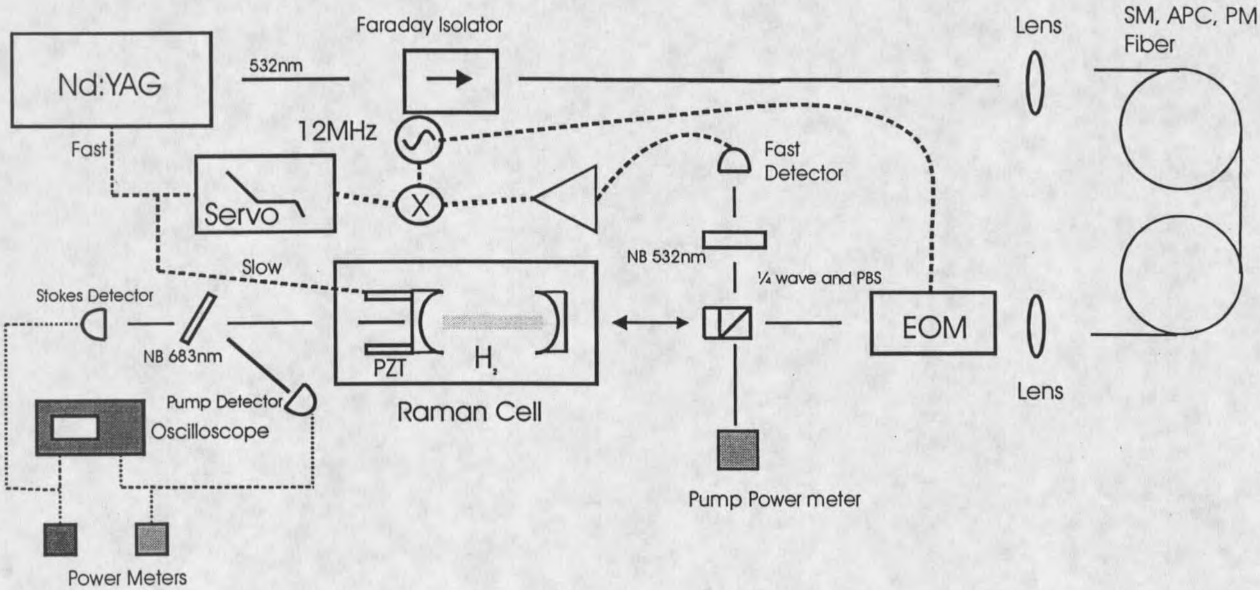

Figure-4.7 Shows the experimental diagram of the cw Raman laser used to make the threshold measurements.

The system is again optically pumped by a frequency-doubled Nd:YAG laser with output powers up to 200mW. The output of this Nd:YAG laser at 532nm was sent though a Faraday isolator to minimize the feedback to the Nd:YAG laser. The optical beam is then launched into a single mode (SM) , angle physical contact (APC), polarization maintaining (PM) optical fiber to provide a variable input power without beam steering. An electro-optic modulator (EOM) was used to place sidebands on the carrier frequency required for locking the pump beam. A polarizing beam splitter (PBS) allowed for monitoring of the beam reflected from the cavity. A fast detector was then used to measure the error signal. A low noise amplifier gave the signal 30db of amplification before the signal was mixed to dc. The error signal entered the servo and slow corrections were sent to the piezoelectric transducer (PZT) on the optical cavity while the fast corrections were sent to pump laser[7].

The finesse of the cavity was measured to be 17,000 ±2000, and the ratio of the input to the output of the cavity was measured to be 0.78 ±0.08. The length of the optical cavity is 7.0 ±0.4cm. The radius of curvature for the mirrors is 1m. The plane wave gain coefficient, α, is $2.5*10^{-9}$ cm/W [4]. The pump (Stokes) wavelength is 532nm (683nm). The experiment was performed in 10atm. of H_2 giving a Raman linewidth of 510MHz [4]. The data was fit with the following parameters: $R_{p(s)} = 0.9998$, $T_{p(s)} = 170$ppm, $A_{p(s)} = 30$ppm, and the gain was scaled by a factor of 2/3. The mirror characteristics are within error bars, and scaling the gain by a factor of 2/3 would correspond to a detuning of 200MHz from the Raman resonance. Figure 4.8a

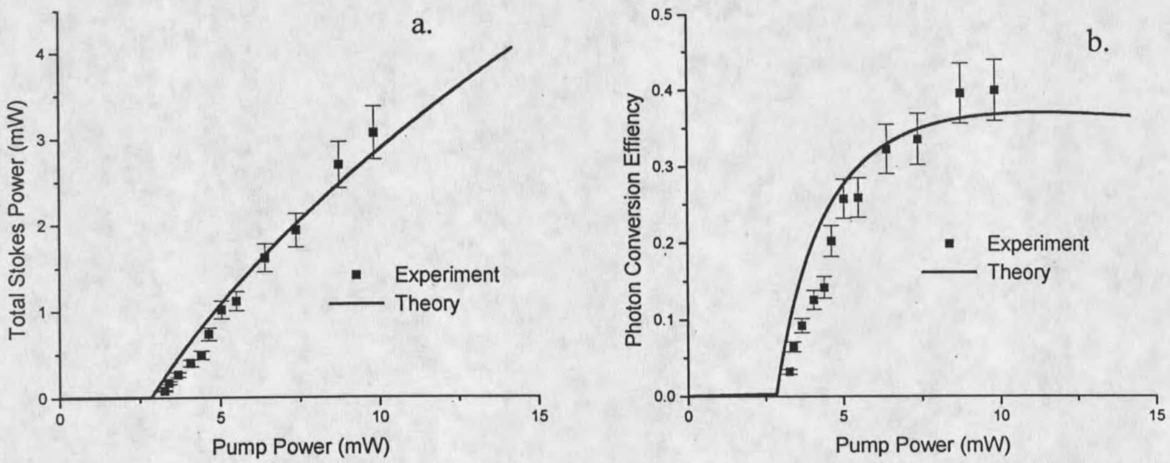

Figure 4.8 Shows the output of the cw Raman laser near threshold: (a) shows the output Stokes power vs. pump power (theory overlaid) (b) shows the photon number conversion efficiency vs. pump power (theory overlaid)

shows the theoretical fit of the output power of the cw Raman laser near threshold, while figure 4.8b shows the theoretical fit of the conversion efficiency near threshold. The maximum output power and conversion efficiency of the cw Raman laser was seen to be at 9.8 mW of pump power producing 3.1mW of Stokes power with a photon conversion efficiency of 40%. Data above 10mW of pump power was not included since at this power the lock was less stable due to relaxation oscillations. The data can be taken at these higher pump rates, however the output of the Raman laser is highly dependent on the servo gain.

Remarks

In this chapter we developed a state-state theory which describes the cw Raman laser very well. However, the relaxation oscillations were present in both experiments, and presented problems in taking data in the region of 3-5 times the threshold of the laser. Remember that the maximum conversion efficiency happens at four times threshold, so locking problems in the 3-5 times threshold region is not surprising. The percent change in the output powers of the Stokes and pump beam is the largest in this region, which presents problems in locking. Once again we appear to have an insurmountable task at hand in these relaxation oscillations, which provides the motivation for the next chapter that mathematically describes these relaxation oscillations, and amplitude noise on the Raman laser.

REFERENCES CHAPTER 4

[1] D. C. MacPherson, R. C. Swanson, and J. L. Carlsten, IEEE J. Quantum Electron. **24**, 2076 (1989).

[2] The intensity buildup inside a high-finesse cavity can found from the standard electric field summation used in standard optics texts. See, for example, E. Hecht and A Zajac, *Optics* (Addison-Wesley, Reading, Mass., 1979), page 305.

[3] B. E. A. Saleh, and M. C. Teich, *Fundamentals of Photonics*, (Addison-Wesley, Reading, Mass., 1991) page 168.

[4] W.K. Bischel and M. J. Dyer, J. Opt. Soc. Am. B **3**, 677 (1986).

[5] The theory uses the following parameters: Using the mirror characteristics given by the quote of the mirror manufacture (R=0.9998, A=20ppm), the plane-wave gain coefficient α=2.5*10^{-9} cm/W [2], and the length of the cavity , $\ell = 7.3cm$. The Math-Cad program can be seen in appendix H.

[6] The mirror characteristics were varied within the experimental error of the measurement of the finesse and the throughput of the cavity to fit the theory.

[7] To insure an overlap of the Stokes cavity resonance with the pump cavity resonance either the cavity or the laser needs to be tuned ~20 GHz. Unfortunately the laser used in this experiment is capable of tuning only 10GHz. Thus a piezo was placed inside the Raman cell to tune the mirror spacing. With a constant voltage applied to the piezo, the cavity spacing drifted as a result of piezo creep. However, the piezo creep was offset by

sending slow corrections to cavity piezo (<10Hz) while sending the fast corrections to the laser (>10Hz).

CHAPTER 5

RELAXATION OSCILLATIONS AND NOISE

Motivation for a Linearized Theory

In chapters 2 and 4 for certain pump rates we saw relaxation oscillations. Normally, these oscillations would not be a problem, because we can operate our cw Raman laser at pump rates where strong relaxation oscillations are not present. However, if we are concerned about the efficiency of the cw Raman laser, the optimal region to run the laser is at four times threshold, where the maximum photon conversion efficiency occurs. Unfortunately this is where the relaxation oscillations are the strongest. So one begins to wonder if there is any hope to remove these relaxation oscillations, or are they here to stay. One optimistic point is that for this region of instability (3-5 times threshold) the strength of the relaxation oscillations was highly dependant on the servo electronics. Thus it may be possible that with faster frequency and phase control we can eliminate these unwanted oscillations. Regardless, to construct this all-knowing servo we need to know more about these relaxation oscillations. In the traditional treatment of relaxation oscillations, we linearize the laser equations and approximate the system as a harmonic oscillator [1].

Linearization of the Cw Raman Laser Equations

Let us start by reviewing the results of the last chapter. The cw Raman laser equations are:

$$\dot{E}_p = -L_p E_p - \frac{\omega_p}{\omega_s} G\left|E_s\right|^2 E_p + k(t) \qquad 5.1a$$

$$\dot{E}_s = -L_s E_s + G\left|E_p\right|^2 E_s. \qquad 5.1b$$

which have the following steady-state values for the pump and Stokes fields:

$$E_{p_{ss}} = \sqrt{\frac{L_s}{G}} \qquad 5.2a$$

$$E_{s_{ss}} = \sqrt{\frac{\omega_s\left(k - L_p E_p\right)}{\omega_p G E_p}}. \qquad 5.2b$$

Now we can begin the linearization of these equations. We start with the following transformations of the pump and Stokes fields:

$$E_p \rightarrow a + a_{ss} \qquad 5.3a$$

$$E_s \rightarrow b + b_{ss} \qquad 5.3b$$

where a and b are allowed to vary in time and a_{ss} and b_{ss} are set to the steady-state values of equations 5.2a and 5.2b. We now substitute equations 5.3a and 5.3b into our cw Raman laser equations, 5.1a and 5.1b, and keep only the linear terms of a and b. After some cumbersome algebra we arrive at the following linearized equations:

$$\dot{a} = -\left(L_p + \frac{\omega_p}{\omega_s} G b_{ss}^2\right) a - 2\frac{\omega_p}{\omega_s} a_{ss} b_{ss} b \qquad 5.4a$$

$$\dot{b} = 2G a_{ss} b_{ss} a \qquad 5.4b$$

Just as a test, let us compare the predictions of the general Raman laser equations to these linearized Raman laser equations and look for similarities and differences in the results.

Figure 5.1a shows how the cw Raman laser is predicted to start up with the intensity build-up in the cavity [3]. We still have the over shoot of the steady-state value of the initial Stokes field. Figure 5.1b shows results by using the non-linear Raman equations [3]. Notice that

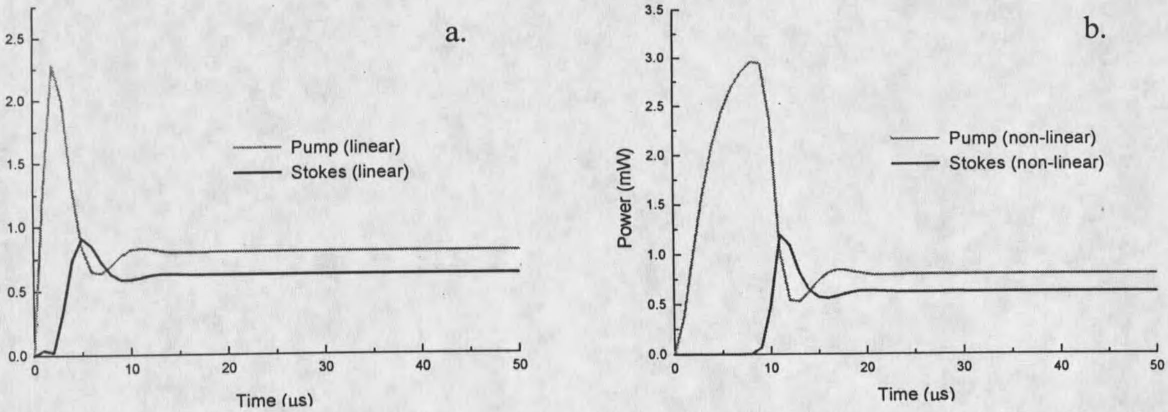

Figure 5.1 Shows how the cw Raman laser starts up: (a) shows the results of the linearized theory while (b) shows the results of the standard theory.

the Stokes field starts about 7μs later than the Stokes of the linearized theory. We can explain this by examining the gain terms for the Stokes fields in both the non-linear and linear theories. The gain of the Stokes field in the non-linear theory is proportional to $\left|E_p\right|^2$ which varies as the pump field builds-up in the cavity, while the linear theory's gain is proportional to $a_{ss}b_{ss}$ which is the steady-state values of the pump and Stokes fields, and does not vary in time. This discrepancy should be expected; when we linearized our Raman equations we dropped the terms that varied like $\left|E_p\right|^2$, with the assumption that $\left|\frac{\Delta E}{E}\right|^2 << 1$. Figure 5.2 shows

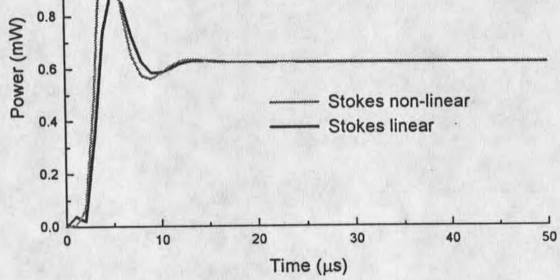

Figure 5.2 Compares the Stokes output of the two theories

the Stokes from the linearized theory plotted with the Stokes from the non-linear theory with the non-linear Stokes displaced so they overlap [3]. From this figure we can see that for small changes in power (later relaxation oscillations) the predictions of the two theories begin to converge. This illustrates the regions where the linearized theory predictions can be considered valid.

Relaxation Oscillations

So our linearized equations were determined to be valid for small deviations about our steady-state values for the pump and Stokes fields. The relaxation oscillations seen in earlier chapters fall into this criteria. As stated earlier in this chapter the traditional treatment of relaxation oscillations models our linearized equations as a simple harmonic oscillator. Let's take a time derivative of equation 5.4b, so we have the following:

$$\ddot{b} = 2Ga_{ss}b_{ss}\dot{a} \qquad 5.5a$$

$$\dot{a} = -\left(L_p + \frac{\omega_p}{\omega_s}Gb_{ss}^2\right)a - 2\frac{\omega_p}{\omega_s}a_{ss}b_{ss}b \qquad 5.5b$$

Now let's substitute $\dot{a}$ of equation 5.5b into 5.5a equation and use the value of a given by equation 5.4b. We arrive at the following differential equation:

$$\ddot{b} + \gamma\dot{b} + \omega_0^2 b = 0 \qquad 5.6$$

where $\gamma = L_p + \frac{\omega_p}{\omega_s}Gb_{ss}^2$ and $\omega_0^2 = \frac{\omega_p}{\omega_s}\left(2Gb_{ss}a_{ss}\right)^2$. Equation 5.6 is just a damped simple harmonic oscillator which has the following solution:

$$b(t) = Ae^{-\gamma t/2}\cos(\omega t + \phi) \qquad 5.7$$

where $\omega^2 = \omega_o^2 - \frac{\gamma^2}{4}$. Figure 5.3 shows how damping constant, γ, and the relaxation oscillation frequency, $\omega/2\pi$, vary as a function of the number of times threshold for mirror reflectivities (transmissions) of 0.9998 (180ppm). We can see that the frequency of the relaxation oscillation increases until it reaches the cavity linewidth of ~200kHz [3]. When the cavity linewidth is reached, the relaxation oscillation frequency starts to decrease because the damping constant, γ, still increases. So some questions may arise. How persistent are these oscillations? How much damping occurs in one oscillation? And is there a sweet spot in pump powers where the cw Raman laser is more prone to oscillate? The first two questions can be answered by calculating how much a relaxation oscillation is attenuated after one oscillation or mathematically:

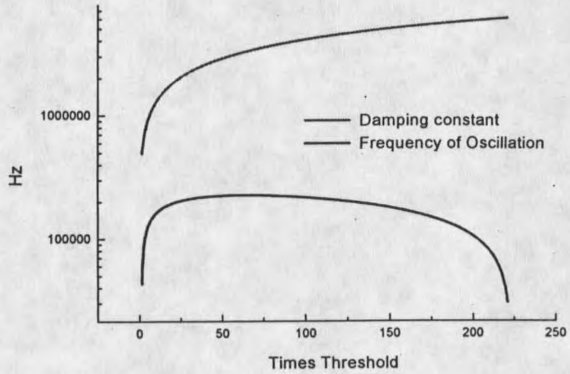

Figure 5.3 Shows the relaxation oscillation frequency and damping constant as a function of the number of times threshold

$$Atten = exp\left(-\frac{\gamma}{2} * \frac{2\pi}{\omega}\right) \tag{5.8}$$

which tells us the attenuation of the oscillation in one period. Figure 5.4 shows the result of this calculation. Notice that we see a peak, or a minimum in the attenuation at four times the threshold of the Raman laser [3]. For pump rates smaller and greater than

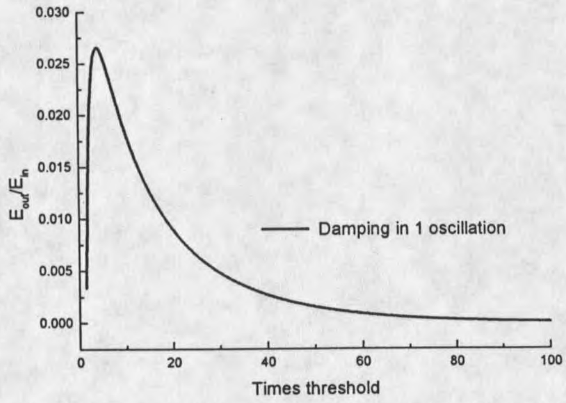

Figure 5.4 Shows damping of relaxation oscillation in one period

four times threshold we see greater attenuation of the relaxation oscillations. This explains why in the previous experiments we saw problems in the Stokes output in the range of 3-5 times threshold. In the previous experiments our servo only had ~30kHz of bandwidth, so frequencies larger than 30kHz experience positive feed-back. Our relaxation oscillations fall into that category, so the relaxation oscillations would experience gain that would sustain the oscillation. As illustrated by figure 5.4 at certain pump rates we are more likely to experience these relaxation oscillations.

Experimental Elimination of Relaxation Oscillations

We now understand the problem at hand, and we can begin to construct a solution. What is needed is a servo that is stable at these higher frequencies, so the oscillations are not fed by the servo. We need to construct a servo that is stable out to the cavity linewidth. Another frequency actuator is needed. An acousto-optic modulator (AOM) can provide small frequency corrections (1-10MHz) in a bandwidths up to 300kHz for a carefully constructed AOM; these limitations are explained in appendix D. The experimental apparatus that uses the AOM is illustrated in figure 5.5. The system is optically pumped by a frequency doubled Nd:YAG with output powers up to

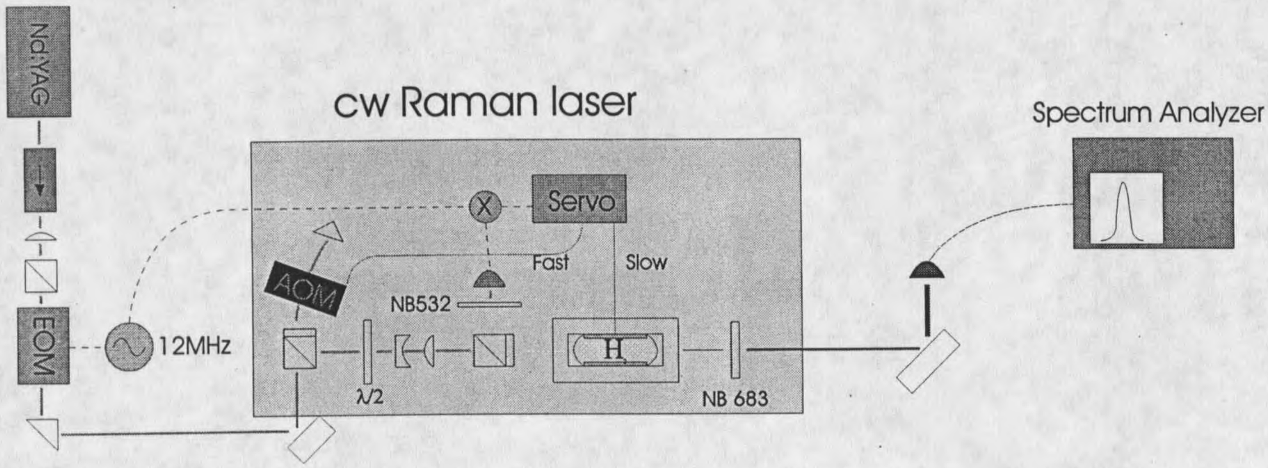

Figure 5.5 Experimental apparatus used to eliminate relaxation oscillations.

200mW. The output of this Nd:YAG laser at 532nm was sent through a Faraday oscillator to minimize the feedback to the laser. The beam is placed through an EOM to place sidebands on the carrier frequency required for locking the pump beam. The beam is double passed though an AOM to minimize beam steering. A half-wave plate allows for rotation of the polarization of the optical beam. The beam travels through a lens pair to mode match the optical beam to the high finesse cavity. After the lens pair the polarizing beamsplitter and quarter waveplate allowed for monitoring of the beam reflected from the cavity. A narrow band filter at 532nm was used to block the Stokes output from the fast detector which was used to measure the error signal. A low-noise amplifier gave the signal 30dB of gain before it was mixed to dc. The error signal entered the servo and the slow corrections were sent to the cavity piezoelectric transducer, and the fast corrections were sent to a voltage controlled oscillator which controlled the AOM. The output of the cavity (Raman laser) was sent through a pelin-broca prism to spatially separate the pump and Stokes beams. Fast detectors (500MHz) allowed for monitoring of the Stokes and pump beams in conjunction with a spectrum analyzer.

Before we look at the amplitude noise of the output of the cw Raman laser, let us briefly define how we will measure it. We will measure the relative intensity noise (RIN) of the laser. We do this by taking the output of the spectrum analyzer, which measures the electrical power supplied by a photo-detector in dBm in a given resolution bandwidth. We want the ratio of the photo-current electrical power noise at a given frequency to the dc electrical power from the photodiode, or mathematically[4]:

$$RIN = 10\log\left(\frac{\Delta P_{diode}}{P_{diode}} * \frac{1Hz}{RB}\right) \quad 5.9$$

where ΔP_{diode} is the electrical power from the photodiode measured by the spectrum analyzer in a resolution bandwidth of RB, and P_{diode} is the dc electrical power generated by the photo-diode. Notice that RIN is a natural or unitless number; however, we "say" that we measure it in dB/Hz which is misleading because it implies that RIN is a frequency when it is just a number. The units stress the fact that we measure the power in a 1 Hz bandwidth. Now let us think about how the photo-detector works. It converts optical power into a current which gives a voltage drop across a resistor. So when we measure the power produced by the photo-detector we actually measure the optical power squared. So a RIN of -20 dB/Hz actually corresponds to power fluctuations of 10% (or -10dB).

In order to lock the laser and produce a Stokes output, the pump laser was locked to the cavity at a power below the cw Raman laser threshold. The pump power is then increased, by varying the half-wave plate, to produce a Stokes output. The relative intensity noise (RIN) of the cw Raman laser was measured and is shown in figure 5.6 at a pump rate of about 4 times threshold. In previous experiments the relaxation oscillations were seen to be about 10% for a pump rate of four times threshold, which would correspond to a RIN of -20dB/Hz. Figure 5.6 shows the measured RIN of the Stokes beam to be less than -90dB/Hz which is 7 orders of magnitude better than previous experiments. From figure 5.6 we can see where the stabilities of our cavity and AOM servos becomes a problem. Notice that the AOM servo becomes unstable at ~160kHz, and the

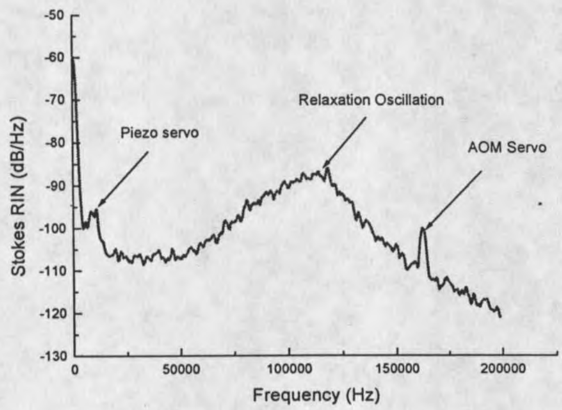

Figure 5.6 Shows the output RIN of the cw Raman laser.

relaxation oscillation occurs at ~115kHz. At 115kHz our AOM servo is being pushed and is starting to have stability issues, but at 115kHz we still have a some phase margin left, so the relaxation oscillations experience the proper feedback, but not enough gain to suppress them totally. We can solve this problem by adding an electro-optic modulator to make corrections at frequencies higher than the cavity linewidth.

So we can now look at the noise on the pump and Stokes beams as a function of the number of times the threshold. Figure 5.7a shows the Stokes output RIN while figure 5.7b

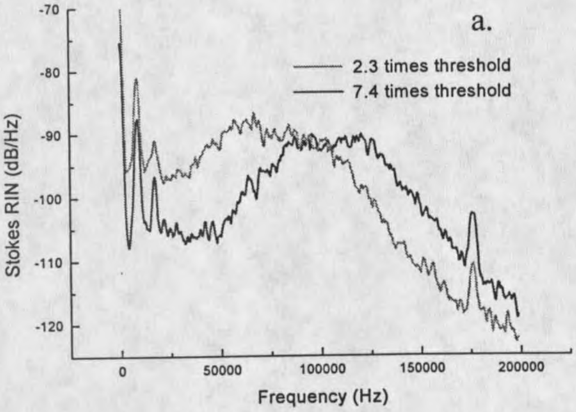

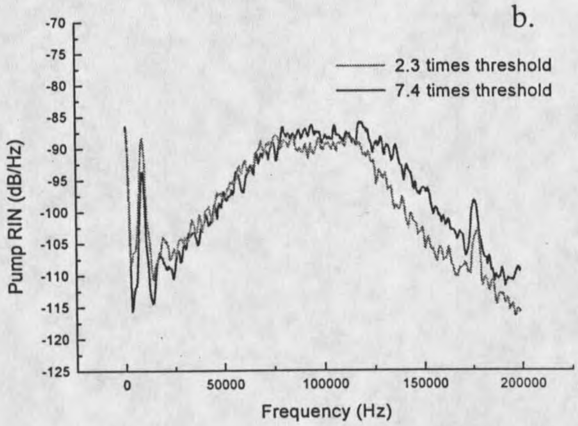

Figure 5.7 Shows the RIN of the (a) Stokes beam and the (b) pump beam for two different pump powers.

show the pump RIN as a function of the number of times threshold. We can see that in both figure 5.7a and figure 5.7b the RIN is dependent on pump power. Both figures contain data for 2.3 times threshold and 7.4 times threshold. We see that the noise of both the pump and the Stokes beams decreases as the pump power increases for frequencies smaller than the cavity linewidth (~100kHz). In both figures we can see the results of the instabilities in the piezo (spikes at ~8kHz) and AOM (spikes ~160kHz) servos. Now let us return to our equations to see if we can predict the amplitude noise response of the cw Raman laser.

Predictions of RIN on the Raman Laser

As seen in the previous section, we can suppress the relaxation oscillations if we have enough bandwidth in the locking servo. Now that the relaxation oscillations are no longer of major importance in the noise spectra of the cw Raman laser, we can start to make predictions of what we expect the noise spectra of the cw Raman laser to be for a given pump laser noise spectra.

Let us think about what the Stokes field thinks amplitude noise is. It is obvious that amplitude noise on the pump laser will be viewed as amplitude noise on the pump laser by the Raman laser. But what about frequency noise on the pump laser? Remember that the Raman linewidth for 10atm. of H_2 is about 510MHz [2]. So if the pump laser has a linewidth of ~1kHz as a result of locking the pump to the cavity, the Raman laser thinks that it is being pumped by a infinitely narrow linewidth laser. The frequency noise on the pump laser would then correspond to a dithering of the pump laser frequency about the cavity linewidth and produce an amplitude modulation on the output of the cavity. Figure 5.8 gives a graphical representation of this effect. We see that a small frequency excursion corresponds to a large amplitude modulation. The Raman linewidth's maximum slope is overlaid to illustrate the point that the cw Raman laser sees a pump that is infinitely narrow in frequency. What we gain from this information is we cannot just measure the RIN of the pump laser when modeling the noise. We need to include the frequency noise of the pump laser as well. Both of these measurements can easily be taken by measuring the RIN at the output of the optical cavity.

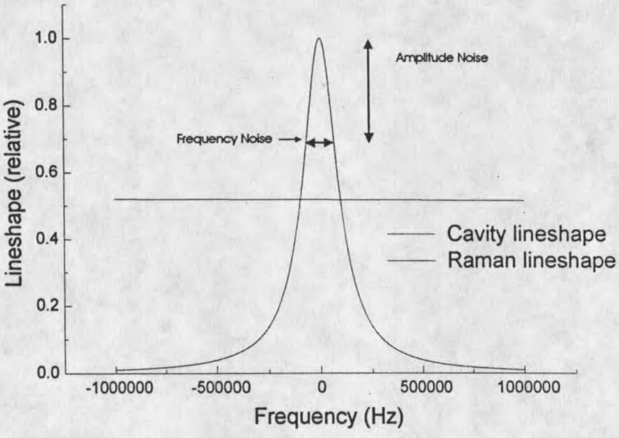

Figure 5.8 Shows illustrates the transformation of frequency noise into amplitude noise.

Figure 5.9 shows the RIN of the pump laser measured at the exit of the cavity below the threshold of the Raman laser and at the front of the cavity. We see that the RIN measured at the front of the cavity is significantly lower than the RIN measured at the exit of the cavity. This means that there is a bit of frequency noise on the pump laser that the cavity turns into amplitude noise. We can use this information to predict what the RIN on the pump and Stokes beams will be. To predict the RIN on the pump and Stokes beams we return to our Raman laser equations and place a noise term on the optical pumping term, k. This gives us the following equations:

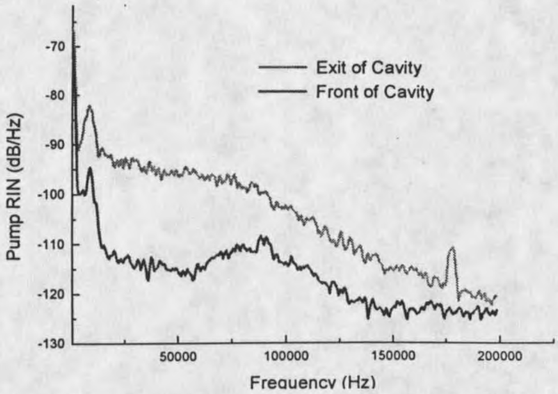

Figure 5.9 Shows the RIN of the laser at the entrance and exit of the cavity

$$\dot{E}_p = -L_p E_p - \frac{\omega_p}{\omega_s} G|E_s|^2 E_p + k(1 + A\sin(\omega t)) \qquad 5.10a$$

$$\dot{E}_s = -L_s E_s + G|E_p|^2 E_s \qquad 5.10b$$

where A and ω are given by the pump noise at the exit of the cavity seen in figure 5.9. Equations 5.10a and 5.10b were numerically integrated for pump values of 2.3, 7.4 and 100 times threshold. The math-cad program used to perform these integrations can be seen in appendix F. Figures 5.10a and 5.10b show the predictions of the theory, for mirror reflectivies (transmissions) of 0.9998 (180ppm) and G as defined in chapter 4 [3]. We see that the theory

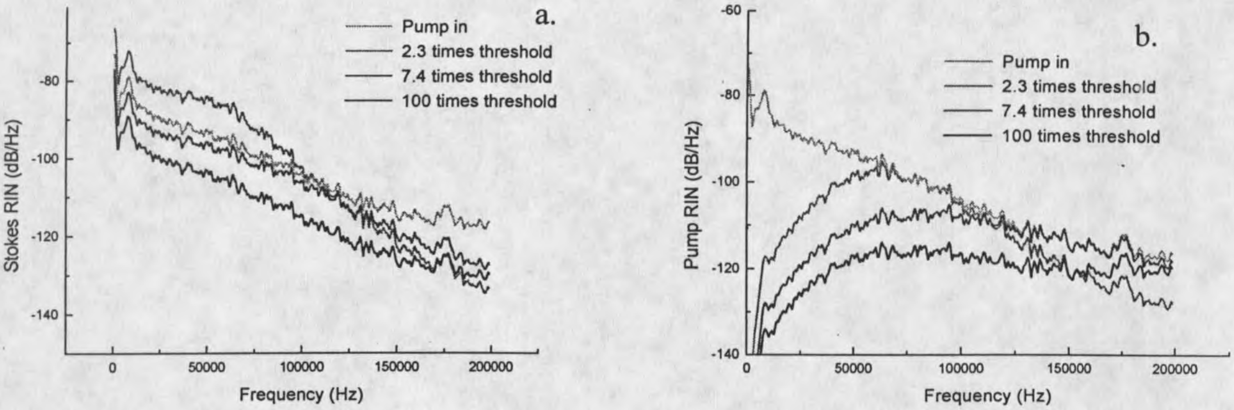

Figure 5.10 Shows the RIN predictions of the theory for the (a) Stokes output and the (b) pump output.

also predicts the reduction of amplitude noise on the pump and the Stokes beams as the pump power increases as seen in figures 5.7a and 5.7b. We see from figure 5.10a that the Stokes RIN is predicted to be slightly larger than the input pump RIN right above threshold, but it drops below the pump RIN at higher pump powers. Now let us take another look at the data from

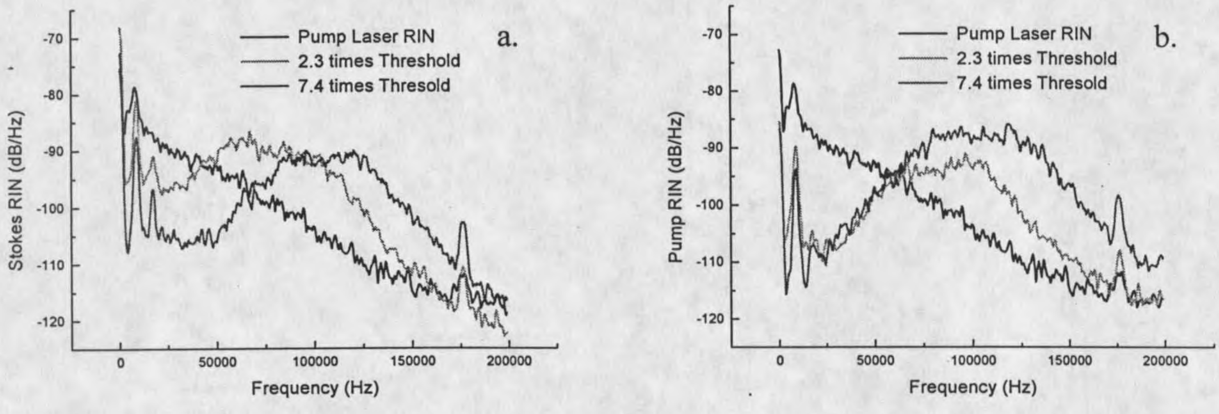

Figure 5.11 Shows the RIN of the (a) Stokes beam and the (b) pump beam at various pump powers with the input pump RIN overlaid.

figures 7a and 7b but let us include the input pump RIN so we can more accurately compare our results with the theory. Figure 5.11a show the Stokes RIN with the input pump RIN overlaid, and Figure 11b show the same for the pump RIN. We see that there is more suppression at the lower frequencies, ~35 dB/Hz for the pump beam, and the RIN appears to peak near the cavity linewidth of about 100kHz, as expected. The theory predicts more RIN reduction in the pump beam than seen in figure 5.11a. Furthermore, the noise of both the pump and the Stokes beams is predicted to remain below the input pump RIN at higher frequencies, which we do not see in figures 5.11a and 5.11b. Remember that we are servoing the pump laser to the cavity linewidth center, and we mentioned in earlier chapters about the Raman laser's sensitivity to the servo gain. In figures 5.12a and 5.12b we show the RIN of the Stokes and the pump beams at ~7 times threshold with slightly different servo gains.

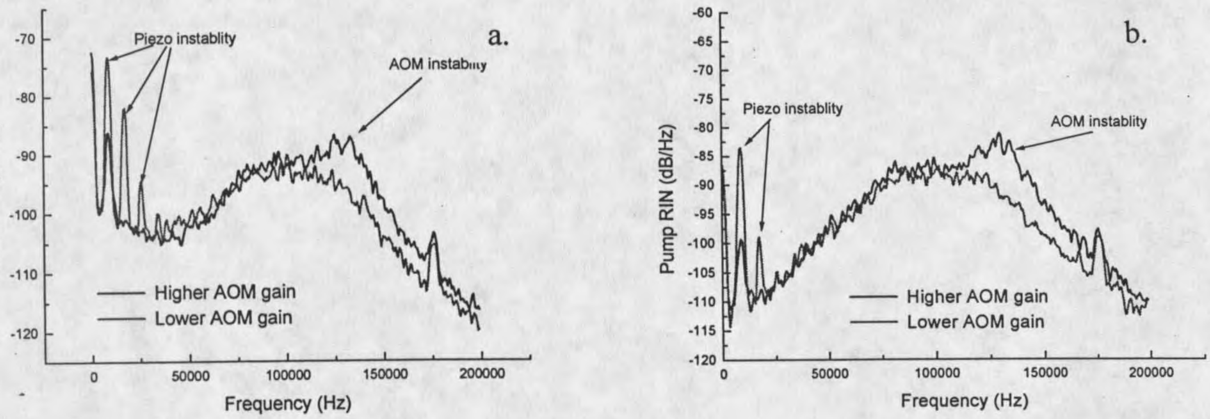

Figure 5.12 Shows the dependence of the (a) Stokes and (b) amplitude noise as the servo gain of the AOM changes

The data for the figures was taken with two different AOM servo gains. Notice if we turn down the AOM servo gain our piezo servo instability becomes more pronounced larger 9kHz oscillation), and if we turn the AOM servo gain up, the relaxation oscillations produce an instability in the AOM servo (~145kHz peaking), so we choose a AOM servo gain that balances these two effects.

Conclusions

In this chapter we found a way to control the relaxation oscillations for our cw Raman laser. Our solution was to increase our servo bandwidth. However, by examining the RIN of the pump laser and the Stokes laser as a function of the pump power we found that the RIN was highly sensitive to the AOM servo gain. We had enough servo bandwidth to reduce the relaxation oscillations, but not enough to have a stable enough servo that could suppress the oscillations totally. A diode pumped Raman laser would be better suited to make RIN measurements predicted by the theory because of the large servo bandwidth when using the current to the diode laser (~1MHz).

We have control of the relaxation oscillations and understand the amplitude noise of the laser, so we only have to measure and describe the Raman laser linewidth to describe the noise characteristics of the cw Raman laser, which leads us to the final chapter.

REFERENCES CHAPTER 5

[1] P. W. Milonni, and J. H. Eberly, *Lasers*, (John Wiley & Sons, New York, NY, 1988), page 366.

[2] W.K. Bischel and M. J. Dyer, J. Opt. Soc. Am. B **3**, 677 (1986).

[3] The theory uses the following parameters: Using the mirror characteristics given by the quote of the mirror manufacture (R=0.9998, A=20ppm), the plane-wave gain coefficient α=2.5*10^{-9} cm/W [2], and the length of the cavity , $\ell = 7.3cm$. The Math-Cad program can be seen in appendix H.

[4] O. Svelto, *Principles of Lasers,* (Plenum Press, New York, NY, 1998) page 298

CHAPTER 6

CW RAMAN LASER LINEWIDTH

Motivation for a Linewidth Measurement

By definition, a single mode laser must be monochromatic or contain just one frequency. So one may ask what is meant by monochromatic. In quantum mechanics we learned that we cannot measure things exactly; there is an error associated with every measurement that we make. We can never know the frequency of a laser to infinite precision, so what is good enough for a laser? Typical optical frequencies are on the order of terahertz (10^{15} Hz). A diode laser has a laser linewidth of about 50MHz, or we know the laser's frequency to about 10ppm. At another extreme, a frequency controlled Helium Neon laser has been shown to have a linewidth less than 50mHz or 1 part in 10^{16} (root Allan variance for a 100s integration time). We see that we have a wide range of possibilities for the linewidth, so it is useful to define the linewidth to distinguish between classes of lasers. We now have a reason to measure the linewidth of our laser, so how do we do it?

Measurement of Laser Linewidth

Depending on the type of laser there are many ways to measure the linewidth. If we start with a diode laser with a linewidth on the order of 50MHz, we can feed the laser light into a high finesse cavity, which can have linewidths on the order of 10-100kHz, and scan across the diode line to take a measurement. However, this method fails when the linewidth of the laser in question is smaller than the cavity linewidth, so we need a method that works for any laser linewidth.

We do not possess the electronics that are fast enough to measure the frequencies in the terahertz frequency band, however, if we have two "identical" lasers that differ in frequency by a giggahertz or less we can beat the lasers together and measure the beat note. The beat note produced will have some uncertainty associated with it, which we will call the linewidth of the laser. Now we have a way to produce a beat note which represents the laser linewidth, so how do we measure it, and how do we interpret the results?

We can place the beat frequency into a spectrum analyzer and measure the linewidth or the beat note. This measurement gives us an idea of how the instantaneous linewidth is jittering and on what time scales. One application of an ultra-stable laser is as an atomic clock. So we would like to know how accurate the beat note (and hence the laser) is over the course of time. Then we would know how accurate our clock could be. In particular we would like to know how our beat note change on time scales larger than 1-10ms (typical time of a sweep of the spectrum analyzer), and are there large variations over the course of an hour or a day?

Thus what we are interested in is how the frequency changes as a function of time. Given two frequency measurements we are interested in the slope, or what is the frequency change divided by the time between measurements. Mathematically we have [1]:

$$y_i^{\tau_o} = \frac{x_{i+1} - x_i}{\tau_o} \qquad 6.1$$

where x_i and x_{i+1} are frequency measurements taken a time τ_0 apart, so y_i is a measure of the frequency jitter scaled by time. Because we want repeatable measurements, we take a family of measurements and then we calculate the variance of these measurements. It turns out that if we take a standard deviation of this family of points, for certain types of noise the standard deviation does not converge. So we take the Allan variance of the data which is defined as the following [1]:

$$\sigma_y(\tau) = \sqrt{\frac{1}{2(n-1)}\sum_{i=0}^{n-1}(y_{i+1}-y_i)^2} \qquad 6.2$$

where n is the number of data points. What we end up with is a linewidth "like" measurement for a given integration time, τ_0. So now we know what measurement we would like to take so now we just need to construct the experimental apparatus to do so.

Experimental Apparatus and Linewidth Measurements

As mentioned in the previous section, in order to take a linewidth measurement for linewidths less than ~100kHz, we need two identical Raman lasers that are separated in frequency by less than 1GHz. If we pump both Raman lasers with the same pump laser we are guaranteed to meet this requirement, because of the Raman linewidth (510MHz) [2]. One may ask: by pumping each Raman laser with the same pump source won't our results be correlated? This is not an unreasonable question to ask. Recall from the previous chapter, because the Raman linewidth is on the order of 510MHz [2], and the pump laser is on the order of 1kHz, due to locking, the Raman laser thinks it is being pumped by an infinitely narrow linewidth laser. The results should not be correlated given the locking schemes are not dependant on the pump laser.

Figure 6.1 is an experimental diagram of the apparatus used to take the linewidth measurements of the cw Raman laser.

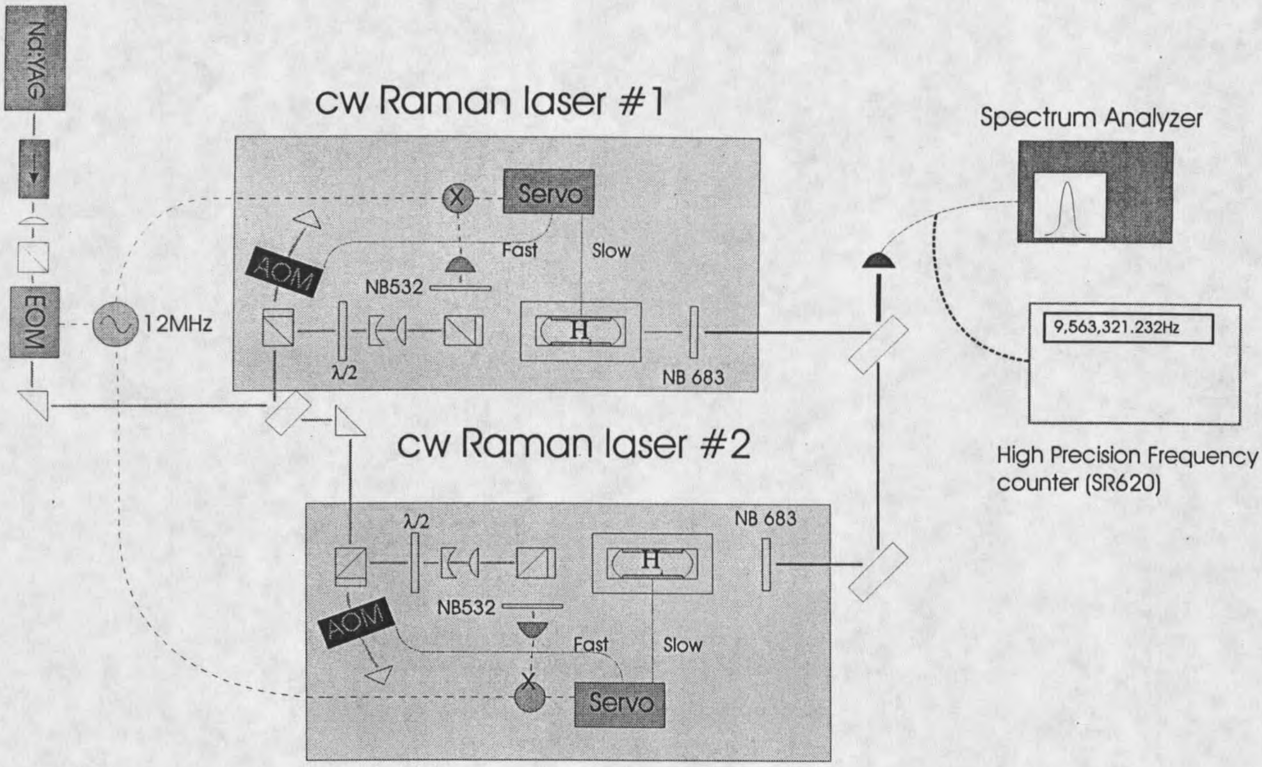

Figure 6.1 Shows the experimental apparatus that is used to take linewidth measurements of the cw Raman laser.

The system is optically pumped by a frequency doubled Nd:YAG laser with output powers up to 200mW. The output of this Nd:YAG at 532nm was sent through a Faraday isolator to minimize the feed-back to the laser. The beam is placed through an EOM to place side-bands on the carrier frequency required for locking the pump beam. The beam is split by a 50/50 beamsplitter to construct two identical cw Raman lasers. The beam is double passed through an AOM (at 80MHz and 110MHz) to minimize beam steering. A half-wave plate allows for rotation of the polarization of the optical beam to provide a variable pump power. The beam travels through a lens pair to mode match the optical beam to the optical cavity. After the lens pair a polarizing beamsplitter and a quarter-wave plate allowed for monitoring of the beam reflected from the cavity. A narrow-band filter (NB) at 532nm was used to block the Stokes from the fast detector used to measure the error signal. A low noise amplifier gave the signal

30dB of amplification before the signal was mixed to dc. The error signal entered the servo and the slow corrections were sent to the piezoelectric transducer (PZT) on the optical cavity while the fast corrections were sent to the a voltage controlled oscillator that controls the AOM. Both cw Raman lasers are identical except for the fact that the AOM's are driven by 110MHz and 80MHz sources so the pump frequencies differ by 60MHz for a double pass. The Stokes beams were overlapped and placed on a fast detector (500MHz) to measure the beat signal. A spectrum analyzer was used to measure the linewidth of the beat frequency. A high precision frequency counter (SR620) was used to calculate the Allan variance for integration times from 1μs to 100s.

The output power of the Raman lasers that reached the fast detector was ~25μW for each laser. A narrow-band filter at 683nm was used to eliminate the pump beam. Figure 6.2 shows the output of the spectrum analyzer. We see that we formed a beat note at 9.557MHz that had a linewidth of 8kHz, which is for two lasers so the linewidth of one laser is just half this value, or 4kHz. We also see structure below 15mV, this is due to jitter in the laser.

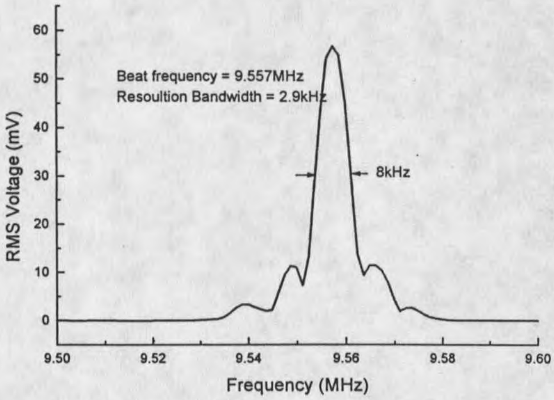

Figure 6.2 Shows a measurement of the linewidth of the beat note formed by two cw Raman lasers

So why do we measure a linewidth of 4kHz? What is the minimum value that the linewidth can be and why do we deviate from that number? Let us walk through a calculation of what we expect the minimum linewidth of the laser to be. First let us think about what we expect the linewidth to depend on. The linewidth of the laser should depend on the physical cavity or resonator, for example, if the cavity has poor mirrors (low reflectivity) the cavity will have a large cavity linewidth, while a cavity with high reflectivity mirrors is going to have a narrow cavity linewidth. So we might expect the following dependency:

$$\Delta\nu_{laser} \propto \Delta\nu_{cavity} \tag{6.3}$$

where $\Delta\nu_{laser}$ is the laser linewidth and $\Delta\nu_{cavity}$ is the cavity linewidth. What is the cavity linewidth? The inverse of the cavity linewidth can be thought of as a lifetime of a photon inside of the cavity. So the smaller the linewidth the longer the photon stays inside the cavity, the longer the photon stays in the cavity the more "identical" photons it can produce by stimulated emission which then produce additional "identical" photons. So we would like to know how many photons the first photon can influence in its lifetime. We cannot measure the photon number directly, because if we placed a meter inside of the cavity we would destroy our interference required for intensity build up. However, we can measure the rate at which the photons are radiating from the cavity by measuring the optical power radiating from the cavity and dividing by the energy per photon. Remember in the steady-state, the number of new photons is equal to the number of photons radiated from the cavity. This will give us a rate of the production of the photons. In the steady-state the gain of photons equals the loss of photons. We can use this number to calculate the number of photons produced in a photon lifetime. The result is:

$$N_{photons} \propto \frac{P_{out}}{h\nu \cdot \Delta\nu_{cavity}} \tag{6.4}$$

where P_{out} is the optical power radiated form the cavity, and $h\nu$ is the energy of one photon. We now can write the following relation for the linewidth dependency:

$$\Delta\nu_{laser} \propto \Delta\nu_{cavity} / N_{photons} = \frac{\left(\Delta\nu_{cavity}\right)^2 \cdot h\nu}{P_{out}}. \tag{6.5}$$

These dependencies are apparent, so it is not shocking that the Schawlow-Townes linewidth has the following functional form [3,4]:

$$\Delta\nu_{laser_{ST}} \geq \frac{\overline{N}_2}{N_2 - N_1} \cdot \frac{h\nu\left(4\pi\Delta\nu_{cavity}\right)^2}{P_{out}} \qquad 6.6$$

where N_a is just the population for the a_{th} state. For a cavity linewidth of ~200kHz, N_2~1 and N_1~0, 200μW of power radiating from the cavity (~8 times the power seen at the detector due to optics), and the wavelength of the output being 683nm, we find the Schawlow-Townes linewidth to be ~10mHz.

We measured a linewidth of 4kHz, which is six orders of magnitude larger than the Schawlow-Townes limit; why? If our cavity was not stable, the resonant frequency would change due to vibrations. How far would our mirrors have to move to correspond to 4kHz? The free-spectral range of our cavity is ~2GHz which corresponds to one half of a wavelength (683nm/2), so 4kHz would correspond to 0.01Å! So we deviate from Schawlow-Townes due to vibrations in the cavity or noise on the piezo driver used to control the spacing of the mirrors.

Since we know what the linewidth of the laser is, now let us examine the stability of the laser. We do this by measuring the beat signal on a high precision frequency counter (SR620) for different integration times. Figure 6.3 show the results of measuring the root Allan variance of the beat signal for integration times from 1μs to 100s. The SR620 calculated the root Allan variance for a sample size of 100 for

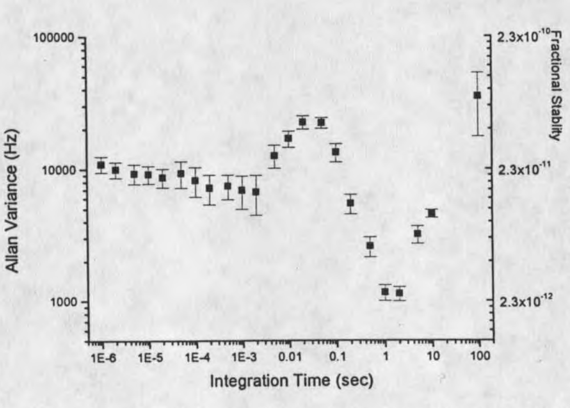

Figure 6.3 Shows the Allan variance of the beat note for various integration times

the integration times of 1μs to 10s and a sample size of 20 for the 100s integration time due to time constraints established by laser lock stability. The root Allen variance at each integration time was measured 20 times so error-bars could be calculated. We see in figure 6.3 that there is a resonance in the cavity for integration time near 0.02 and 0.01 seconds or between 50-100Hz. This resonance is most likely caused by line noise at 60Hz either vibrational or a small ground loop in the system. The Allan variance has a minimum of 1.1kHz at an integration time of 1sec. The cavity drift takes over on the time scale of 10 to100 seconds.

Conclusions

We measured the linewidth of the laser to be 4kHz, which is attributed to the vibrations of the cavity. These vibrations appear in the root Allan variance at integration times of ~10ms, most likely caused by 60Hz sources.. The cavity drift became significant for times scales larger than 10s.

REFERENCES CHAPTER 6

[1] D. W. Allan, IEEE Transactions on Ultrasonics, Ferroelectrics, and Frequency control, **UFFC-34**, 647 (1987).

[2] W.K. Bischel and M. J. Dyer, J. Opt. Soc. Am. B **3**, 677 (1986).

[3] P. W. Milonni, and J. H. Eberly, *Lasers*, (John Wiley & Sons, New York, NY, 1988), page 348.

[4] A. L. Schawlow and C. H. Townes, Phys. Rev., **112**, 1940 (1958).

CHAPTER 7

CONCLUDING REMARKS

In this thesis we describe the construction of the first non-resonant cw Raman laser in H_2. We saw a threshold on the order of a couple of milli-watts which is six to seven orders of magnitude smaller than the power used to produce Raman shifted light in previous pulsed experiments. A time-dependent theory was developed which can be manipulated to predict the threshold of the Raman laser, steady-state values for the pump and the Stokes fields, as well as, relaxation oscillations and the relative intensity noise of the cw Raman laser. Experimental techniques for building servos to accurately control the pump laser were learned and techniques for producing low-noise AOM and piezo drivers were developed.

The future of this field has many exciting possibilities. We can now build lasers at many new frequencies. Because of the low threshold, we can pump the Raman lasers with inexpensive low amplitude noise diode lasers. The amplitude noise reduction that was seen in chapter 5, makes one wonder what would happen if we used a squeezed source as the pump source for the Raman laser. The possibilities seem endless, and offer many directions for this field to grow.

APPENDICES

APPENDIX A

LOCKING

In order for the cw Raman laser to reach threshold, there needs to be an intensity build up of the pump laser inside of the high finesse cavity (HFC). In order for the intensity build up the pump laser must the resonant with the HFC, which can be done by passive or active feed-back. Passive feed-back uses optical feed-back from the HFC to coerce the pump laser to lase at the cavity frequency. This method is possible with diode lasers because of their large gain profiles, which increases the chances of an overlap of a laser mode with the cavity mode. However, the laser used to pump the cw Raman laser is a diode-pumped miser crystal Nd:YAG which only has a bandwidth of ~20GHz which is much smaller than the tens of nanometers of a diode laser, so passive feed-back is impractical.

There are two common ways of using active feed-back to lock a pump laser to a HFC. The first and simplest is fringe locking. This method uses the throughput of the HFC. A servo is designed to hold the power at one half of the maximum value, this method is impractical for the cw Raman laser because we need the intensity build up inside of the cavity. A second method is the Pound-Drever-Hall method for locking where side bands are placed on the pump frequency. A beat note is produced and an error-signal is formed, this method was chosen for the work in this thesis.

Pound-Drever-Hall Locking

An electro-optic modulator (EOM) is used to modulate the phase of the input laser beam. The EOM is driven by a sine wave generator at a known frequency, ω_m. So we can write the electric field of the laser in the following manner:

$$E(t) = E_0 \exp\left(-i\left(\omega t + \beta \sin(\omega_m t)\right)\right) \qquad \text{A.1}$$

where β is the modulation depth. We now expand our field using the Bessel functions as our basis function leaving:

$$E(t) = E_o e^{-i\omega t}\left(J_o(\beta) + J_1(\beta)e^{-i\omega_c t} + J_{-1}(\beta)e^{i\omega t} + \ldots\right) \qquad \text{A.2}$$

where J_n are Bessel functions. Now we assume that the modulation is small, and making the approximations for the Bessel functions: $J_o \approx 1 - \frac{\beta^2}{2} \approx 1$, and $J_1 \approx -J_{-1} \approx \frac{\beta}{2}$ we can write our field as:

$$E(t) = E_o e^{-i\omega t}\left(1 + i\beta \sin(\omega_m t)\right). \qquad \text{A.3}$$

We now know what the EOM does to the laser field, so we can look to see what happens when place an optical cavity into the system. Figure A.1 shows an optical cavity to illustrate how we produce an error signal. We use a beam splitting polarizer with a quarter wave plate to monitor the reflected beam from the cavity. We then place the reflected beam, which includes the leaked beam from the cavity, on a fast photo detector. We then use the signal generator with an appropriate phase shift to mix the beat signal seen at the detector to dc. Let us examine mathematically how this works.

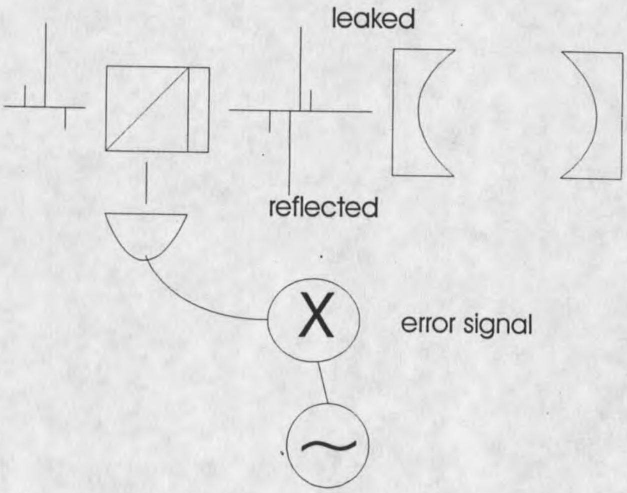

Figure A.1 Shows how the error signal is produced.

We want to know the laser field that the photo detector sees. The field is a combination of the reflected field from the cavity and the field leaked form the cavity. Let us start by writing the reflected pump beam.

$$E_r(t) = -rE_o e^{-i\omega t}\left(1 + i\beta \sin(\omega_m t)\right) \qquad \text{A.4}$$

where r is $\sqrt{R}$. Now we need to write an expression for the field leaked from the cavity. We start with the following differential equation that describes the cavity.

$$\dot{E} = -LE - i\theta E + K \qquad \text{A.5}$$

where L accounts for the losses in the cavity, θ is the detuning from the center of the cavity and K is a pumping term. This equation is solved in a manner similar to the method used in chapter VI, which yields:

$$E_{leaked}(t) = E_0 e^{-i\omega t}\left(\frac{t_m}{2}\cdot\frac{k}{L+i\theta}\left(1-e^{-(L+i\theta)t}\right)\right) \qquad \text{A.6}$$

where t_m is the transmission of the mirrors. We just consider times where the field inside the cavity is well established, this leaves:

$$E_{leaked}(t) = E_0 e^{-i\omega t}\left(\frac{t_m}{2}\cdot\frac{k}{L+i\theta}\right). \qquad \text{A.7}$$

The detector measures the power of the optical field. The output of the photo detector will be proportional to:

$$Out \propto \left(E_r(t) + E_{leaked}(t)\right)^2 \qquad \text{A.8}$$

The output of the photo detector then enters the mixer, which multiplies the signal by $\sin(\omega_m t)$. The output of the mixer will contain components at dc, ω_m, $2\omega_m$, etc.. We are just concerned with the near dc component, so we can build filters to eliminate the higher frequencies. If we just look at the dc components, we find the following dependency of the error signal:

$$Error(\theta) \propto t_m k\left(\frac{\theta}{\theta^2+L^2} - \frac{\beta(\theta-\omega_m)}{2(\theta^2+L^2)} - \frac{\beta(\theta+\omega_m)}{2(\theta^2+L^2)}\right) \qquad \text{A.9}$$

We now have an expression for the error signal as a function of cavity detuning. Figure A.2 shows typical error signal. The cavity frequency is scanned from 15MHz below the carrier frequency to 15MHz above the cavity frequency. We see that our error signal changes sign as we scan though the carrier frequency, which is needed if we want to lock to the center of the cavity resonance. Another point of importance is the fact that the error signal maintains the proper sign for frequency excursions up to the modulation frequency.

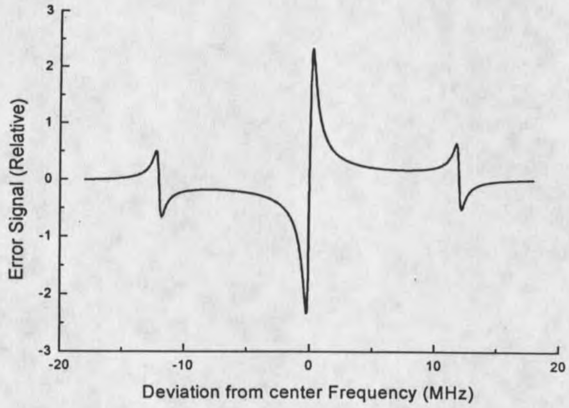

Figure A.2 Shows the error signal as a function of cavity detuning

We now know the mathematics behind the error signal.

APPENDIX B

SERVO DESIGN

In appendix A, we learned how to create an error signal by placing side-bands on the carrier frequency by modulating the phase of the laser beam. Now we need to learn how to use this information that the error signal provides to lock the laser to a high finesse cavity. We need to build electronics to control the laser and servo it to the center of the cavity line.

The first thing that we need to learn is how to control the frequency of the laser. Lasers can be tuned in many ways: adjusting the current to the laser, changing the temperature of the laser, or stressing the lasing medium in some way. The frequency can also be tuned externally by using an electro optic modulator to vary the phase of the laser beam or an acousto optic modular to vary the frequency of the laser. There are many ways to vary the frequency, but the important question is: How much does the frequency change for a give voltage and how fast can we control the frequency? The transfer function is a measure of the frequency actuators response to a given input. These are important functions to know when one is trying to build a servo to control the laser.

The basic scheme to make a servo is the following: our error signal monitors the laser frequency, we see the laser drift so our servo tells the laser to do the opposite, or we give it negative feed-back.. So our servo is 180° out of phase with the laser drift. Now if we think back to figure-1b we see that the phase of the frequency actuator changes as we go through the corner, so our phase will change from -180° to -270°. Our electronics that we use to construct these servos are not perfect so at high frequencies they will add more phase shift. It is unavoidable that we will cross over from negative feed-back to positive feed-back. When we are trying to control the laser with positive feed-back we will create an oscillation. In order to prevent this, the frequencies with receive positive feed-back must be attenuated. We do this with an integrator. Figures B.1a and B.1b show the desired response. We create the integrators response by placing a capacitor in series with a resistor and using the combination as a feed-back impedance for a operational amplifier (op-amp). The voltage gain of an op-amp is just $-\frac{Z_2}{Z_1}$, where Z_2 is the feed-back impedance and Z_1 is the input impedance to the operational amplifier used in an inverting mode.

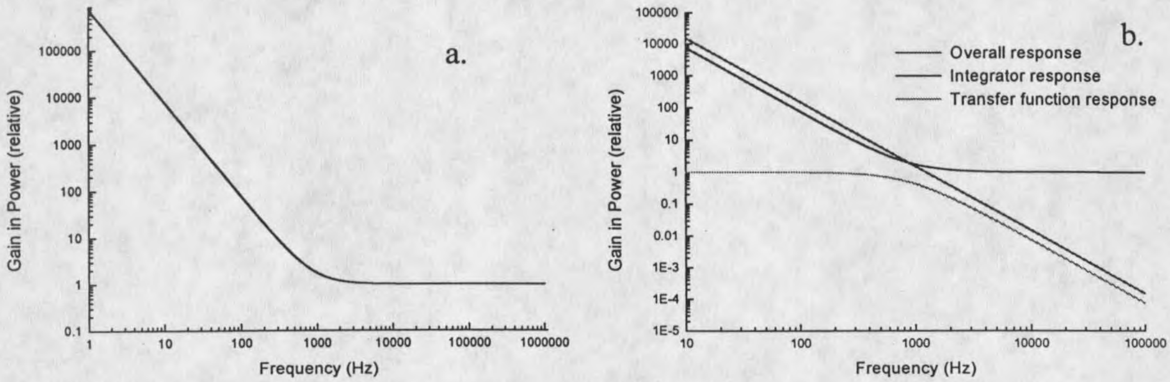

Figure B.1 Shows the (a) servo response and the desired (b) overall response of the locking system.

We see at low frequencies the capacitor has a large impedance, so the gain is large. However, there will be a frequency where the impedance of the resistor is larger than the capacitor, so the resistor sets the gain. Figure B.1a shows this, we see a -20dB/dec slope for the capacitor and a flat response at higher frequencies caused by the resistor. Ideally we adjust this corner to match the corner of our transfer function, this gives a smooth gain profile and the phase does not change from -270°, and we have a fall off of -20dB/dec in the region of positive feed-back. Figure 1b shows our over-all goal. We know have an idea of what we want to do, use an integrator to match the transfer function an give us a -20dB/dec fall off, so we can design a servo to do so.

Figure B.2 shows a servo which was originally designed by Jan Hall of Pound-Drever-Hall, with a few changes to make the servo more practical for our use.

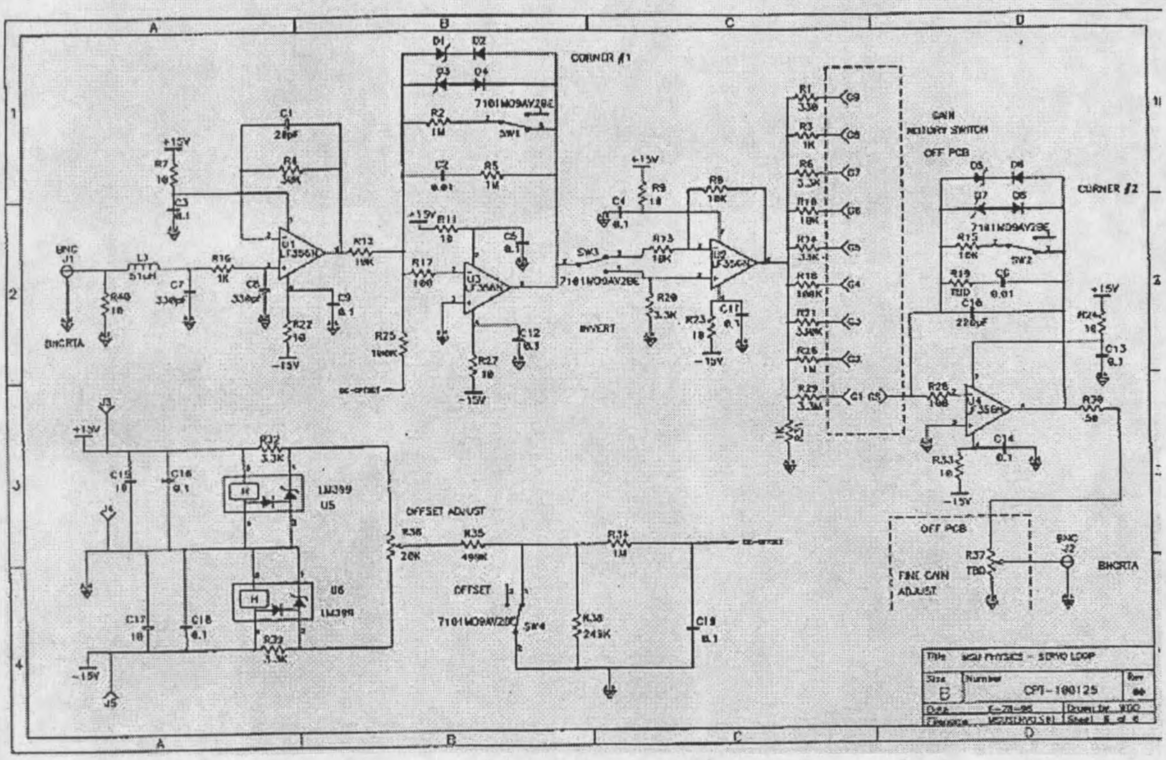

Figure B.2 A schematic of the servo board

We will go stage by stage and describe what happens. Our error signal enters through the BNC J1, and is dropped across a resistor R40. Typically the value of R40 is 50Ω, this impedance matches the BNC cable with the circuit. We then go through some low pass filters which set the maximum bandwidth of the servo. We then enter our first op-amp, U1, which is used as a buffer, the capacitor and resistor used in feed-back help prevent parasitic oscillation caused by a stay capacitance between the + and - input ports. We then enter our first integrator, U3, with a low-noise dc basis to zero our error signal. Resistor R5 and capacitor C2 are chosen to match the corner in the transfer function. Because of the large dc gain of an integrator a by-pass resistor R2 is used until the laser is close to lock then removed by throwing a switch. The zener diode and signal diode pair provide a clamp on the voltage so the op-amp is never railed. R17 is a resistor that reduces the tendency for the op-amp to oscillate. Because we are not guaranteed that the slope for every frequency transducer is the same, we have an optional invert stage, U2, to assign the proper sign to our feed-back. We now enter our final stage which consists of an array of resistors to set the gain of the servo, and an optional second integrator, U4, for the work in this thesis R19 and C6 we not used. We then leave the servo though a 10-turn pot that gives us fine control of our gain.

The method of locking the laser follows these steps. First the servo is tuned to match the transfer function of the frequency actuator. The frequency of the cavity and laser are tuned with in the side-bands produced by the EOM. The gain is increased with R2 in the circuit. Once we are close to the cavity center the switch is thrown removing R2 and leaving a pure integrator, the gain is increased until an oscillation is seen, the gain is reduced until the oscillation disappears. The oscillation is cause by positive feed-back so the gain was reduced. So we have a locked laser.

APPENDIX C

PIEZO DRIVER

In this appendix we will discuss the design of a low noise high voltage piezo driver. In this thesis we use a piezo inside the Raman cavity to control the spacing to the mirrors. So if we apply a voltage to the piezo we change the length of the cavity, hence, change the frequency which the resonant frequency of the cavity. If we know the free-spectral range of the cavity (2GHz), and the amount of voltage required to move a free-spectral range (27V) we can calculate the frequency change for a give voltage. For the cavities used in this thesis this number is about 75 MHz/V. So noise in the piezo driver on the order of 1mV, would give us a minimum linewidth of 75kHz. This is the level of typical piezo drivers that can be purchased over the counter. So if we want a stable cavity or laser we need to improve on this number.

Figure C.1 shows a low noise piezo driver that was constructed with some guidance from Michael Jefferson of IBM.

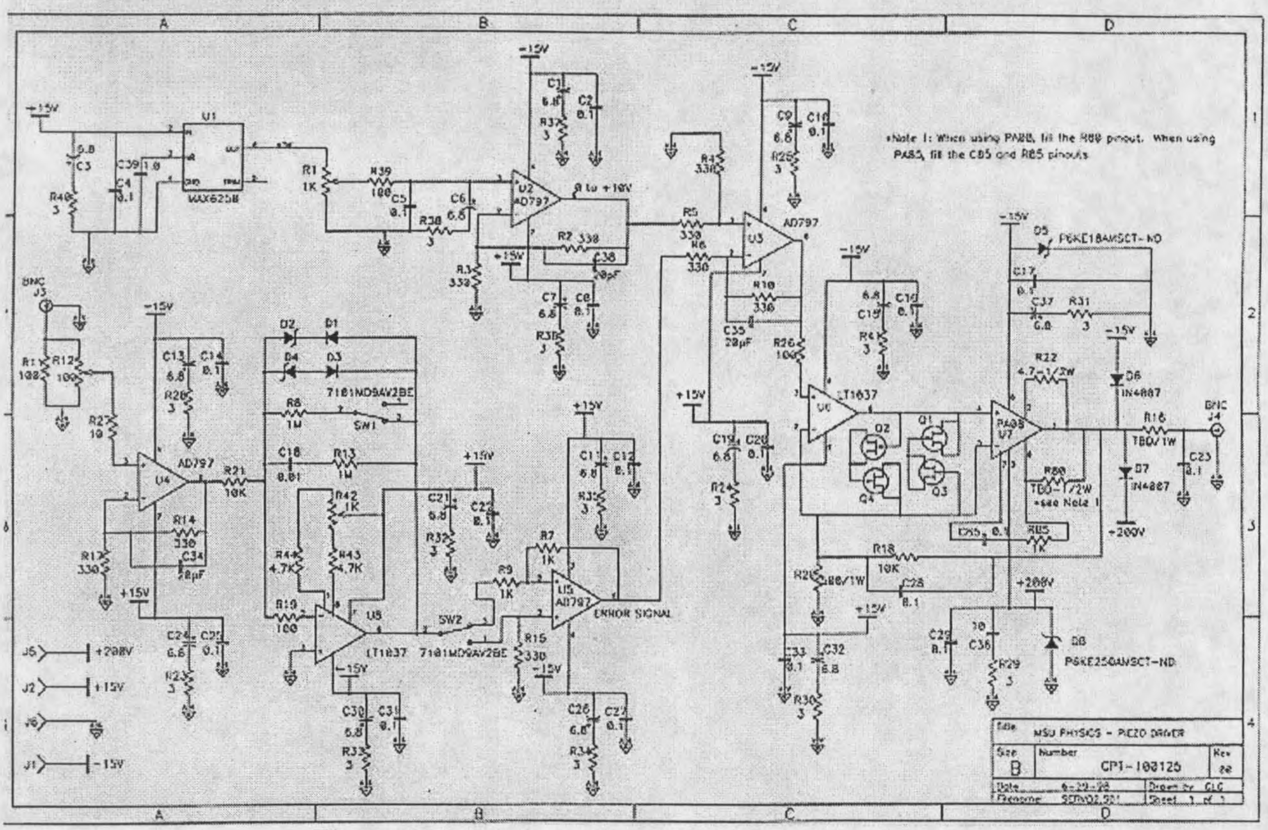

Figure C.1 A Schematic of the Piezo driver board

The error signal enters the driver at the BNC, J3. The error signal is dropped across a 50Ω pot to provide impedance matching and a variable gain. The error signal then enters a low noise buffer, U4, which then enters the integrator U8 who's function is described in appendix B. We then enter an optional invert and reach a difference amplifier U3, which sums our error signal with a DC bias produced by a low noise voltage reference. The out output of the difference amplifier is place into the high-voltage stage. This high voltage stage is a combination of two op-amps. The first op-amp is low noise and it thinks that its output is after the high voltage stage U7, because that is where the feed-back resistor is. So it controls the output of the high-voltage stage giving us low noise. Because of the cost of the high voltage stage (~$200), some protection components were added, Q1-4, and voltage suppressors on the power supplies. The high voltage the leaves the piezo driver through a resistor which is chosen to give the desired bandwidth of the servo by forming a low pass filter with the piezo. The noise of this system is limited by the IC's that are chosen so we will show a list of the chips used in the circuit.

LT1007	U8, U5, and U6
AD797	U4, U2, and U3
MAX6250	U1 (low noise 5V ref, limiting piece in servo)
PA08 or 85	U7 high voltage stage

These IC were chosen because of their stability and low noise.

The noise of the servo was compared to commercially available high voltage devices, a Thor labs piezo driver and a new-focus piezo driver. The rms. voltage was measured by matching the output impedances of each device and placing the voltage across the piezo inside the cavity. The New focus driver had 3,200μV_{rms}, the Thor labs piezo driver had 700μV_{rms}, while the above piezo driver had 1μV_{rms}, which would correspond to 75 Hz. This is the driver that is used through this thesis.

APPENDIX D

AOM DRIVER

This appendix describes the AOM driver used in this thesis. An acousto optic modulator works by generation an acoustic wave in a crystal, which then shifts the frequency of the laser beam inside the crystal. We want to use an AOM to frequency control the laser, so we need to know some things about the AOM. The acoustic wave is generated by a piezo which is driven by a voltage to frequency converter. The velocity of the acoustic wave is 3,630m/s, and the wave has to travel 3mm to reach the beam in the crystal, this corresponds to a delay of 826ns. So the usable bandwidth for locking with the AOM is $f_{AOM} \sim \frac{1}{2\pi t_d}$, where t_d is the time delay of the AOM. This gives a bandwidth of 190kHz. However, if the AOM can still respond to higher frequencies, but with the improper feed-back, so we need to be careful with the noise in the electronics. The transit time of the acoustic wave across the beam diameter is ~25 ns which corresponds to about 6MHz, where noise can be placed on the AOM and no possibility of removal. So we need to construct a low noise AOM driver that is quiet out to frequencies up to 6MHz.

Figure D.1 shows the schematic of the AOM driver used in this thesis. The error signal enters through the BNC labeled J7. There is a high-pass filter that can be used to eliminate cross

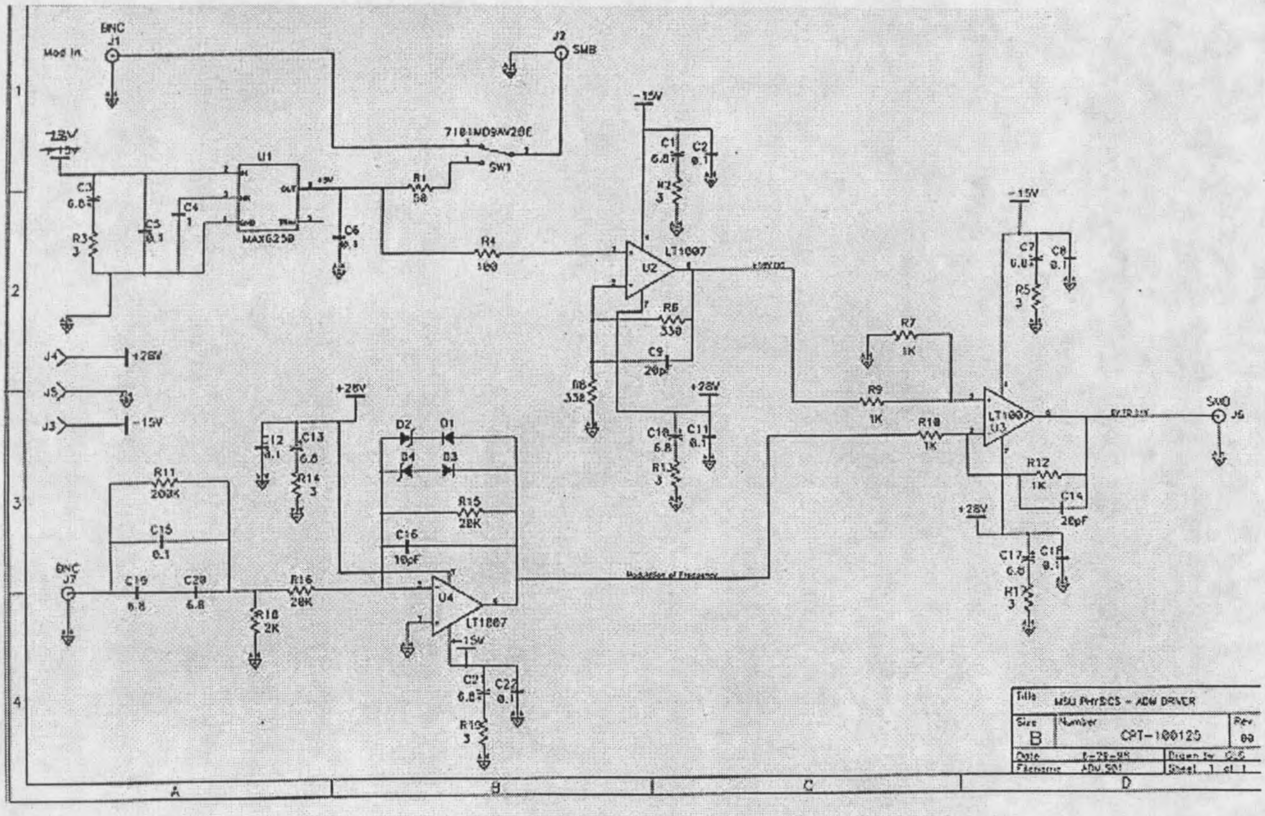

Figure D.1 A schematic of the AOM driver board

talk from the slow servo. We then enter a low noise op-amp that clamps the voltage between ±4V, so the voltage to frequency converter is not damaged. We then enter a difference amplifier that sums the error signal to a dc signal and the output goes to the AOM. The AOM has a center frequency of 80MHz which corresponds to an input voltage of 10VDC. So the dc basis is tuned to this voltage. If a R6 is replaced with a trimpot the center frequency can be changed. The board is driven by -15V and +28V, so the output can be tuned from 6-14V. The +28V is used because the AOM voltage to frequency converter requires +28V. The board also has a +5V output that turns on the oscillator, with the option of being externally controlled by BNC, J1. This driver provides a low-noise 10V output that can be changed by the error-signal

APPENDIX E

AOM TEMPERATURE CONTROLLING

This appendix describes the need to temperature control the AOM. Normally the input polarization of the beam entering an AOM is linearly polarized and sent down one of the axes of the crystal. However, because we are doing a double pass, to minimize beam steering, we use a polarizing beamsplitter and a quarter wave plate to separate the double-passed beam. So we have circularly polarized light entering the AOM which has a slight birefringence, which changes the polarization state of the beam so the polarizing beamsplitter does not work as planned. Furthermore, the piezo is being driven by 1W of RF power so when we tune the AOM we change the temperature of the AOM crystal, hence changing the beam's polarization due to the birefringence of the AOM. This results in drastic power fluctuations.

We can eliminate these fluctuations by temperature controlling the AOM. Figure E.1 shows the results of temperature controlling the AOM. We can see when the AOM is turned on both the powers change drastically, however after 10 minutes the temperature controlled AOM stabilizes, while the uncontrolled AOM keeps oscillating. So by temperature controlling the AOM we can eliminate, or cancel the effects of the birefringent crystal.

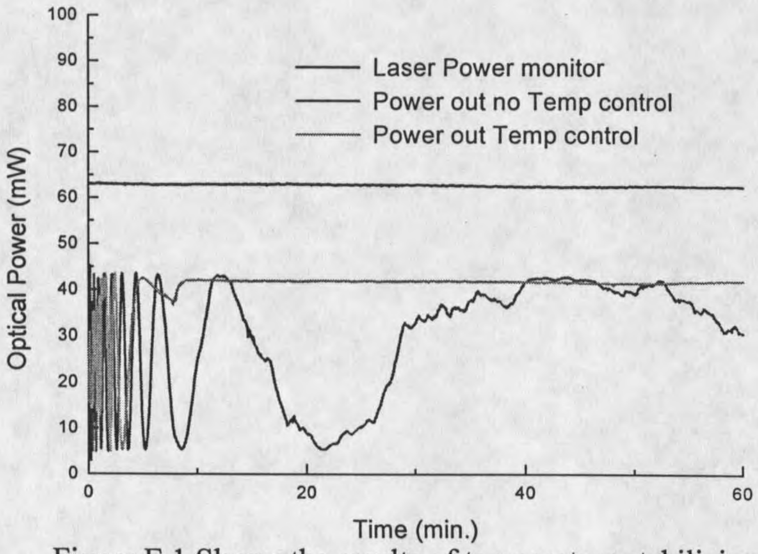

Figure E.1 Shows the results of temperature stabilizing the AOM.

APPENDIX F

PUMPING SYSTEM

This appendix describes the pumping system used to evacuate the cavity of air and fill it with H_2. When one uses these high reflectivity mirrors (A<15ppm), one needs to pay special care to the environmental conditions when a Raman cavity is constructed. Some examples: a normal roughing pump can deposit oil on the mirrors and adversely affect the properties of the mirrors; in addition, any dust in the H_2 tank that reaches the cavity will also degrade the performance of the cw Raman laser. To ensure the cleanliness of the mirrors the Raman cavities are assembled under a hood and the cavity, and H_2 lines are pumped down by an absorption pump, and a 0.5 miron filter was placed after the H_2 tank. Figure F.1 illustrates the pumping system.

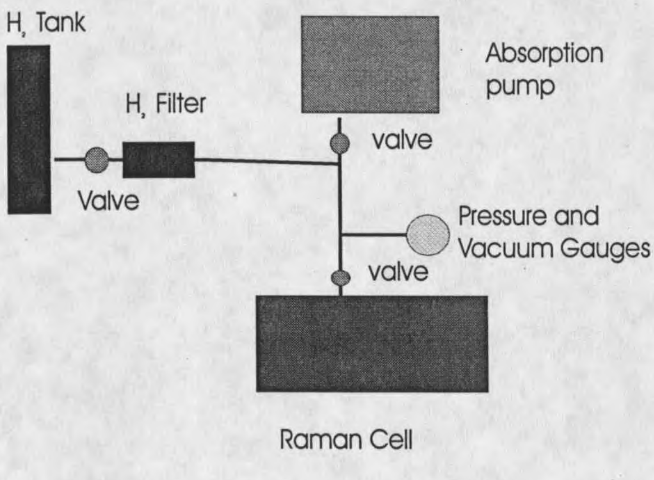

Figure F.1 Shows the pumping system used in this thesis.

APPENDIX G

RAMAN CAVITY

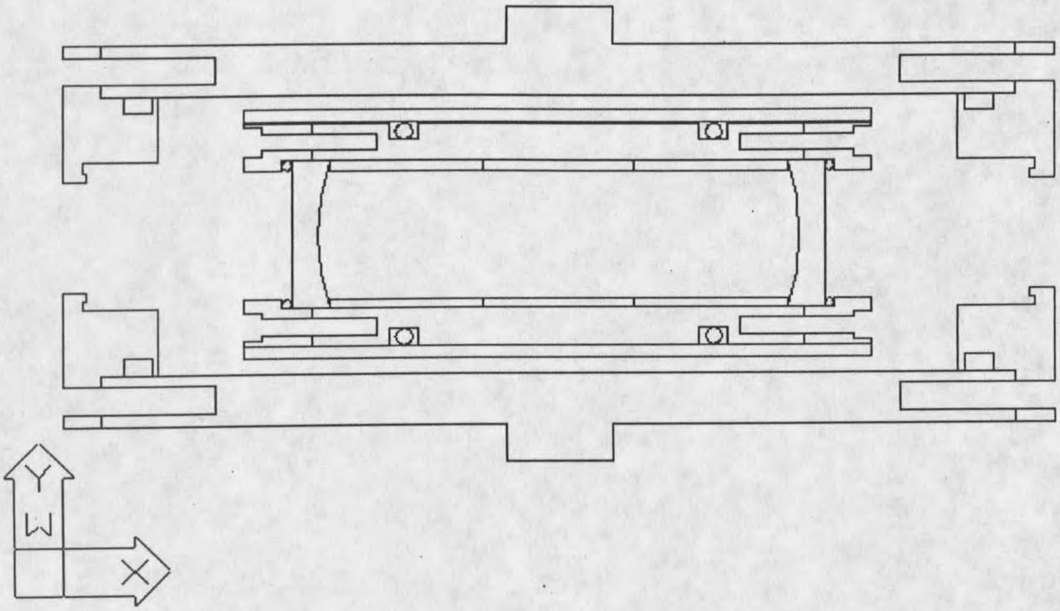

Figure G.1 The Raman cavity

This is the a diagram of the current cw Raman laser. The mirrors are spaced by 3 cylindrical piezos. And the cavity is vibration isolated by o-rings and sorbathane. The cavity is enclosed and is designed to safely hold 10atm. of H_2 (windows are limit).

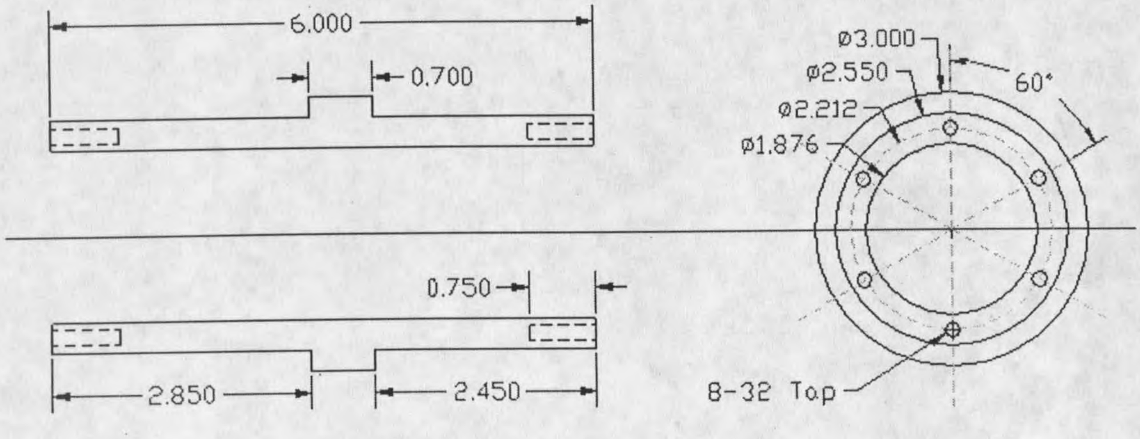

Figure G.2 The Raman cavity housing

This picture shows the housing of the cw Raman laser cavity.

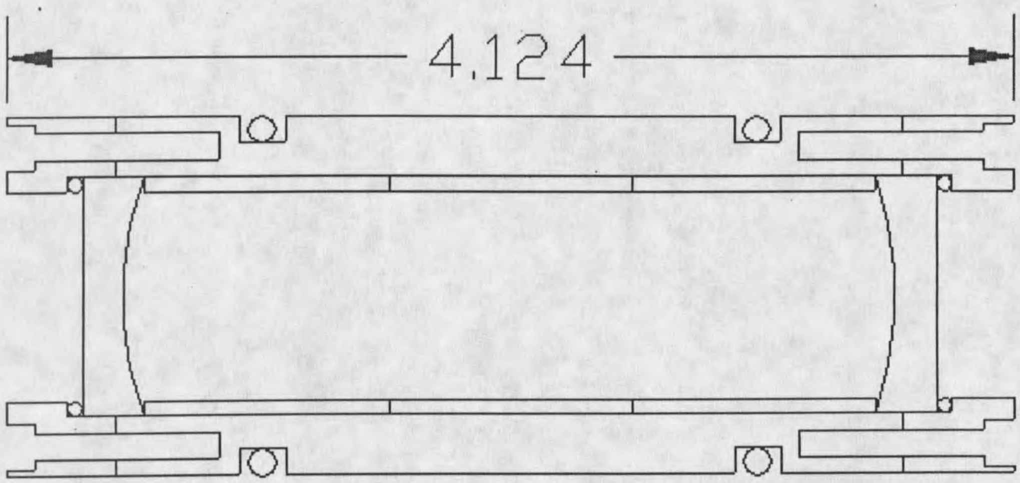

Figure G.3 The mirror holders

This figure shows the cavity section of the cw Raman laser, we can see the mirrors are held in contact with the piezos by compressed o-rings. The two o-rings that are on the outside of the cavity serve as vibration isolation.

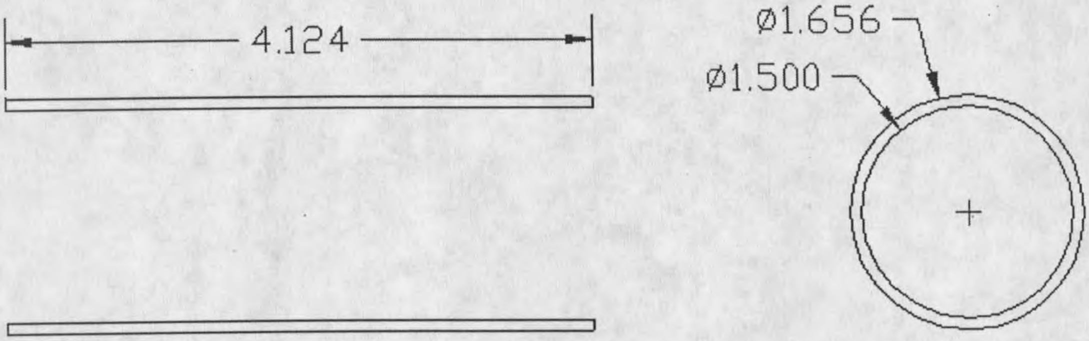

Figure G.4 Isolation cylinder

This cylinder sides over the cavity of figure G.3 and sorbathane is placed around the exterior of the cylinder to provide more vibration isolation from the cavity housing. The cw Raman cavity was designed by John Carlsten and Pete Roos, and constructed by Pete Roos

APPENDIX H

MATH-CAD PROGRAMS

This appendix contains the computer programs used in this thesis. They are Math-Cad programs.

Program list:

I	Calculates the start of the Raman laser for both the normal and linearized theories
II	Calculates the steady-state values for the pump and Stokes beams
III	Calculates the relaxation oscillation frequencies and damping
IV	Converts spectrum analyzer data into RIN
V	Calculates the RIN on the pump and the Stokes beams give a pump RIN

Program I

This program integrates the pump and Stokes equations

I. Let's model the mirror first:

A. Pump:

$R_p := 0.9998$ $\quad T_p := 180 \cdot 10^{-6}$ $\quad A_p := 1 - R_p - T_p$

B. Stokes' :

$R_s := R_p$ $\quad T_s := T_p$ $\quad A_s := A_p$

II. Let's define some constants:

$c := 3 \cdot 10^{10}$ cm/sec $\quad \psi := \sqrt{\dfrac{1 \cdot 10^{14}}{(4 \cdot \pi \cdot c)^2}}$ $\quad \psi = 2.653 \cdot 10^{-5}$

$L := 7.28$ cm (cavity length)

$R := 50$ cm (radius of curvature)

$b := \sqrt{(2 \cdot R - L) \cdot L}$ cm (confocal parameter)

$\lambda_p := 532 \cdot 10^{-7}$ cm (pump wavelength)

$$\lambda_s := \left(\frac{1}{\lambda_p} - 4155\right)^{-1}$$

$\lambda_s = 6.83 \cdot 10^{-5}$ cm (Stokes' wavelength)

$\upsilon_p := \dfrac{1}{\lambda_p}$ $\quad \upsilon_s := \dfrac{1}{\lambda_s}$ pump and Stokes frequencies

$$\alpha := 2.5 \cdot 10^{-9} \cdot \frac{\left[\left(8.48 \cdot 10^4\right)^2 - \left(\dfrac{1}{532 \cdot 10^{-7}}\right)^2\right]^2}{\left(\dfrac{1}{532 \cdot 10^{-7}} - 4155\right)} \cdot \frac{\upsilon_p - 4155}{\left[\left(8.48 \cdot 10^4\right)^2 - \upsilon_p^{\,2}\right]^2}$$ plane wave gain coefficient

$\alpha = 2.5 \cdot 10^{-9}$ cm/W

$$G := \frac{1}{2} \cdot \left(\frac{1}{4} \cdot \alpha \cdot c \cdot \psi\right)$$

$G = 2.487 \cdot 10^{-4}$ 1/sec*W $\quad g := G \quad g = 2.487 \cdot 10^{-4}$

$L_p := -\dfrac{c}{2 \cdot L} \cdot \ln(R_p)$ $\quad L_p = 4.121 \cdot 10^5$ 1/sec losses in pump mirrors

$L_s := -\dfrac{c}{2 \cdot L} \cdot \ln(R_s)$ $\quad L_s = 4.121 \cdot 10^5$ 1/sec losses in Stokes mirrors

Threshold Powers:

$$\mathrm{Area} := \frac{L \cdot (\lambda_p + \lambda_s)}{4 \cdot \mathrm{atan}\left(\dfrac{L}{b}\right)}$$ $\mathrm{Area} = 8.094 \cdot 10^{-4}$ Average area through a focus

$$E_{thres} := \frac{L \cdot L_p}{c} \cdot \sqrt{\frac{L_s}{T_p} \cdot \frac{1}{g}} \qquad E_{thres} = 303.462$$

$$P_{thres} := \frac{1}{2} \cdot \psi \cdot E_{thres}{}^2 \cdot Area \qquad P_{thres} = 9.886 \cdot 10^{-4}$$ Raman threshold in Watts

$Times := 4$ Number of time threshold

$$E_{in} := \sqrt{Times \cdot E_{thres}}$$

$K := \frac{c}{L} \cdot \sqrt{T_p} \cdot E_{in}$ Pump Rate

$x \equiv \begin{pmatrix} 0 \\ 1.5 \cdot 10^{-3} \end{pmatrix}$ Initial conditions

$K = 3.356 \cdot 10^{10}$

$$D(t,x) := \begin{bmatrix} \left(-L_p \cdot x_0\right) + K - \frac{\lambda_s}{\lambda_p} \cdot (g) \cdot \left(x_1\right)^2 \cdot x_0 \\ -L_s \cdot x_1 + (g) \cdot \left(x_0\right)^2 \cdot x_1 + 1 \cdot 10^7 \end{bmatrix}$$

$$Z := Bulstoer\left(x, 0, 100 \cdot 10^{-6}, 100, D\right)$$

$i := 0..3 \quad n := 0..100 \quad m := 1..100$

This section calculates the fields and powers leaving the cavity

Pump:

Front

$$Epf(n) := -\sqrt{R_p} \cdot E_{in} + \frac{1}{2} \cdot \sqrt{T_p} \cdot Z_{n,1}$$

$$Ppb(n) := \frac{1}{2} \cdot \psi \cdot Area \cdot Epb(n)^2$$

back

$Epb(n) := \frac{1}{2} \cdot \sqrt{T_p} \cdot Z_{n,1}$ field

$Ppf(n) := \frac{1}{2} \cdot \psi \cdot Area \cdot Epf(n)^2$ power

Stokes:

front

$$Esf(n) := \frac{1}{2} \cdot \sqrt{T_p} \cdot Z_{n,2}$$

$$Psf(n) := \frac{1}{2} \cdot \psi \cdot Area \cdot Esf(n)^2$$

back

$Esb(n) := \frac{1}{2} \cdot \sqrt{T_p} \cdot Z_{n,2}$ field

$Psb(n) := \frac{1}{2} \cdot \psi \cdot Area \cdot Esf(n)^2$ power

$P(n) := P_{thres} \cdot Times$ Input pump power

$\%(n) := \left[\frac{\frac{\lambda_s}{\lambda_p} \cdot (Psf(n) + Psb(n))}{P(n)} \right] \cdot 100$ Photon conversion efficiency

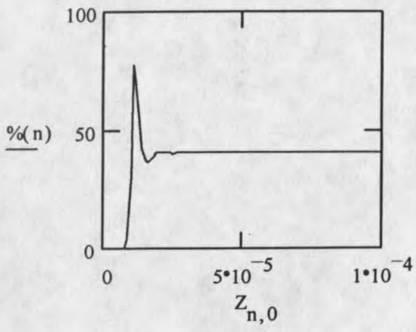

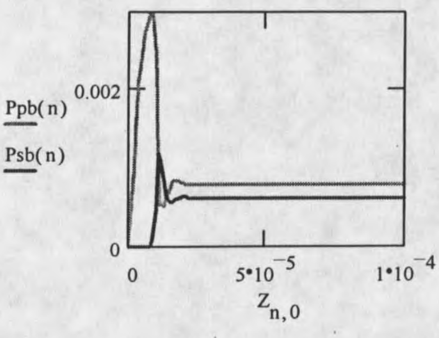

Writes the results to a data file

$Data_{n,0} := Z_{n,0}\cdot 1\cdot 10^{6}$ Time in micro seconds

$Data_{n,1} := Ppb(n)\cdot$ 100(pump at exit of cavity in mW

$Data_{n,2} := Ppf(n)\cdot$ 100(pump at front of cavity in mW

$Data_{n,3} := Psb(n)\cdot$ 100(Stokes at exit of cavity in mW

$Data_{n,4} := Psf(n)\cdot$ 100(Stokes at front of cavity in mW

$Data_{n,5} := \%(n)$ Conversion efficiency

$Data_{n,6} := P(n)$ pump in (marker)

$WRITEPRN(start) := Data$ Writes to a data file: start.prn

This section tests out the linearized theory

$a_{ss} := \sqrt{\dfrac{L_s}{g}}$ $\quad a_{ss} = 4.071\cdot 10^{4}$ pump field in the steady-state

$b_{ss} := \sqrt{\dfrac{\lambda_p\cdot\left(K - L_p\cdot a_{ss}\right)}{\lambda_s\cdot g\cdot a_{ss}}}$ $\quad b_{ss} = 3.593\cdot 10^{4}$ Stokes field in the steady-state

$x := \begin{pmatrix} -a_{ss} \\ -b_{ss} \end{pmatrix}$ initial conditions

$$DD(t,x) := \begin{bmatrix} -\left(L_p + \dfrac{\lambda_s}{\lambda_p}\cdot g\cdot b_{ss}^{\,2}\right)\cdot x_0 - 2\cdot\dfrac{\lambda_s}{\lambda_p}\cdot g\cdot a_{ss}\cdot b_{ss}\cdot x_1 \\ 2\cdot g\cdot a_{ss}\cdot b_{ss}\cdot x_0 \end{bmatrix}$$ linearized Raman equations

$ZZZ := Bulstoer\left(x, 0, 100\cdot 10^{-6}, 100, DD\right)$ integrates the linearized Raman equations

$ZZ_{n,1} := ZZZ_{n,1} + a_{ss}$ pump field

$ZZ_{n,2} := ZZZ_{n,2} + b_{ss}$ Stokes field

The pump and Stokes fields and powers at the front and the back of the cavity

pump:

front | back

$Af(n) := -\sqrt{R_p}\cdot E_{in} + \frac{1}{2}\cdot\sqrt{T_p}\cdot ZZ_{n,1}$ $\quad Ab(n) := \frac{1}{2}\cdot\sqrt{T_p}\cdot ZZ_{n,1}$ field

$Paf(n) := \frac{1}{2}\cdot\psi\cdot Area\cdot Af(n)^2$ $\quad Pab(n) := \frac{1}{2}\cdot\psi\cdot Area\cdot Ab(n)^2$ power

Stokes:

Front | back

$Bf(n) := \frac{1}{2}\cdot\sqrt{T_p}\cdot ZZ_{n,2}$ $\quad Bb(n) := \frac{1}{2}\cdot\sqrt{T_p}\cdot ZZ_{n,2}$ field

$Pbf(n) := \frac{1}{2}\cdot\psi\cdot Area\cdot Bf(n)^2$ $\quad Pbb(n) := \frac{1}{2}\cdot\psi\cdot Area\cdot Bb(n)^2$ power

$bbb := 0..70$

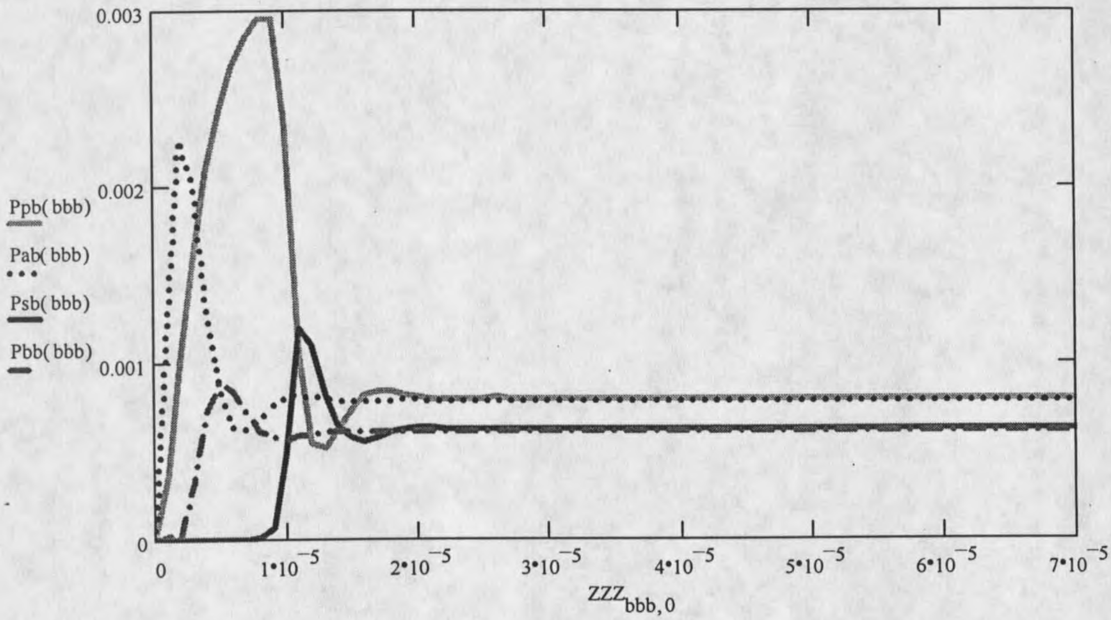

$Data2_{n,0} := ZZZ_{n,0}$ time in seconds

$Data2_{n,1} := Ppb(n)$ pump at back (normal)

$Data2_{n,2} := Psb(n)$ Stokes at back (normal)

$Data2_{n,3} := Pab(n)$ pump at back (linearized)

$Data2_{n,4} := Pbb(n)$ Stokes at back (linearized)

WRITEPRN(start2) := Data2 writes to a data file: start2.prn

Program II

This program takes the steady-state limit of the pump and Stokes equations

I. Let's model the mirror first:

A. Pump:

$R_p := 0.99978$ $\text{Ratio} := .86$ $T_p := (1 - R_p)\cdot\text{Ratio}$ $T_p = 1.849\cdot 10^{-4}$ $A_p := 1 - R_p - T_p$

$A_p = 3.01\cdot 10^{-5}$

B. Stokes' :

$R_s := R_p$ $T_s := T_p$ $A_s := A_p$

II. Let's define some constants:

$c := 3\cdot 10^8$ m/s $\psi := \sqrt{\dfrac{1\cdot 10^{14}}{(4\cdot\pi\cdot c)^2}}$ $\psi = 2.653\cdot 10^{-3}$

$L := 0.06$ m (cavity length)

$R := 1$ m (radius of curvature)

$b := \sqrt{(2\cdot R - L)\cdot L}$ m (confocal parameter)

$\lambda_p := 532\cdot 10^{-9}$ m (pump wavelength)

$\lambda_s := \left[\left(\dfrac{1}{\lambda_p\cdot 100} - 4155\right)\cdot 100\right]^{-1}$ $\lambda_s = 6.83\cdot 10^{-7}$ m (Stokes' wavelength)

$\upsilon_p := \dfrac{1}{\lambda_p\cdot 100}$ $\upsilon_s := \dfrac{1}{\lambda_s\cdot 100}$

$$\alpha := 2.5\cdot 10^{-11}\cdot\frac{\left[\left(8.48\cdot 10^4\right)^2 - \left(\dfrac{1}{532\cdot 10^{-7}}\right)^2\right]^2}{\left(\dfrac{1}{532\cdot 10^{-7}} - 4155\right)}\cdot\frac{\upsilon_p - 4155}{\left[\left(8.48\cdot 10^4\right)^2 - \upsilon_p^{\,2}\right]^2}$$

$\alpha = 2.5\cdot 10^{-11}$ m/W

$\text{Fac} := .66$

$G := \dfrac{1}{8}\cdot\psi\cdot\alpha\cdot c$ $G = 2.487\cdot 10^{-6}$ 1/sec*W $g := G\cdot\text{Fac}$

$L_p := -\dfrac{c}{2\cdot L}\cdot\ln(R_p)$ $L_p = 5.376\cdot 10^5$ 1/sec

$L_s := -\dfrac{c}{2\cdot L}\cdot\ln(R_s)$ $L_s = 5.376\cdot 10^5$ 1/sec

Let's do some steady-state theory.

$$A := \frac{L\cdot(\lambda_p + \lambda_s)}{4\cdot\operatorname{atan}\left(\dfrac{L}{b}\right)}$$

Threshold of the laser

$$E_{thres} := \frac{L}{c \cdot \sqrt{T_p}} \cdot L_p \cdot \sqrt{\frac{L_s}{g}} \quad E_{thres} = 4.525 \cdot 10^{3}$$

$$A = 1.047 \cdot 10^{-7}$$

$$P_{thres} := \frac{1}{2} \cdot \psi \cdot E_{thres} \cdot E_{thres} \cdot A \quad P_{thres} = 2.843 \cdot 10^{-3}$$

$$mm := 1000 \qquad n := 1 .. mm$$

$$P_{in}(n) := \left(1 + \frac{n \cdot 4}{mm}\right) \cdot P_{thres}$$

The steady state Approximation:

$$k(n) := \frac{c}{L} \cdot \sqrt{T_p} \cdot \sqrt{\frac{2 \cdot P_{in}(n)}{\psi \cdot A}}$$

$$P_{pump}(n) := \frac{1}{2} \cdot \psi \cdot \frac{k(n)}{T_p} \cdot k(n) \cdot \left(\frac{L}{c}\right)^2 \cdot A$$

$$E_{sexit}(n) := \frac{1}{2} \cdot \sqrt{T_s} \cdot \left[\frac{k(n) - L_p \cdot \sqrt{\frac{L_s}{g}}}{g} \cdot \frac{\lambda_p}{\lambda_s} \cdot \sqrt{\frac{g}{L_s}}\right]^{.5}$$

$$P_{sexit}(n) := \frac{1}{2} \cdot \psi \cdot E_{sexit}(n) \cdot E_{sexit}(n) \cdot A$$

$$S(n) := \frac{1}{1 - 2 \cdot \sqrt{\frac{R_p}{T_p} \cdot \frac{g}{L_s} \cdot P_{in}(n)}}$$

$DD_{n,0} := 1000 P_{pump}(n)$ Pump power

$DD_{n,1} := 2 \cdot 1000 P_{sexit}(n)$ Total Stokes power

$DD_{n,2} := \frac{683}{532} \cdot \frac{DD_{n,1}}{DD_{n,0}}$ Conversion efficiency

WRITEPRN(thres) := DD Writes to data file: thres.prn

Program III

This program computes the frequencies of the relaxation oscillations

I. Let's model the mirror first:

A. Pump:

$R_p := 0.999$ $T_p := 180\cdot10^{-6}$ $A_p := 1 - R_p - T_p$

B. Stokes' :

$R_s := R_p$ $T_s := T_p$ $A_s := A_p$

II. Let's define some constants:

$c := 3\cdot10^{10}$ cm/sec $\psi := \sqrt{\dfrac{1\cdot10^{14}}{(4\cdot\pi\cdot c)^2}}$ $\psi = 2.653\cdot10^{-5}$

$L := 7.28$ cm (cavity length)

$R := 50$ cm (radius of curvature)

$b := \sqrt{(2\cdot R - L)\cdot L}$ cm (confocal parameter)

$\lambda_p := 532\cdot10^{-7}$ cm (pump wavelength)

$\lambda_s := \left(\dfrac{1}{\lambda_p} - 4155\right)^{-1}$ $\lambda_s = 6.83\cdot10^{-5}$ cm (Stokes' wavelength)

$\upsilon_p := \dfrac{1}{\lambda_p}$ $\upsilon_s := \dfrac{1}{\lambda_s}$

$$\alpha := 2.5\cdot10^{-9}\cdot\frac{\left[\left(8.48\cdot10^4\right)^2 - \left(\dfrac{1}{532\cdot10^{-7}}\right)^2\right]^2}{\left(\dfrac{1}{532\cdot10^{-7}} - 4155\right)}\cdot\frac{\upsilon_p - 4155}{\left[\left(8.48\cdot10^4\right)^2 - \upsilon_p^{\,2}\right]^2}$$

$\alpha = 2.5\cdot10^{-9}$ cm/W

$G := \dfrac{1}{2}\cdot\left(\dfrac{1}{4}\cdot\alpha\cdot c\cdot\psi\right)$ $G = 2.487\cdot10^{-4}$ 1/sec*W $g := G$ $g = 2.487\cdot10^{-4}$

$L_p := -\dfrac{c}{2\cdot L}\cdot\ln\left(R_p\right)$ $L_p = 4.121\cdot10^5$ 1/sec

$L_s := -\dfrac{c}{2\cdot L}\cdot\ln\left(R_s\right)$ $L_s = 4.121\cdot10^5$ 1/sec

Threshold Powers:

$\text{Area} := \dfrac{L\cdot\left(\lambda_p + \lambda_s\right)}{4\cdot\operatorname{atan}\left(\dfrac{L}{b}\right)}$ $\text{Area} = 8.094\cdot10^{-4}$

$E_{thres} := \dfrac{L\cdot L_p}{c}\cdot\sqrt{\dfrac{L_s}{T_p}\cdot\dfrac{1}{g}}$ $E_{thres} = 303.462$

$P_{thres} := \dfrac{1}{2}\cdot\psi\cdot E_{thres}^{\,2}\cdot\text{Area}$ $P_{thres} = 9.886\cdot10^{-4}$

$n := 3..1000$

$\mathrm{Times}(n) := 1 + n\cdot\frac{220}{1000}$ This variable ramps the pump power

$E_{in}(n) := \sqrt{\mathrm{Times}(n)\cdot E_{thres}}$

$K(n) := \frac{c}{L}\cdot\sqrt{T_p}\cdot E_{in}(n)$

Let's test out the linearized theory

$a_{ss} := \sqrt{\frac{L_s}{g}}$ $\quad a_{ss} = 4.071\cdot 10^4$

$b_{ss}(n) := \sqrt{\frac{\lambda_p\cdot\left(K(n) - L_p\cdot a_{ss}\right)}{\lambda_s\cdot g\cdot a_{ss}}}$ $\quad b_{ss}(1) = 1.162\cdot 10^4$

$\gamma(n) := L_p + \frac{\lambda_s}{\lambda_p}\cdot g\cdot b_{ss}(n)^2$ $\quad \omega_0(n) := \sqrt{\frac{\lambda_s}{\lambda_p}\cdot\left(2\cdot g\cdot b_{ss}(n)\cdot a_{ss}\right)^2}$

$\omega(n) := \sqrt{\omega_0(n)^2 - \frac{\gamma(n)^2}{4}}$ $\quad f(n) := \frac{1}{2\cdot\pi}\cdot\omega(n)$

$m := 2..1000$

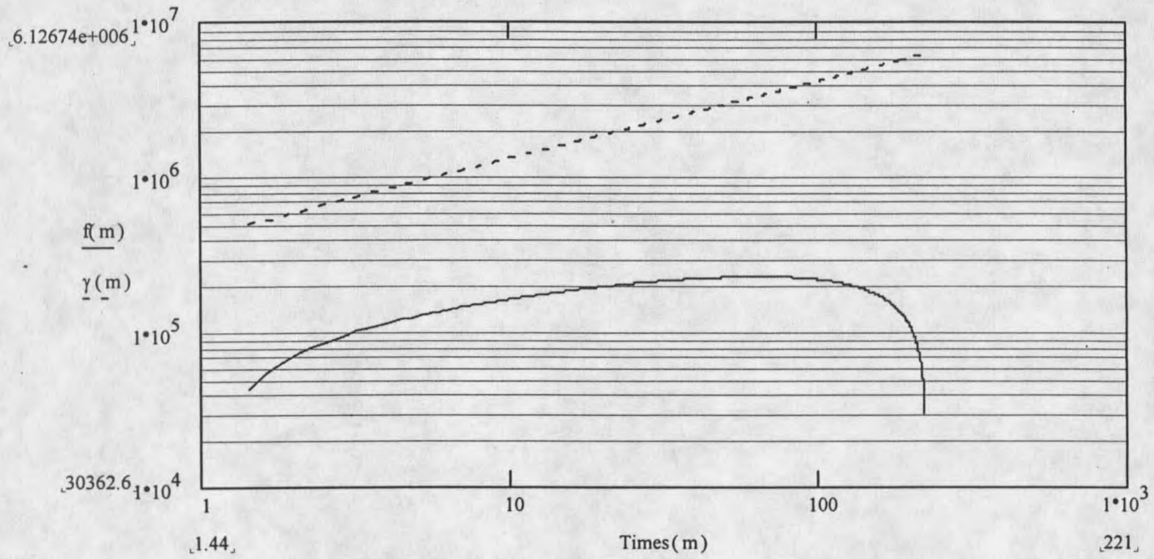

Now let's calculate how much damping occurs in one oscillation

$$\mathrm{Damping}(n) := e^{\frac{-\gamma(n)}{2} \cdot 2 \cdot \frac{\pi}{\omega(n)}}$$

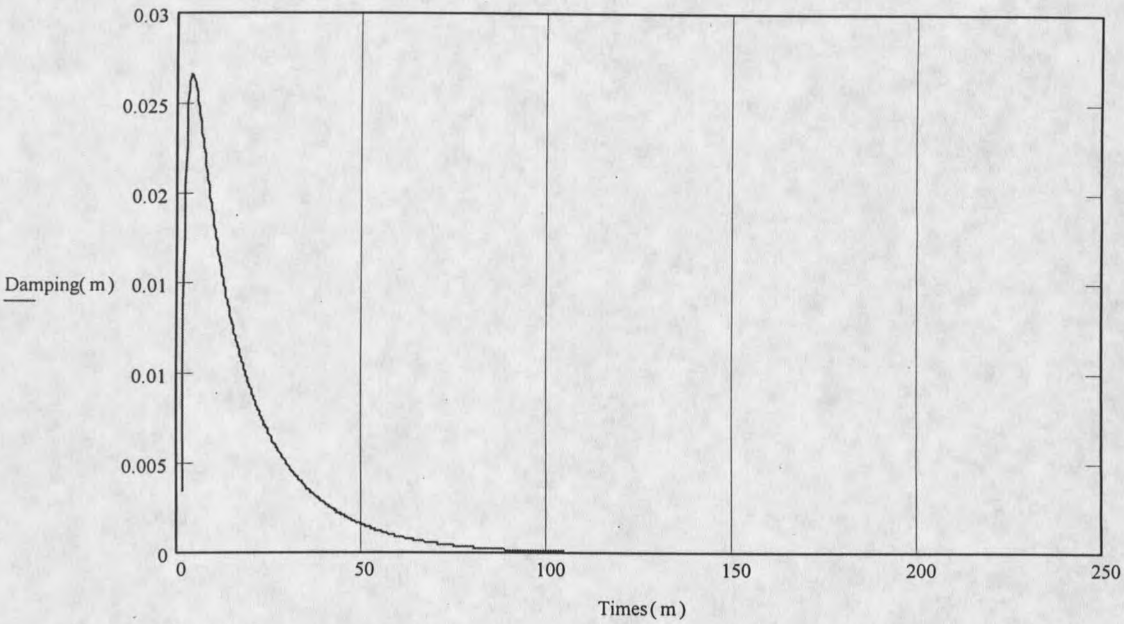

$Z_{m,0} := \mathrm{Times}(m)$

$Z_{m,1} := f(m)$

$Z_{m,2} := \gamma(m)$

$Z_{m,3} := \mathrm{Damping}(m)$

WRITEPRN(relax) := Z writes to a data file: relax.prn

Program IV

This program converts the spectrum analyzer data into RIN.

This section reads in the data file

$X := \mathrm{READPRN}(s90g1) \quad A := \mathrm{rows}(X) \quad A = 399 \qquad n := 0..A-1$

Now we want to convert the data to RIN

$V_{dc} := \frac{7.3}{2}\,\mathrm{V} \qquad R := 50\Omega$

$P_{dc} := \frac{V_{dc}^{2}\cdot 1000}{R}\,\mathrm{mW} \qquad RB := 1200\,\mathrm{Hz}$

$\mathrm{correction} := 10\cdot\log\left(P_{dc}\right) + 10\cdot\log(RB) \quad \mathrm{correction} = 55.048$

$Z_{n,0} := X_{n,0}$ Frequency $\qquad Z_{n,1} := X_{n,1} - \mathrm{correction}$

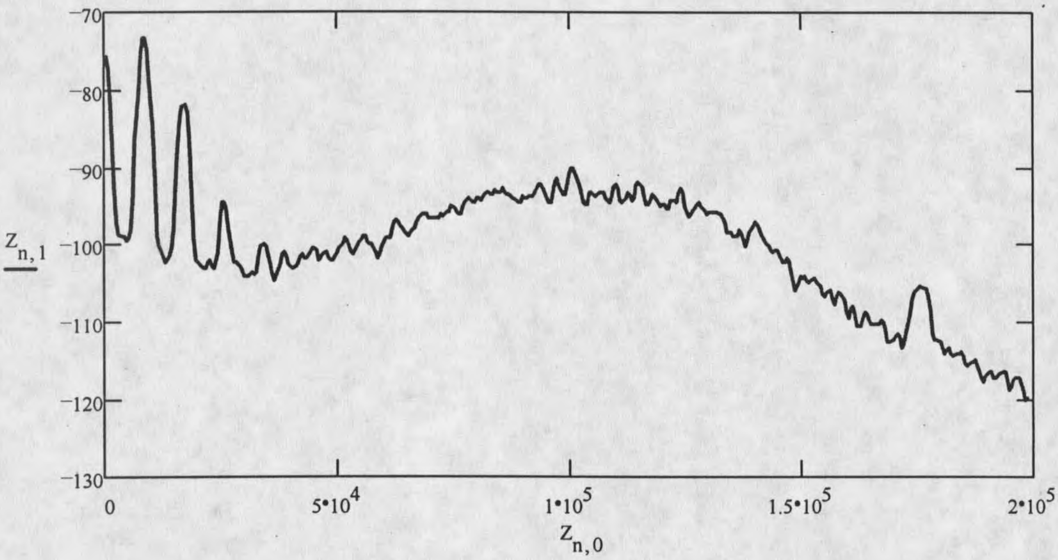

$\mathrm{WRITEPRN}(s90g1r) := Z$ writes the RIN to a data file

Program V

This program integrates the pump and Stokes equations

I. Let's model the mirror first:

A. Pump:

$R_p := 0.9998'$ $\quad T_p := 110 \cdot 10^{-6}$ $\quad A_p := 1 - R_p - T_p$ $\quad A_p = 2 \cdot 10^{-5}$

B. Stokes' :

$R_s := .9997\text{ɩ}$ $\quad T_s := 180 \cdot 10^{-6}$ $\quad A_s := 1 - R_s - T_s$

II. Let's define some constants:

$c := 3 \cdot 10^{10}$ cm/sec $\qquad \psi := \sqrt{\dfrac{1 \cdot 10^{14}}{(4 \cdot \pi \cdot c)^2}} \qquad \psi = 2.653 \cdot 10^{-5}$

$L := 7.28$ cm (cavity length)
$R := 50$ cm (radius of curvature)
$b := \sqrt{(2 \cdot R - L) \cdot L}$ cm (confocal parameter)
$\lambda_p := 532 \cdot 10^{-7}$ cm (pump wavelength)

$$\lambda_s := \left(\frac{1}{\lambda_p} - 4155\right)^{-1}$$

$\lambda_s = 6.83 \cdot 10^{-5}$ cm (Stokes' wavelength)

$\upsilon_p := \dfrac{1}{\lambda_p} \qquad \upsilon_s := \dfrac{1}{\lambda_s}$

$$\alpha := 2.5 \cdot 10^{-9} \cdot \frac{\left[\left(8.48 \cdot 10^4\right)^2 - \left(\dfrac{1}{532 \cdot 10^{-7}}\right)^2\right]^2}{\left(\dfrac{1}{532 \cdot 10^{-7}} - 4155\right)} \cdot \frac{\upsilon_p - 4155}{\left[\left(8.48 \cdot 10^4\right)^2 - \upsilon_p^{\,2}\right]^2}$$

$\alpha = 2.5 \cdot 10^{-9}$ cm/W

$G := \dfrac{1}{2} \cdot \left(\dfrac{1}{4} \cdot \alpha \cdot c \cdot \psi\right) \quad G = 2.487 \cdot 10^{-4}$ 1/sec*W $\quad g := G \quad g = 2.487 \cdot 10^{-4}$

$L_p := -\dfrac{c}{2 \cdot L} \cdot \ln\left(R_p\right) \quad L_p = 2.679 \cdot 10^5$ 1/sec

$L_s := -\dfrac{c}{2 \cdot L} \cdot \ln\left(R_s\right) \quad L_s = 4.533 \cdot 10^5$ 1/sec

Threshold Powers:

$\text{Area} := \dfrac{L \cdot \left(\lambda_p + \lambda_s\right)}{4 \cdot \operatorname{atan}\left(\dfrac{L}{b}\right)} \quad \text{Area} = 8.094 \cdot 10^{-4}$

$E_{thres} := \dfrac{L \cdot L_p}{c} \cdot \sqrt{\dfrac{L_s}{T_p} \cdot \dfrac{1}{g}} \quad E_{thres} = 264.631$

$P_{thres} := \frac{1}{2}\cdot\psi\cdot E_{thres}{}^{2}\cdot Area \quad P_{thres} = 7.518\cdot 10^{-4}$

$Times := 5.6 \quad E_{in} := \sqrt{Times\cdot E_{thres}} \quad K := \frac{c}{L}\cdot\sqrt{T_{p}}\cdot E_{in} \quad K = 2.707\cdot 10^{10}$

The steady-state values:

$a_{ss} := \sqrt{\frac{L_{s}}{g}} \quad a_{ss} = 4.27\cdot 10^{4} \qquad b_{ss} := \sqrt{\frac{\lambda_{p}\cdot\left(K - L_{p}\cdot a_{ss}\right)}{\lambda_{s}\cdot g\cdot a_{ss}}} \quad b_{ss} = 3.386\cdot 10^{4}$

Let us read in the pump RIN data file

$Pump := READPRN(Pump1) \quad A := rows(Pump) \quad A = 399 \quad list := 0..A-1$

Col. 0 is the frequency, and col 1 is the SA data. We now need to convert the SA data into RIN

$RB := 1200Hz \quad Volt := \frac{4.56}{2}V \quad R := 50\Omega \quad DCP := \frac{Volt^{2}}{R}\cdot 1000 \quad DCP = 103.968 \ mW$

Now we can convert to RIN

$RBa := 10\cdot\log(RB) \quad RBa = 30.792 \quad DCPa := 10\cdot\log(DCP) \quad DCPa = 20.169$
$Correction := RBa + DCPa \quad Correction = 50.961$

$RIN_{list,0} := Pump_{list,0} \quad RIN_{list,1} := Pump_{list,1} - Correction$

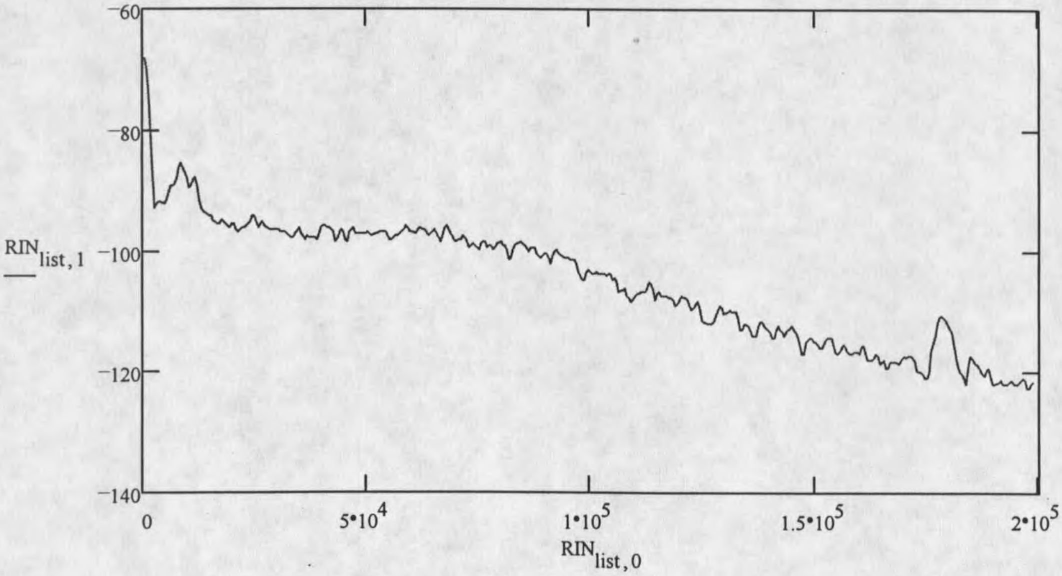

Now we have the pump fluctuations in RIN, now we want to place these fluctuations in to an amplitude for the pumping term (in Field). Remember RIN goes like the optical power squared, so it will vary like the Field to the 4th power. The RIN is also measured in RMS.

$Amp_{list,0} := RIN_{list,0}$ Frequency of the oscillation

$Amp_{list,1} := \sqrt{2 \cdot 10^{\frac{1}{40} \cdot RIN_{list,1}}}$ Relative amplitude of the oscillation (in Field)

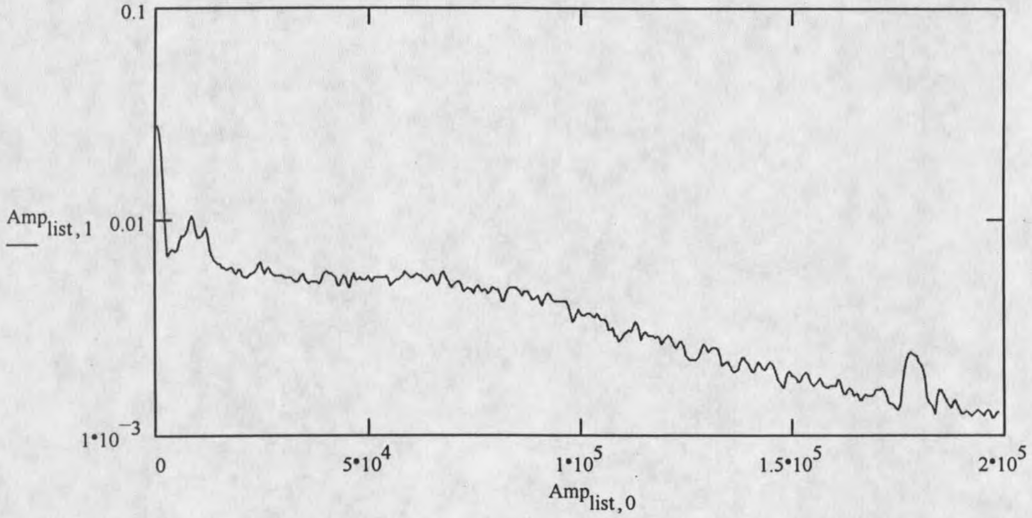

Now we want to place this noise into the cavity pumping k(f) and generate what we would expect to see in the output Stokes and Pump fields above threshold!
This program finds the noise spectra for the pump and Stokes beams after threshold:

$$\mathrm{Answer}\left(D, \mathrm{List}, \mathrm{Amp}, a_{ss}, b_{ss}\right) := \left\| \begin{array}{l} \text{for } k \in 0..\mathrm{List}-1 \\ \quad \left\| \begin{array}{l} f \leftarrow \mathrm{Amp}_{k,0} \\ \mathrm{Time} \leftarrow \dfrac{2}{f} \\ A \leftarrow \mathrm{Amp}_{k,1} \\ x \leftarrow \begin{bmatrix} a_{ss} \\ b_{ss} \\ 2 \cdot \pi \cdot f \\ A \end{bmatrix} \\ Z \leftarrow \mathrm{Bulstoer}(x, 0, \mathrm{Time}, 1500, D) \\ \text{for } s \in 0..1399 \\ \quad \left\| \begin{array}{l} \mathrm{Pump}_s \leftarrow Z_{s+100,1} \\ \mathrm{Stokes}_s \leftarrow Z_{s+100,2} \end{array} \right. \\ \mathrm{Noise}_{k,0} \leftarrow f \\ \mathrm{Noise}_{k,1} \leftarrow 2 \cdot \dfrac{\max(\mathrm{Pump}) - \min(\mathrm{Pump})}{\max(\mathrm{Pump}) + \min(\mathrm{Pump})} \\ \mathrm{Noise}_{k,2} \leftarrow 2 \cdot \dfrac{\max(\mathrm{Stokes}) - \min(\mathrm{Stokes})}{\max(\mathrm{Stokes}) + \min(\mathrm{Stokes})} \end{array} \right. \\ \mathrm{Noise} \end{array} \right.$$

Now we need to write the differential equation for the system

$$D(t,x) := \begin{bmatrix} \left[\left[-L_p \cdot x_0 + K \cdot \left(1 + x_3 \cdot \sin\left(x_2 \cdot t\right)\right) \right] - \dfrac{\lambda_s}{\lambda_p} \cdot g \cdot \left(x_1\right)^2 \cdot x_0 \right] \\ -L_s \cdot x_1 + g \cdot \left(x_0\right)^2 \cdot x_1 \\ 0 \\ 0 \end{bmatrix}$$

$$Z := \mathrm{Answer}\left(D, A, \mathrm{Amp}, a_{ss}, b_{ss}\right)$$

Now we need to convert the noise into a RIN

$ZZ_{list,0} := Z_{list,0}$ Frequency of oscillation

$ZZ_{list,1} := 40 \cdot \log\left(\dfrac{Z_{list,1}}{2 \cdot \sqrt{2}}\right)$ Pump RIN

$ZZ_{list,2} := 40 \cdot \log\left(\dfrac{Z_{list,2}}{2 \cdot \sqrt{2}}\right)$ Stokes RIN

$ZZ_{list,3} := RIN_{list,1}$ Pump In RIN

WRITEPRN(RINQ) := ZZ Writes the data to a file RINQ.prn